COUPLED AND UNCOUPLED PANEL

RESPONSE TO SONIC BOOM

TYPE INPUTS

By

GERALD D. WHITEHOUSE
"

Bachelor of Science
University of Missouri-Rolla
Rolla, Missouri
1958

Master of Science
Oklahoma State University
Stillwater, Oklahoma
1964

Submitted to the faculty of the Graduate
College of the Oklahoma State University
in partial fulfillment of the
requirements for the degree of
DOCTOR OF PHILOSOPHY
May, 1967

COUPLED AND UNCOUPLED PANEL

RESPONSE TO SONIC BOOM

TYPE INPUTS

Thesis Approved:

R. L. Lowery
Thesis Adviser

P. Dransfield

Lee Harrisberger

David L. Hichs

D. D. Durham
Dean of the Graduate School

ii

PREFACE

Development of the supersonic transport aircraft has
created wide concern for the overpressures that the gener-
ated sonic boom will cause on structural elements. The
elements that are most likely to be damaged and that occur
in abundance are glass windows. Extensive research has
been conducted on the response of panels in the past, but
little work has been directed toward the transient response
of panels and applying the results for the understanding of
panel response to sonic booms.

The dynamic response of structural members such as
large glass windows and flexible ceilings, is a difficult
problem, due to the acoustical interaction that results
from a sonic boom pressure wave. This study is to further
the understanding of panel and panel cavity coupled transient
oscillations to sonic boom type inputs. This area will
become increasingly important as sonic boom flights become
more frequent in this country.

I wish to express my gratitude to the National Science
Foundation for the traineeship that enabled sufficient funds
to undertake the study.

I wish to express my appreciation to Dr. R. L. Lowery,
who served as my adviser throughout the years of my graduate

iii

TABLE OF CONTENTS

LIST OF TABLES

LIST OF FIGURES

LIST OF SYMBOLS

x,y,z	Refers to the x,y,z direction in rectangular coordinate system
$\ddot{x},\dot{x}$	Second derivative with respect to time, first derivative with respect to time
h	Thickness of panel
Q_0	Intensity of a continuously distributed load
P	Pressure
P_0	Height of pressure pulse
p_0	Static reference pressure
γ	Weight of material per unit volume
ρ	Density of material
ρ_0	Density of air at standard atmospheric conditions
E	Modulus of elasticity in tension or compression
μ	Poisson's ratio
D	Flexure rigidity of plate
a	Dimension of panel along x-direction
b	Dimension of panel along y-direction
τ_1	Positive pressure duration of N-wave
τ	Time duration of N-wave
ζ,ζ_{rs}	Damping factor, damping factor for rs mode
q_{rs}	Generalized displacement for rs mode
ω_{rs}	Angular undamped rs^{th} natural frequency
r,s,u,v	Indexes of mode functions

Φ_{rs}	Normal mode function for the rs^{th} mode
ω_{dr}	Damped natural angular frequency
K	Variable to adjust shape of pressure wave (for instance K=2 for idealized N-wave)
U	Potential energy
T	Kinetic energy
m	Actual mass of the panel
c, C_{rs}	Damping coefficient, damping coefficient for rs mode
$F(x,y,t)$	Force time history
$h(t)$	Impulsive response, system response to impulse
ϵ_x	Strain in the x-direction
ϵ_y	Strain in the y-direction
L_{rs}	Generalized forcing function
Ψ	Dummy variable of integration for variable t
σ_x	Stress in x-direction of a element on surface of panel
σ_y	Stress in y-direction of a element on surface of panel
Z_{rs}	Absolute displacement of panel in a direction perpendicular to x-y axis
M_{rs}	Generalized mass for rs^{th} mode
T	Fundamental Period of System
γ^1	Ratio of specific heats

CHAPTER I

INTRODUCTION

Definition of the Problem

Sonic boom test conducted in Oklahoma City in 1964 gave
indications that various building enclosures can behave in
the manner of a Helmholtz resonator. The question arises as
to what effect the pressure oscillations inside the structure
have on the flexible panels contained in the enclosure.
The residual cavity pressure oscillations during sonic booms
create secondary driving forces and can adversely affect
structural elements such as windows and flexible ceilings.

The transient response of a panel coupled to a Helmholtz
resonator subjected to a N-wave pulse analogizes this problem,
which will often be encountered in future response studies
of building enclosures. The coupled system is shown in
Figure 1 and the idealized N-wave representing the sonic
boom is shown in Figure 2. The system is a coupled dis-
tributed system, in which the panel response is affected by
the parameters of the cavity.

The problem, therefore, is to investigate the response
of the panel when the resonator is subjected to a transient
N-wave, and to develop methods for predicting the panel
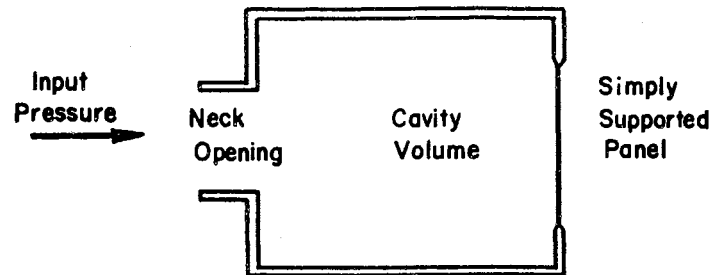
Figure 1. Panel Coupled to Helmholtz Resonator
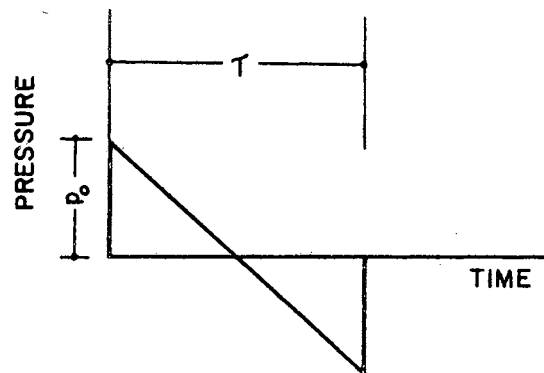
Figure 2. Transient Pressure Pulse

response.

Purpose and Scope of the Study

Incidents occurring in the area of structural response to transient inputs such as sonic booms, indicate that portions of the structures, such as ceilings, windows and walls may achieve amplitudes of sufficient magnitude to cause destruction.

A portion of a news article which appeared in the Washington C. H., Ohio, Journal Herald, June 10, 1966, reads as follows:

> A sonic boom thundered over the Washington C. H., Ohio, yesterday morning shattering windows and causing an estimated $30,000 damage.
> Wright-Patterson Air Force base officials said an F-IC Phantom jet fighter-bomber from the base was conducting tests in the area at the time.
> "The plane flew right over town, from northeast to southwest," said Patrolman Dennis Brown who was on duty in his cruiser. "There was a loud cracking noise - it cracked my eardrums - and then all these windows commenced popping out," Brown said.
> Several residents compared it to a tornado. One woman said the concussion struck like a big suction cup. Another resident told of seeing a window screen pulled off by suction created by the boom.
> The boom broke 20 to 30 plate glass windows in downtown stores, toppled furniture in private homes, rattles dishes out of cabinets, bent metal doors and snapped loose ceiling material, residents reported.

This incident involving the breaking of plate glass windows indicated that stress levels had been reached on the order of the ultimate strength of glass. A discussion taken from reference (1), states:

Aside from the obvious variation due to incon-
sistencies in the shape of the pressure wave, another
unusual effect was observed in some of the displace-
ment recordings. On the records, corresponding to
Flights 4, 5, 6, 7 and 8 of July 28, relatively high
readings were taken for both the differential trans-
former and the strain gauge. The fact that both
readings were high suggests that the window actually
was driven by some force to a considerable amplitude
and that the instruments were not in error.

The strain and displacement traces show the
window to be vibrating at a low frequency, about
5 cps. This is unexpected since the natural frequency
of the window was found to be on the order of 25 cps
also checked with the calculated natural frequency.

It can be seen in some of the recordings that
the peak strain (and displacement) can occur after
the pressure wave is past. The logical explanation
for this is that a secondary driving function has
been generated after the wave has passed.

In the first incident, an overflight caused extreme

damage to a community and probably was a result of a human

error in altitude and speed. The second incident originated

in a controlled flight test in which various portions of

the structure were instrumentated for obtaining response

data. The two cases need to be related to understand the

phenomena of the sonic boom effects on non-load carrying

members, such as windows. The first case was probably

one in which pressure caused by the sonic boom was of

sufficient magnitude so that all large glass windows in

the vicinity having a natural period nearly equal to the

forcing period of the pressure wave, were driven to large

stress amplitudes. The second incident could be one in

which large amplitudes were achieved due to the panel-

cavity coupling. However, the window did not break because

the natural frequency of the panel was well above the

resonant frequency of the cavity.

Development of supersonic aircraft has created much concern for the probability of damage to residential dwellings and structural elements such as walls, windows and ceilings. In the near future, many structures throughout the country will experience at least one sonic boom shock wave daily. As a consequence, the sonic boom has generated interest in the study of transient panel oscillations and panel-cavity coupled oscillations.

The method for accomplishing the objective was to investigate both analytically and experimentally the transient response of: (a) a simply supported panel in a baffle and (b) a simply supported panel coupled to a Helmholtz resonator. The transient input to the resonator was achieved by the use of an electronic generated N-wave pulse driving a transducer.

The analytical study consisted of a multi-mode analysis of the transient response of the simply supported panel in a baffle, and a lumped mathematical model investigation of the panel-cavity coupled transient oscillations. The effect of damping is included in both analysis.

The experimental work required the design and the construction of a simply supported aluminum panel, a test resonator, and the development of adequate instrumentation for generating the transient pressure pulse. Input pressures, cavity response, and panel response were measured for N-wave transient pulse inputs. Responses were correlated with

analytical predictions.

One consequence of the experimental investigation was to verify that the lumped parameter, damped, two degree-of-freedom system sufficed in predicting the transient response of the panel in the wall of the resonator.

An analysis was performed of an actual case of structural damage that occurred during a supersonic flight. A comparison of the results is given between a continuous system analysis and an idealization as a lumped parameter system.

Previous Work

Mathematical analysis of various plate configurations with various loading functions found in the technical literature are numerous. Most of the documented cases involve deflection solutions to a statically applied load. Vibration analysis of plates were confined mainly to the area of steady state analysis. Very little emphasis has been placed on the investigation of transient panel response.

Plate vibrations probably started with the published works of Lord Rayleigh (20), Timoshenko (28, 29) and Lamb (13). Timoshenko gives the solution for simply supported vibrating plate. Mixed boundary conditions of the plate -, i.e., when one or more of the sides are clamped, free, simply supported, etc; - are difficult to handle. The Rayleigh-Ritz method (14) had been used to solve this type of problem. It is a numerical technique based on energy

relations.

Previous work on the transient vibration of plates was restricted mainly to the undamped case, and to cases for simple forcing input such as step functions.

Ungar (31) was probably the original investigator in the area of panel response to moving loads. He investigated the response of simply supported rectangular plates to sinusoidally oscillating shocks. Traveling shock waves parallel to the edges of the plate were used as inputs. The response was obtained by use of Lagrange's equations using generalized coordinates. Specialized expressions were obtained for moving pressure discontinuities, and results were applied in the area of response of panels on flight vehicles.

Crocker (10), in a recent publication, investigated analytically the response of an undamped simply supported panel to sonic boom type inputs, with normal and grazing incidence waves. He showed the traveling wave to be less severe than the normal incidence wave. The experimental work consisted of the strain response of a small panel mounted in a tube in which an explosive charge was detonated to simulate the pressure pulse.

Cheng (7) investigated the dynamic effects of sonic boom on beams and plates. A theoretical analysis for simply sup-ported and clamped conditions was investigated for normal incidence pressure waves. The undamped case was treated and solution was obtained by the use of a trignometric

series. Practical implications of sonic booms on building structures were discussed.

Mase (16) investigated analytically the transient response of a linear, viscoelastic panel for a uniform load step input. The plate was assumed to be of a Kelvin type material. The deflection expression was obtained by solving the equation of motion using operational calculus. Termwise inversion of the resulting transform is very cumbersome to obtain the time response.

Bowles and Sugarman (5) conducted an experimental investigation of static load tests on large rectangular glass panels. The average failure stress for the glass was about 6000 psi. Rate of loading had an appreciable effect: failure strength increased as the rate of loading increased.

The effect of coupling the panel to the resonator required an understanding of the Helmholtz resonator. Helmholtz was the original investigator or the resonator. He investigated vowel sounds using the resonator for an amplification device. Rayleigh (20) and others (15, 23, 25, 26, 27) conducted steady state response analysis on various configurations of resonators. Their investigations contributed greatly to the area of wave filters.

Simpson (24) investigated the transient response of the Helmholtz resonator and showed the resonator to behave like a simple oscillator for large wave lengths of sound. Simpson verified the undamped idealized model results by

measured cavity pressures.

Pretlove (19) investigated coupled panel oscillations. A rectangular panel which covered one side of a rectangular enclosure was the situation that was considered. An analytical expression was derived for the free oscillations of the panel. The results are applicable only to a simple rectangular enclose backing the panel.

Ostergren (17) investigated the time response of an undamped two degree-of-freedom system for step inputs. This was a specific application to cushioning and packaging of equipment. His results show that the ratio of the upper and lower mass is the significant influential parameter on the response to a step input. Other analysis have been performed for transient analysis for simple forcing functions. The introduction of damping in the system and a transient excitation as the N-wave increases the difficulty in obtaining a solution. A general transient response analysis of the damped two degree-of-freedom system has not been performed.

CHAPTER II

THE TRANSIENT RESPONSE OF A SIMPLY SUPPORTED
PANEL TO A N-WAVE PRESSURE PULSE ARRIVING
AT NORMAL INCIDENCE

The analysis of the vibrating panel in a baffle has
been performed by many acousticians (28,3). Steady state
analysis, or the condition in which a constant driving
force at one frequency is applied to the panel, has been
the primary approach. Transient response analysis is not
as straight forward as steady state analysis. The concept
of mechanical impedance becomes extremely complicated in
the transient case in which excitation can occur at more
than one frequency.

A transient or aperiodic input represents a pulse type
condition in which a multi-frequency situation exists. The
frequency spectrum of a N-wave shaped pulse can be obtained
easily by the method of the Fourier integral and a plot of
the frequency versus the amplitude, will show that the
frequency spectrum of the pulse is continuous.

The presence of finite amplitudes of each frequency in
the transient pulse, and the fact that a distributed system
such as the simply supported panel has natural frequencies
above the fundamental causes concern in the transient

analysis.

A distributive dynamic system has associated with it normal modes which exhibit orthogonal properties. If the system is considered to be a linear structure and deflections are small enough for the theory of elasticity to hold, the dynamic response of the system can be analyzed in terms of its normal mode oscillations. A distributive system in the form of a simply supported panel with a transient N-wave arriving at normal incidence is illustrated in Figure 3.
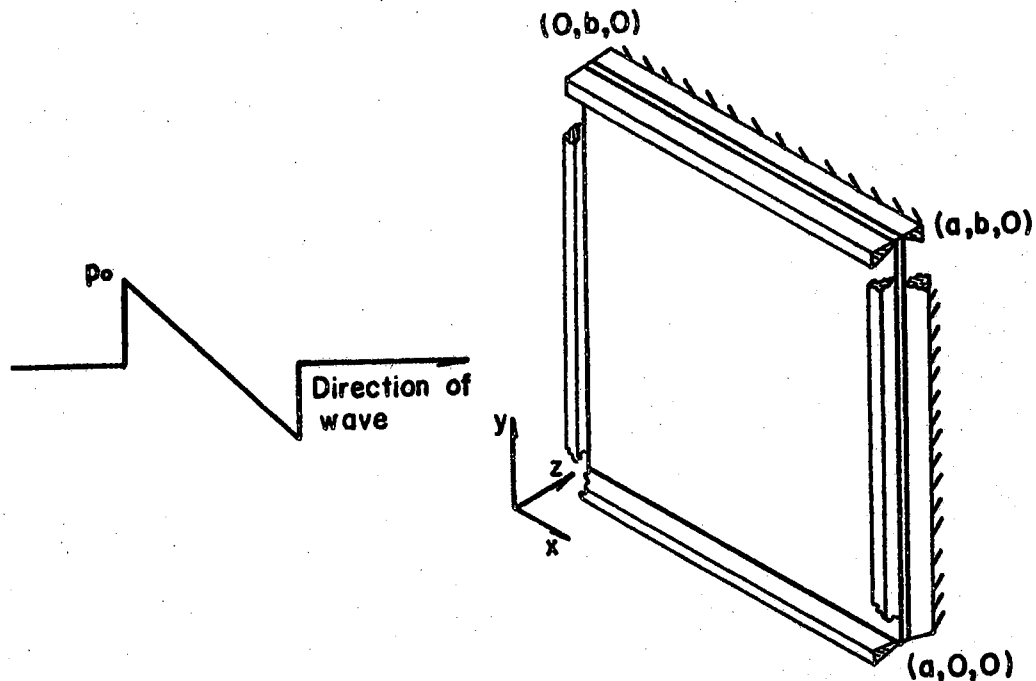
Figure 3. Simply Supported Plate with Transient Input Pressure Pulse

If x and y represent a space coordinate defining a point on the structure, and z is the oscillatory displace-

ment, the equation of motion for the system can be written as,

$$m\ddot{z} + c\dot{z} + D(z) = F(x,y,t) \tag{2-1}$$

where

m = mass of system,

c = damping coefficient,

F(x,y,t) = forcing function,

and D(z) = differential operator,

$$D(z) = \frac{\partial^4 z}{\partial_x^4} + 2\frac{\partial^4 z}{\partial_x^2 \partial_y^2} + \frac{\partial^4 z}{\partial_y^4} \quad \text{for plates.}$$

The normal modes can be found from the equation,

$$m\ddot{z} + D(z) = 0. \tag{2-2}$$

Assuming a solution of the form,

$$z_{rs} = \Phi_{rs}(x,y) e^{i\omega_{rs}t}, \tag{2-3}$$

where

r, s = indexes representing mode numbers,

Φ_{rs} = mode function

ω_{rs} = circular undamped frequency,

and then by substituting the expression (2-3) into (2-2) yields

$$D(\Phi_{rs}) = m\omega^2_{rs} \Phi_{rs}(x,y). \tag{2-4}$$

The mode function Φ_{rs} is orthogonal which indicates that no coupling exists between normal modes and the

relation,

$$\int_0^b \int_0^a m \ \Phi_{rs} \ (x,y) \ \Phi_{uv} \ (x,y) \ dx \ dy$$

$$= \begin{cases} 0 & r \neq u \\ & s \neq v \\ \int_0^b \int_0^a m \ \Phi_{rs}^2 \ dx \ dy & r = u \\ & s = v \end{cases} \qquad (2-5) \ .$$

is satisfied.

If viscous damping is small, then cross coupling between the modes can be neglected, and the relation

$$\int_0^b \int_0^a c \ \Phi_{rs} \ (x,y) \ \Phi_{uv} \ (x,y) \ dx \ dy$$

$$= \begin{cases} 0 & r \neq u \\ & s \neq v \\ 2 \zeta \omega_{rs} \int_0^b \int_0^a m \ \Phi_{rs}^2 \ dx \ dy & r = u \\ & s = v \end{cases} \qquad (2-6)$$

where

ζ = damping factor,

is satisfied.

The assumed solution of (2-1) takes the form

$$z_{rs} \ (x,y,t) = \sum_{r=1}^{\infty} \sum_{s=1}^{\infty} \Phi_{rs} \ (x,y) \ q_{rs}(t) \ , \qquad (2-7)$$

where q_{rs} is the generalized displacement.

Then the differential equation for the panel is given by substituting (2-7) into (2-1) resulting in the following

expression:

$$m \sum_{r=1}^{\infty} \sum_{s=1}^{\infty} \Phi_{rs}(x,y)\,\ddot{q}_{rs} + c \sum_{r=1}^{\infty} \sum_{s=1}^{\infty} \Phi_{rs}(x,y)\,\dot{q}_{rs}$$

$$+ m \sum_{r=1}^{\infty} \sum_{s=1}^{\infty} \omega_{rs}^{2}\,\Phi_{rs}(x,y)\,q_{rs} = F(x,y,t) \,. \qquad (2\text{-}8)$$

Multiplying each side by Φ_{uv} and integrating with respect to x and y, one obtains:

$$\ddot{q}_{rs} + 2\zeta_{rs}\,\omega_{rs}\,\dot{q}_{rs} + \omega_{rs}^{2}\,q_{rs}$$

$$= \frac{1}{M_{rs}} \int_{0}^{b} \int_{0}^{a} F(x,y,t)\,\Phi_{uv}(x,y)\,dx\,dy \quad, \qquad (2\text{-}9)$$

where M_{rs} is the generalized mass and is represented by

$$M_{rs} = \int_{0}^{b} \int_{0}^{a} m\,\Phi_{rs}^{2}(x,y)\,dx\,dy \,. \qquad (2\text{-}10)$$

The damping factor is defined as;

$$\zeta_{rs} = \frac{1}{2\,M_{rs}\,\omega_{rs}} \int_{0}^{b} \int_{0}^{a} c\,\Phi_{rs}^{2}(x,y)\,dx\,dy, \qquad (2\text{-}11)$$

and the generalized force is given by,

$$L_{rs} = \int_{0}^{b} \int_{0}^{a} F(x,y,t)\,\Phi_{rs}(x,y)\,dx\,dy. \qquad (2\text{-}12)$$

Comparing the expression (2-9) with the well-known differential equation of a spring-mass system with viscous damping, one can observe the similarity that enables the multi-degree of freedom system to be analyzed.

The expression for the damped single degree-of-freedom oscillator is,

$$\ddot{x} + 2\zeta_i \omega_i \dot{x} + \omega^2 x = \frac{F(t)}{m} \ .$$ (2-13)

The solution of (2-12) where $F(t)$ is a dirac function, being a pulse of zero time duration and infinite height, is given in almost any advanced text book on vibrations and takes the form,

$$h(t) = \frac{e^{-\zeta_i \omega_i t}}{M_i \omega_i \sqrt{1 - \zeta_i^2}} \ Sin\sqrt{1 - \zeta_i^2} \ \omega t \ .$$ (2-14)

By the use of Duamel's integral sometimes known as the convolution integral, the expression (2-9) can be solved for any force time history $F(x,y,t)$, knowing the solution for the system response given in (2-13). The convolution integral states, that knowing the impulsive response $h(t)$, the response to any arbitrary excitation $f(t)$ is given by the convolution of $f(t)$ and $h(t)$. This is usually noted by

$$x(t) = h(t) * f(t) = \int_0^t h(t - \Psi) \ f(\Psi) \ d\Psi \ .$$ (2-15)

Ψ is a dummy variable.

The generalized displacement $q_{rs}(t)$, is given by the expression,

$$q_{rs}(t) = \int_0^t \int_0^b \int_0^a L_{rs}(\Psi) \, h_{rs}(t - \Psi) \Phi_{rs}(x,y) dx \, dy \, d\Psi. \quad (2\text{-}16)$$

The mode function Φ_{rs} for a simply supported panel is

$$\Phi_{rs}(x,y) = \text{Sin} \frac{r\pi x}{a} \text{Sin} \frac{s\pi y}{b} . \quad (2\text{-}17)$$

This mode function enables the boundary conditions, of deflection equal to zero at x=0, x=a, y=0, y=b, and the moments equal to zero at x=0, x=a, y=0, y=b, or mathematically stated,

$$Z_{rs}(t) = 0 \qquad \text{at} \qquad x=0, \ x=a$$
$$\qquad\qquad\qquad\qquad y=0, \ y=b$$
$$\frac{\partial^2 Z_{rs}}{\partial x^2} = 0 \qquad \text{at} \qquad x=0, \ x=a \qquad\qquad (2\text{-}18)$$
$$\frac{\partial^2 Z_{rs}}{\partial y^2} = 0 \qquad \text{at} \qquad y=0, \ y=b .$$

The strains in the x-direction and y-direction from the theory of elasticity (see reference 3) can be expressed by,

$$\epsilon_x = \frac{-h}{2} \frac{\partial^2}{\partial x^2} [Z_{rs}(t)] \qquad\qquad (2\text{-}19)$$

and

$$\epsilon_y = \frac{-h}{2} \frac{\partial^2}{\partial y^2} [Z_{rs}(t)] . \qquad\qquad (2\text{-}20)$$

The resulting stress in the x and y directions are,

$$\sigma_x(x,y,t) = \frac{E}{1-\mu^2} [\epsilon_x + \mu\epsilon_y] \qquad (2\text{-}21)$$

and

$$\sigma_y(x,y,t) = \frac{E}{1-\mu^2} [\epsilon_y + \mu\epsilon_x] \quad . \qquad (2\text{-}22)$$

The Transient Input

The idealized N-wave pressure signatures, shown in Figure 2 , can be described,
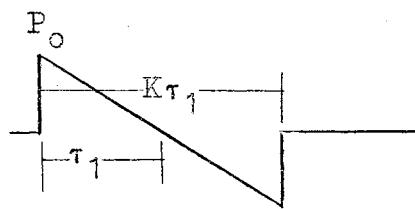
$$P = 0 \quad \text{for} \quad t < 0$$

$$P = P_o(1 - \frac{t}{\tau_1}) \quad \text{for } 0 < t \leq K\tau_1$$

$$P = 0 \quad \text{for } K\tau_1 < t \quad . \qquad (2\text{-}23)$$

For a symmetrical N-wave, K = 2.0.

The generalized displacement for the forcing time era,

$$0 < t < K\tau_1$$

$$q_{rs}(t) = \int_o^t \int_o^b \int_o^a \frac{P_o}{M_{rs}\omega_{dr}} (1 - \frac{\Psi}{\tau_1}) \ e^{\frac{-C_{rs}(t-\Psi)}{2M_{rs}}}$$

$$\qquad (2\text{-}24)$$

$$\cdot \text{Sin} \frac{r\pi x}{a} \text{ Sin} \frac{s\pi y}{b} \text{ Sin } \omega_{dr}(t-\Psi) \ dx \ dy \ d\Psi$$

and for the residual time era,

$$K\tau_1 < t$$

$$q_{rs}(t) = \int_0^{K\tau_1} \int_0^b \int_0^a \frac{P_0}{M_{rs}\,\omega_{dr}} \left(1 - \frac{\Psi}{\tau_1}\right) e^{\frac{-C_{rs}(t-\Psi)}{2M_{rs}}}$$

(2-25)

$$\cdot \text{Sin} \frac{r\pi x}{a} \text{Sin} \frac{s\pi y}{b} \text{Sin } \omega_{dr}(t-\Psi) \, dx \, dy \, d\Psi \, .$$

Note: Ψ is a dummy variable for the time integration.

If the damping is zero, i.e., $C_{rs} = 0$, the expressions are simplified and integration yields, for the forced time era;

$$0 < t \leq K\tau_1$$

(2-26)

$$q_{rs}(t) = \frac{4abP_0}{rs\pi^2 M_{rs}\omega_{rs}^2} \left[1 - \frac{t}{\tau_1} - \text{Cos } \omega_{rs}t + \frac{\text{Sin } \omega_{rs}t}{\tau_1\,\omega_{rs}}\right] ,$$

and for the residual era:

$$K\tau_1 < t$$

$$q_{rs}(t) = \frac{4ab\,P_0}{rs\pi^2 M_{rs}\,\omega_{rs}^2} \left\{ (1-K)\,\text{Cos }[\omega_{rs}(K\tau_1 - t)] \right.$$

$$+ \frac{\text{Sin}}{\tau_1\omega_{rs}} [\omega_{rs}(K\tau_1 - t)] - \text{Cos } \omega_{rs}t$$

$$\left. + \frac{\text{Sin } \omega_{rs}t}{\omega_{rs}\tau_1} \right\} .$$

(2-27)

The expressions (2-22) and (2-23) with the damping coefficient included can be integrated without an undue amount of labor, if they are first expanded using trigonometric identies. The algebraic manipulations are tedious, and it

does not appear to be extremely useful to non-dimensionalize the expressions.

The resulting integration of expressions (2-22) and (2-23), yield (2-28) and (2-29). Although the following expressions may not appear in their simplest form, nevertheless, they lend themselves to easy numerical computations on the digital computer. The displacement for the time interval,

$$0 < t \leq K\tau_1 \qquad (2-28)$$

$$q_{rs}(t) = \frac{4abP_o}{rs\pi^2 M_{rs} \omega_{dr}} \left\{ e^{-\alpha t} \quad \text{Sin } \omega_{dr}t \left[\frac{e^{\alpha t}}{\alpha^2 + \omega_{dr}^2} \right. \right.$$

$$\left. (\alpha \text{ Cos } \omega_{dr}t + \omega_{dr} \text{ Sin } \omega_{dr}t) - \frac{\alpha}{\alpha^2 + \omega_{dr}^2} \right]$$

$$- \text{ Cos } \omega_{dr}t \left[\frac{e^{\alpha t}}{\alpha^2 + \omega_{dr}^2} (\alpha \text{ Sin } \omega_{dr}t - \omega_{dr} \text{ Cos } \omega_{dr}t) \right]$$

$$- \frac{\text{Sin } \omega_{dr}t}{\tau_1} \left[\left[\frac{t e^{\alpha t}}{\alpha^2 + \omega_{dr}^2} (\alpha \text{ Cos } \omega_{dr}t + \omega_{dr} \text{ Sin } \omega_{dr}t) \right] \right.$$

$$- \frac{e^{\alpha t}}{\alpha^2 + \omega_{dr}^2} \left[(\alpha^2 - \omega_{dr}^2) \text{ Cos } \omega_{dr}t + 2\alpha\omega_{dr} \text{ Sin } \omega_{dr}t \right]$$

$$\left. - \frac{(\alpha^2 - \omega_{dr}^2)}{(\alpha^2 + \omega_{dr}^2)^2} \right] + \frac{\text{Cos } \omega_{dr}t}{\tau_1} \left[\frac{t e^{\alpha t}}{\alpha^2 + \omega_{dr}^2} (\alpha \text{ Sin } \omega_{dr}t \right.$$

$$\left. - \omega_{dr} \text{ Cos } \omega_{dr}t) - \frac{e^{\alpha t}}{(\alpha^2 + \omega_{dr}^2)^2} \left[(\alpha^2 - \omega_{dr}^2) \cdot \right. \right.$$

$$\text{Sin } \omega_{dr}t - 2 \alpha\omega_{dr} \text{ Cos } \omega_{dr}t\Big]\Big]\Big\}$$

For the residual time era;

$$K\tau_1 < t \tag{2-29}$$

$$q_{rs}(t) = \frac{4ab\ P_0 e^{-\alpha t}}{rs\pi^2 M_{rs}\omega_{dr}} \left\{ \text{Sin } \omega_{dr}t \left[\frac{e^{\alpha K\tau_1}}{\alpha^2 + \omega_{dr}^2} \cdot \right.\right.$$

$$\left. (\alpha \text{ Cos } \omega_{dr}K\tau_1 + \omega_{dr} \text{ Sin } \omega_{dr}K\tau_1) - \frac{\alpha}{\alpha^2 + \omega_{dr}^2} \right]$$

$$- \text{ Cos } \omega_{dr}t \left[\frac{e^{\alpha K\tau_1}}{\alpha^2 + \omega_{dr}^2} (\alpha \text{ Sin } \omega_{dr}K\tau_1 - \omega_{dr} \text{ Cos } \omega_{dr}K\tau_1) \right.$$

$$\left. + \frac{\omega_{dr}}{\alpha^2 + \omega_{dr}^2} \right] - \frac{\text{Sin } \omega_{dr}t}{\tau_1} \left[\left[\frac{K\tau_1 e^{\alpha K\tau_1}}{\alpha^2 + \omega_{dr}^2} (\alpha \text{ Cos } \omega_{dr}K\tau_1 \right.\right.$$

$$\left. + \omega_{dr} \text{ Sin } \omega_{dr}K\tau_1) \right] - \frac{e^{\alpha K\tau_1}}{(\alpha^2 + \omega_{dr}^2)^2} \left[(\alpha^2 - \omega_{dr}^2) \cdot \right.$$

$$\left. \text{Cos } \omega_{dr}K\tau_1 + 2\alpha\ \omega_{dr} \text{ Sin } \omega_{dr}K\tau_1 \right] + \frac{\alpha^2 - \omega_{dr}^2}{(\alpha^2 + \omega_{dr}^2)^2} \right]$$

$$+ \frac{\text{Cos } \omega_{dr}t}{\tau_1} \left[\frac{K\tau_1 e^{\alpha K\tau_1}}{\alpha^2 + \omega_{dr}^2} (\alpha \text{ Sin } \omega_{dr}K\tau_1 - \omega_{dr} \text{ Cos } \omega_{dr}K\tau_1) \right.$$

$$- \frac{e^{\alpha K\tau_1}}{(\alpha^2 + \omega_{dr}^2)^2} \left[(\alpha^2 - \omega_{dr}^2) \text{ Sin } \omega_{dr}K\tau_1 \right.$$

$$\left. - 2\alpha \ \omega_{dr} \ \text{Cos} \ \omega_{dr} \ K\tau_1 \right] - \frac{2\alpha \ \omega_{dr}}{(\alpha^2 + \omega_{dr}^2)^2} \right] \right\}$$

Displacement and Stress Modal Participation
Factors for the Transient N-wave

It is well known that the dynamic response of a multi-degree of freedom system or a distributed system can be described as the sum of products; (normal mode shape) X (corresponding dynamic response function). Furthermore, if the loading function is spacewise constant, then the sum of the products takes the form,

$$\sum_{i=1}^{\infty} \sum_{j=1}^{\infty} \left[\begin{array}{c} \text{Contribution of the } i^{th}, j^{th} \\ \text{mode} \end{array} \right] \times \left[\begin{array}{c} i^{th}, j^{th} \text{ dynamic re-} \\ \text{sponse function} \end{array} \right].$$

A quantitative examination of the contribution of the higher modes for the transient response of the panel to a N-wave is performed. The displacement and stress modal participation factors are computed by using the expression given previously. The stress modal participation factor is given as the relative contribution of that particular mode to the maximum dynamic stress to the fundamental mode for the transient N-wave. The stress modal participation factor will not necessarily be of the same magnitude as the corresponding participation factor for the displacement response.

Table I is a tabulation of the stress modal participation factors for the simply supported plate with a N-wave

of $\tau = T$, and shows distinctly why a fundamental mode assumption is a valid assumption for idealizing the dynamic system.

The contributions of the higher modes can be examined in different ways. Investigators have stated that higher modes cannot be neglected in analysis of panel stresses (10). The stress modal participation factors are admittedly higher than the corresponding displacement factors. Mode shapes such as the 3,7 and the 3,9 contribute as much as 3 per cent to the stress amplitude. However, these two modes have a sign reversal and tend to cancel themselves. Analytical work on the transient response of a panel of a necessity has to be performed on the digital computer. To compute the displacement for a given point (x,y) using expressions (2-28) and (2-29) for a given time t is a tedious chore. A detailed time history would require numerous points and would be extremely time consuming. A convenient and practical method is to analyze the number of modes, stopping at even numbers, such as 3,3 or 5,5 or 9,9. An analysis of the transient response to the N-wave and considering the first 25 modes, the error in the maximum displacement is less than 1 per cent and the corresponding maximum stress, less than 3 per cent. This is for the aspect ratio $(\frac{b}{a})=1.0$ and could vary somewhat for very small or very large ratios. A difference of less than 3 per cent in the maximum stress certainly would justify a fundamental mode assumption.

TABLE I

DYNAMIC MODAL CONTRIBUTION FACTORS FOR TRANSIENT N-WAVE

Displacement	Stress	Mode
1.0000000	1.0000000	1,1
+.0020900	+.0165000	1,3
-.0008300	+.0091500	1,5
+.0000146	+.0091500	1,7
-.0000146	-.0027450	1,9
-.0042900	-.0082300	3,1
+.0001192	+.0110000	3,3
-.0002330	-.0000920	3,5
-.0000146	-.0302000	3,7
-.0001455	+.0283500	3,9
+.0001162	+.0027400	5,1
-.0000874	-.0027400	5,3
+.	+.0055000	5,5
+.0000291	+.0338000	5,7
+.0000146	-.0320000	5,9
+.0000437	+.0009150	7,1
-.0000582	-.0018300	7,3
+.0000146	+.0018300	7,5
+.0000146	-.1189000	7,7
-.0000146	+.0027460	7,9
+.0000146	-.0082400	9,1
+.	+.0002015	9,3
+.0000146	+.0001920	9,5
+.	+.0005315	9,7
+.0000146	-.0004760	9,9

Total deviation of 25 modes as compared to fundamental mode only, b/a = 1.0

.3%   2.42%

CHAPTER III

ANALOG COMPUTER SIMULATION OF A PANEL
COUPLED TO THE RESONATOR

The use of a mathematical model to predict the response
or the performance of a physical system is desirable because
of the ease and speed of obtaining results. The analog
computer offers a means for obtaining an accurate and fast
solution of simultaneous differential equations. The
analog computer is also very effective for examining
parameter changes in the mathematical model.

The lumped parameter idealization of the system repre-
sents the air in the neck of the resonator as a mass, the
air in the cavity volume as a spring, and the inclusion of
a viscous damper associated with the energy dissipation of
the resonator. The panel was represented in a similar
fashion, having mass, stiffness and damping.

The differential equations derived from the lumped
parameter system that governs the motion of the system is
based on the schematic diagram in Figure 4. The following
assumptions are applicable:

1. The panel is represented by the contribution
    of the fundamental mode of vibration. This
    assumption hardly involves any error in the

displacement-time response, but it will be shown
later that the stress response will be in error
by about 3 per cent when compared to the response
using a 25 mode contribution.

2. Undamped, uncoupled, natural frequencies of both
the panel and the resonator, are preserved in
the calculation of an equivalent mass and an
equivalent lumped parameter model is shown in
Appendix A.

3. The damping coefficients for the resonator (C_r)
and for the panel (C_p) used in the analysis, were
obtained experimentally as outlined in Chapter V.

4. The lumped parameter model serves as an adequate
representation for describing the response of
the system on the basis of the reduction to an
equivalent system as demonstrated in Appendix A.
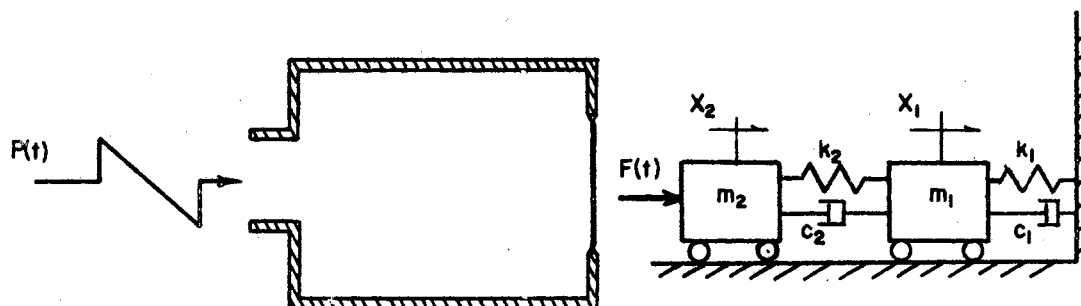
Figure 4. Lumped Parameter Idealization of Panel
Coupled to the Resonator

The differential equations governing the motion of the system can be obtained by the use of Newton's laws:

$$m_a \frac{d^2 x_2}{dt^2} + C_r \frac{dx_2}{dt} + k_r x_2 - k_r x_1 - C_r \frac{dx_1}{dt} = F(t) \qquad (3\text{-}A)$$

$$m_p \frac{d^2 x_1}{dt^2} + (C_p + C_r) \frac{dx_1}{dt} + (k_r + k_p) x_1 - k_r x_2$$

$$- \frac{C_r dx_2}{dt} = 0 \qquad (3\text{-}B)$$

where

m_a = mass of air in neck of resonator

k_r = stiffness of air in resonator

C_r = damping of resonator

m_p = equivalent mass of panel

k_p = equivalent spring constant of plate

C_p = equivalent damping of plate

$F(t)$ = forcing function (N-wave).

Expressions (3-A) and (3-B) are linear, simultaneous, equations which are readily solvable for both the transient and steady state solution if the forcing function $F(t)$ is of a simple form. By use of operator calculus, one can obtain a closed form for the solution and solve for the response of x_1 or x_2 as a function of time. The solution of the equations (3-A) and (3-B) when $F(t)$ is in the form of a N-wave is extremely complex and time consuming.

The analog computer is a useful tool for solving the differential equations if the forcing input can be generated electronically. Equations 3-A and 3-B are written in standard

form for insertion in the analog computer, by solving for the highest order derivative of the principal variable in each equation. The second derivative of x_1 and x_2 are separated in each equation. The revised equations are;

$$\frac{d^2x_2}{dt^2} = \frac{-C_r}{m_a} \frac{dx_2}{dt} - \frac{k_r x_2}{m_a} + \frac{k_r x_1}{m_a} + \frac{C_r}{m_a} \frac{dx_1}{dt} + \frac{F(t)}{m_a} \qquad (3\text{-}C)$$

$$\frac{d^2x_1}{dt^2} = \frac{-(C_p + C_r)}{M_p} \frac{dx_1}{dt} - \frac{(k_r + k_p)}{m_p} + \frac{k_r x_2}{m_p} + \frac{C_r}{m_p} \frac{dx_2}{dt}. \qquad (3\text{-}D)$$

Scaling of the equations so the computer time was 100 times the real time results in the following expressions:

$$10^{-4}\ddot{x}_2 = -.0092833\dot{x}_2 - 84.444x_2 + 184.444x_1$$
$$+ .009283\dot{x}_1 + 2.0868F(t) \qquad (3\text{-}E)$$

$$10^{-4}\ddot{x}_1 = -.006929\dot{x}_1 - 50.0424x_1 + 10.7268x_2$$
$$+ .001179\dot{x}_2 . \qquad (3\text{-}F)$$

A N-wave forcing input on the lower mass of the system was achieved utilizing an integrator, a clock, a comparator, and a relay. A constant voltage was integrated as the clock started running at zero. This integrated voltage was constantly monitored by a comparator. As the voltage reached a preset value, set on the comparator, the relay was energized cutting off the integrator and applying a step voltage which enabled the system to return to zero voltage. The generated N-wave could be varied to any height, slope,

or time duration, within the limits of the scaled equations.

Calculated system constants appropriate to the lumped parameter analysis were set on the computer, and the forcing function applied. The time response of the computer model was observed and recorded on a x-y plotter. Displacement, velocity, or acceleration could be obtained. Figure 25 is a typical recorded trace.

The upper portion of the mathematical two degree-of-freedom was represented by fixed parameters. The experimental objectives were to investigate primarily one panel configuration; thus k_1 and m_1 were held constant. The frequency of the lower system was changed by altering the parameters, k_2 and m_2. In the experimental apparatus the mass of air in the resonator depended on the size of the neck. Plots shown in Figures 5 and 6 were obtained using the mass of the air in the specific neck, that was used in the experimentation.

Indicial response of the two degree-of-freedom system is shown in Figure 5. The ratio of the frequency of the lower portion of system to the upper portion is not sharply tuned and as long as this ratio is approximately 1.2 to 1.3, the response of the upper mass is significant.

The computer was then set at the values for the frequency ratio obtained above, and a series of N-waves were used to excite the lower mass. The time duration of the N-wave was varied for each run.

Figure 6 is a plot of the response of the mass m_1

referenced to the static displacement, and the variation of

the forcing period referenced to the natural period of

the lower portion. An arbitrary parameter τ_{12} is plotted

in Figure 6 as the horizontal axis.

This study is not an all inclusive parametric study.
To completely encompass every possible variation of the
parameters is a laborious procedure, and probably would
not yield any more conclusive information than what was
obtained. The analysis was limited, in the respect that
the size of the panel had dictated the type and size of
resonator. The analog study produced plots of the time
response for the various time ratios of the N-wave. The
main contribution of the analog work to this investigation
was the predicted time response plots of the transient
response of the system. This enabled an experimental veri-
fication and a comparison with the idealized model response.
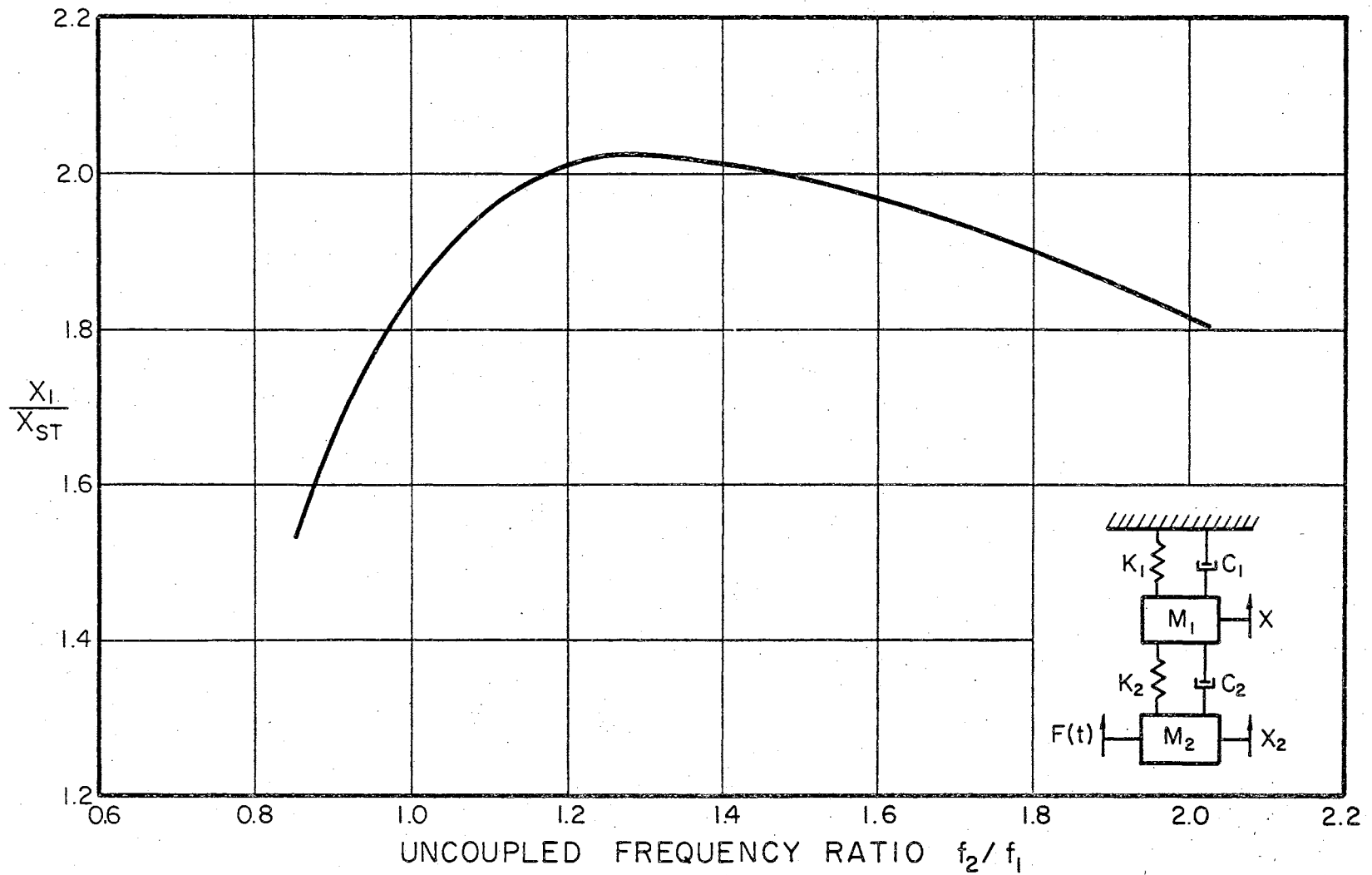
Figure 5. Frequency Effect on Indicial Response of Upper Mass
$\zeta_1 = \zeta_2 = 0.005$
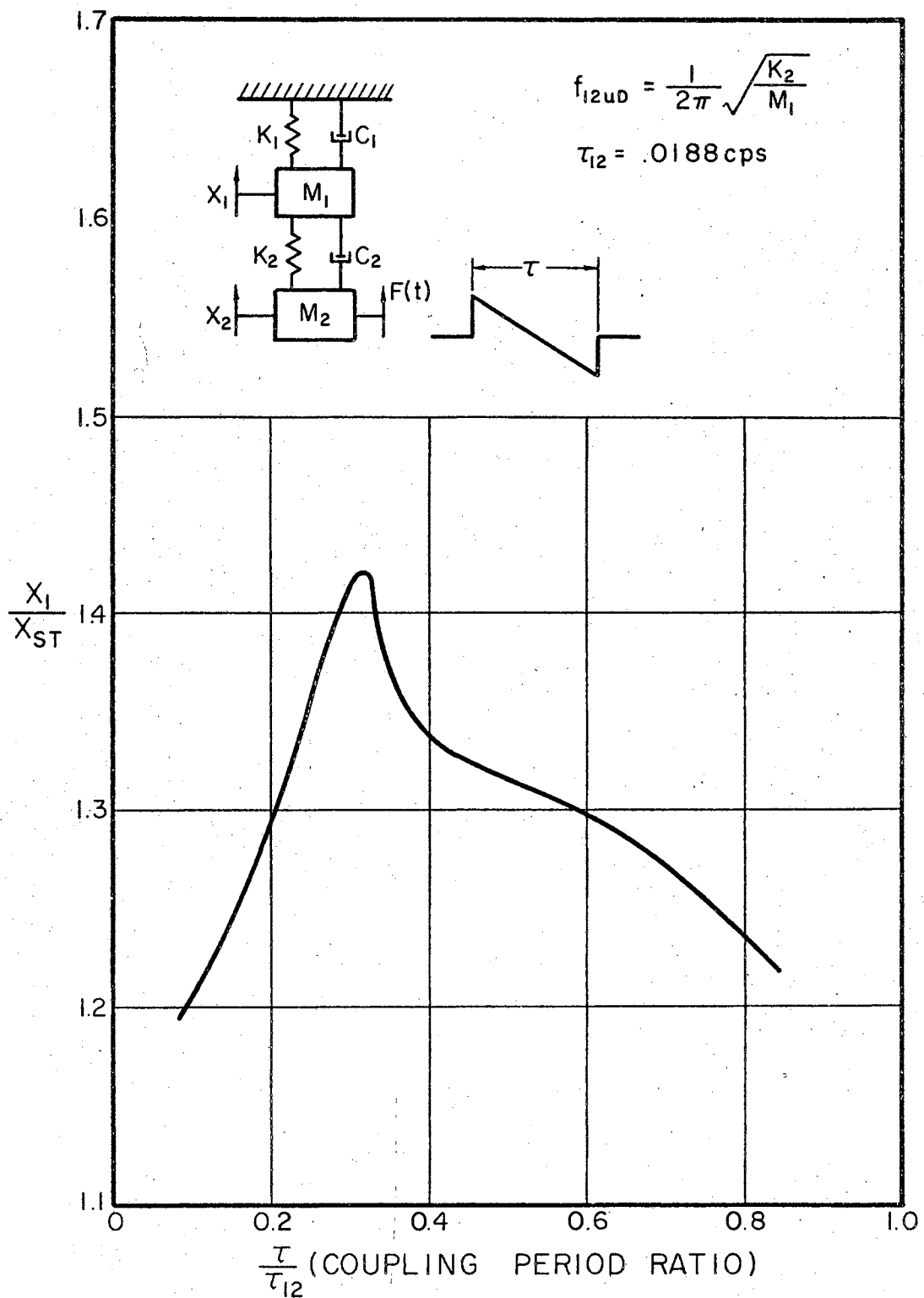
Figure 6. Forcing Duration Effect on Upper Mass $\dfrac{f_2}{f_1} = 1.25$, $\zeta_1 = \zeta_2 = 0.05$

CHAPTER IV

EXPERIMENTAL APPARATUS AND INSTRUMENTATION

An experimental model was designed and constructed to
test the validity of the predicted panel response. The
model was designed to enable testing of, (a) the panel in
a baffle and, (b) a panel in the wall of the Helmholtz
resonator, with a minimum amount of work in changing from
one configuration to the other. The size of the test
resonator was dictated by the frequency of the panel. The
frequency of the resonator was varied by changing the depth
of the cavity.

Simply Supported Panel

A panel 9x9x0.041 inches was constructed from sheet
aluminum. The panel was mounted on knife edges to achieve
the simply supported edge conditions. Difficulty in
achieving absolute moment free edge conditions occurred
when the panel was tightened to eliminate air leakage
around the periphery. The panel was mounted in the baffle
in the manner illustrated in Figure 7 and Figure 8. The
baffle was mounted at the termination of an acoustic delay
line, which was pulsed by an electronic generating device.
The baffle was moved a short distance from the end of the
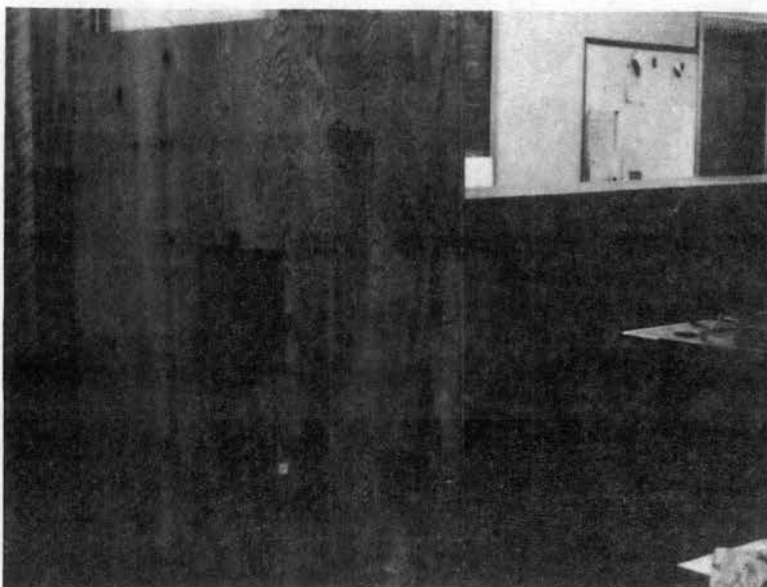
Figure 7. Panel Mounting With Associated
Instrumentation
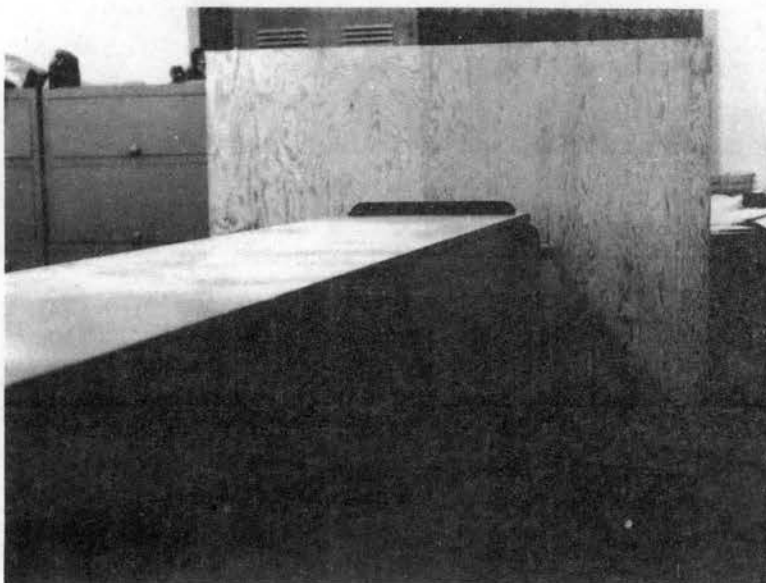
Figure 8. Panel Mounted at Termination of
Plane Wave Tube

tube, to eliminate the loading effect of the tube. This termination offset minimized the loading effect on the driving system, and caused a negligible effect on the acoustic input to the panel. A semiconductor strain gauge mounted at the center of the panel was used to measure the center strain.

The Plane Wave Tube

The plane wave tube, used as the intermediate device in the mechanical acoustical testing apparatus, consisted of a 32 ft. tube of about 200 in^2 cross sectional area. The pressures over the cross section at the end of the tube were uniform. The entire driving aparatus is shown in Figure 9. The driving device, a 12 inch loudspeaker, performed adequately in the range 80-175 cps over which the tests were conducted. Transient response of the speaker prevented an exact simulation of the desired pressure pulse. However, simulation was close and was enhanced by its' excellent reproducability.

Test Resonator

The test resonator was constructed from a tube of inside diameter 11.5 inches and wall thickness of $\frac{1}{4}$-inch. Different resonator lengths were obtained by varying the position of a O-ringed plug inside the tube as illustrated in Figure 10. The panel was mounted at the termination of the resonator using the same support conditions as were
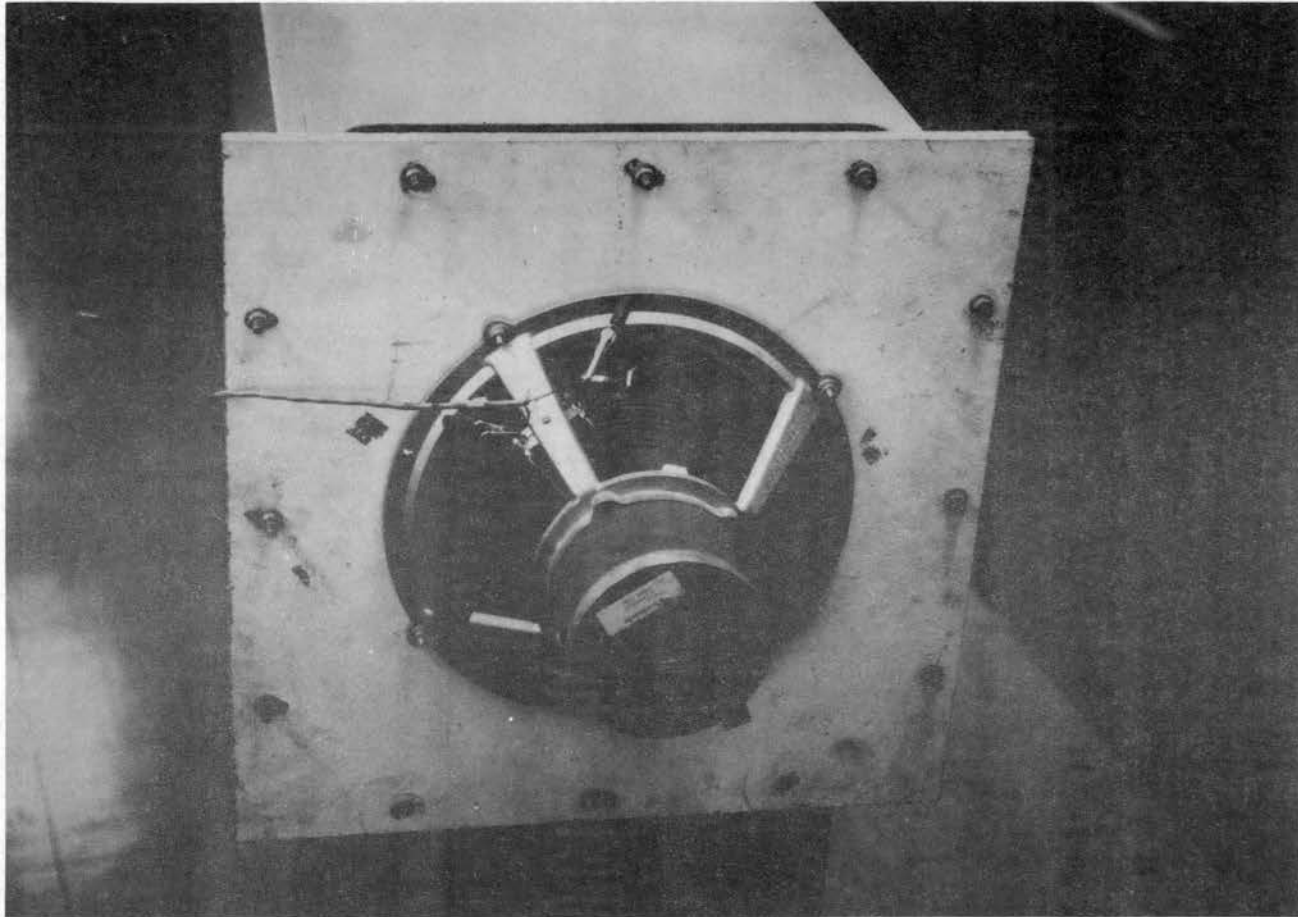
Figure 9. Loudspeaker Used as a Driving Unit on 32 Foot
Plane Wave Tube
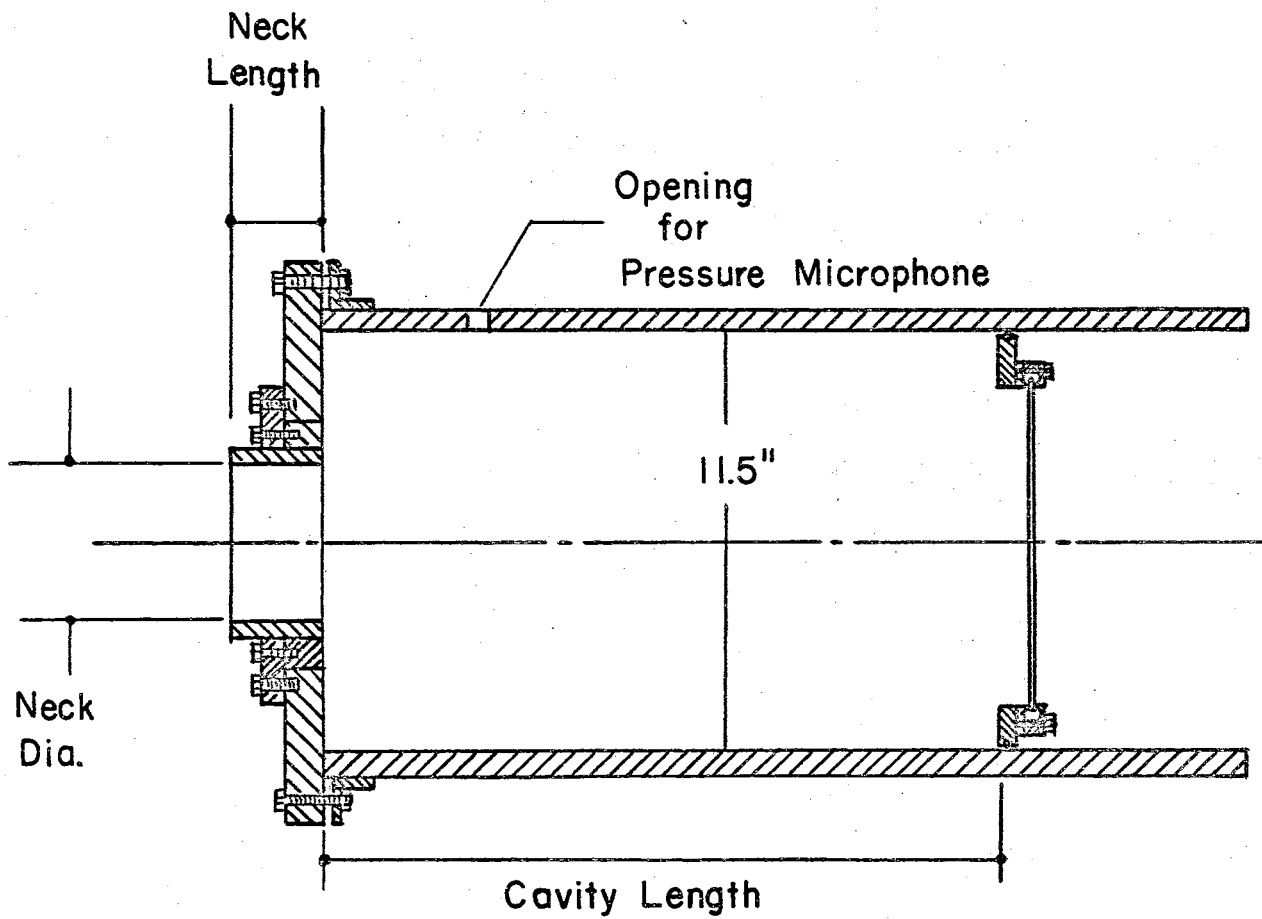
Figure 10. Cross-Sectional View of Plate-Resonator Coupled
Configuration Used in Testing

used in the baffled case. Condenser microphones were used
at three different locations in the resonator to measure
pressure magnitudes. A photographic view of the test
resonator showing the pressure microphones is illustrated
in Figure 11.

Pressure Variations Inside the Test Resonator

It has been found that the operating frequency above
which the Helmholtz resonator does not behave as a simple
system, should be such that the wave length of the incoming
sound is sixteen times the characteristic dimension of the
cavity (3,21). Figure 12 shows a typical recorded trace of
input and cavity pressures.

The reason for the restriction on the wave length is to
insure that the higher modes are not excited. A wave length
of incoming sound two to three times the characteristic
dimension would be cause for concern. However, experimental
results for incoming sound of wave length eight times the
characteristic dimension of the cavity showed very little
deviations in pressure at various points in the resonator.
Figure 13 displays recordings of three pressure microphones
located inside the resonator. The microphones were placed
at (a) in the rear of the cavity, (b) four inches from the
neck, and, (c) eight inches from the neck at a 90 degree
rotation from the microphone nearest the neck. The transient
input signal for this recording was a N-wave of wave length
approximately eight times the largest dimension of the cavity.

Pressure Microphones
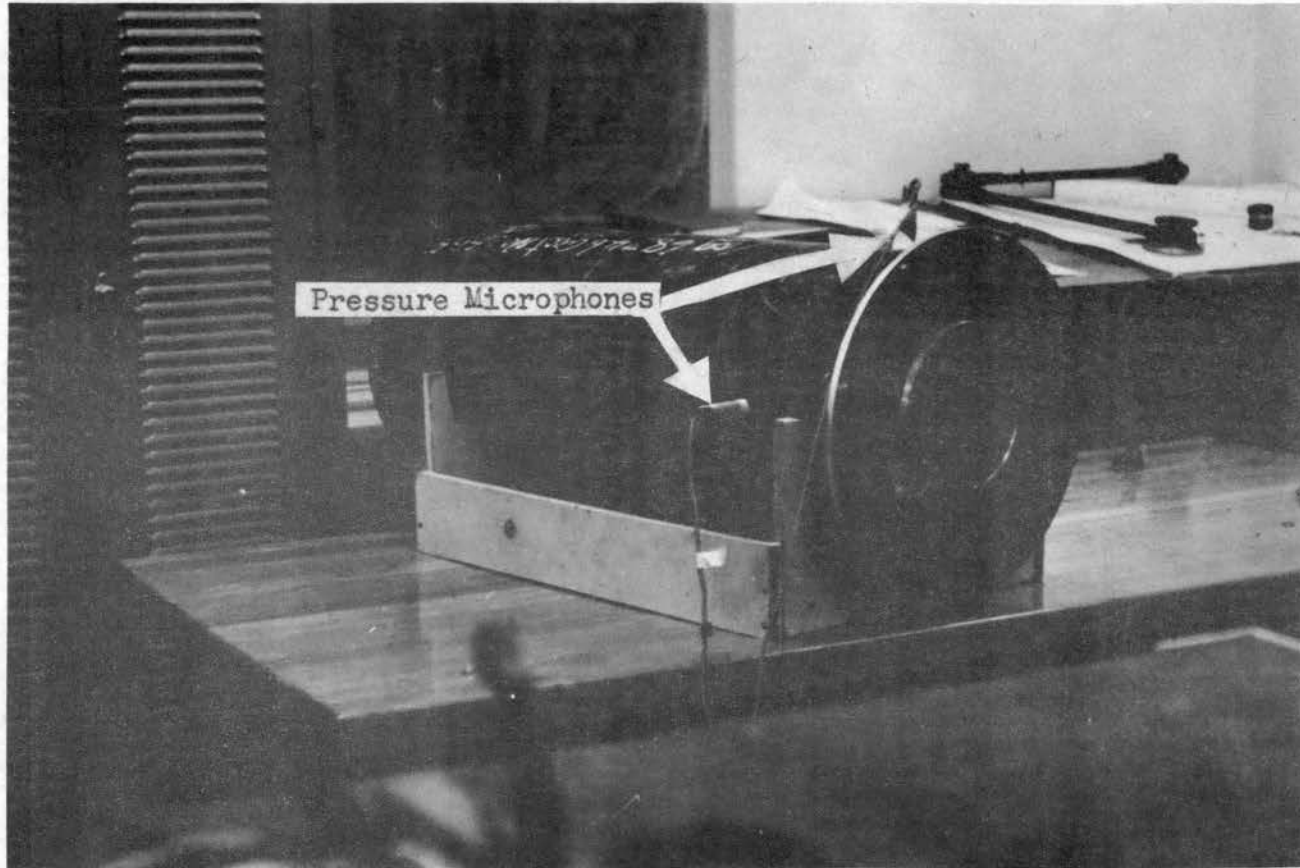
Figure 11. Test Resonator Showing Pressure Microphones
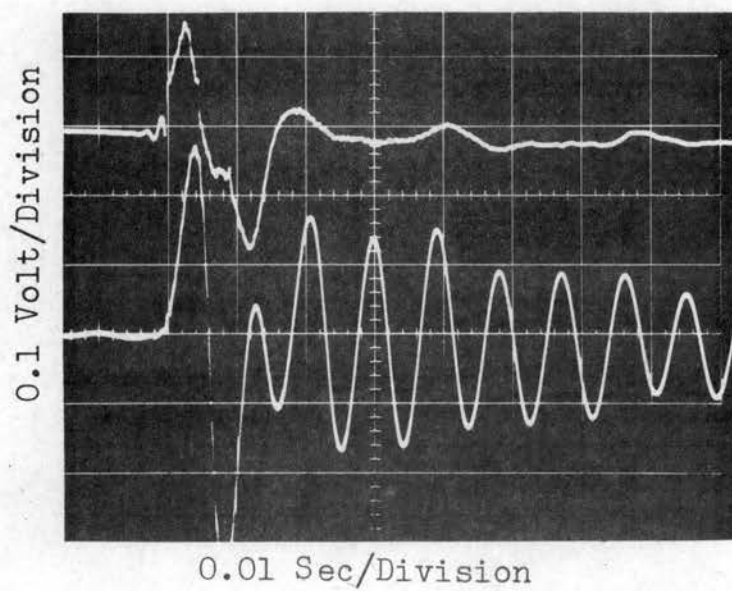
Figure 12.   Typical Trace Showing N-wave
Input and Cavity Response
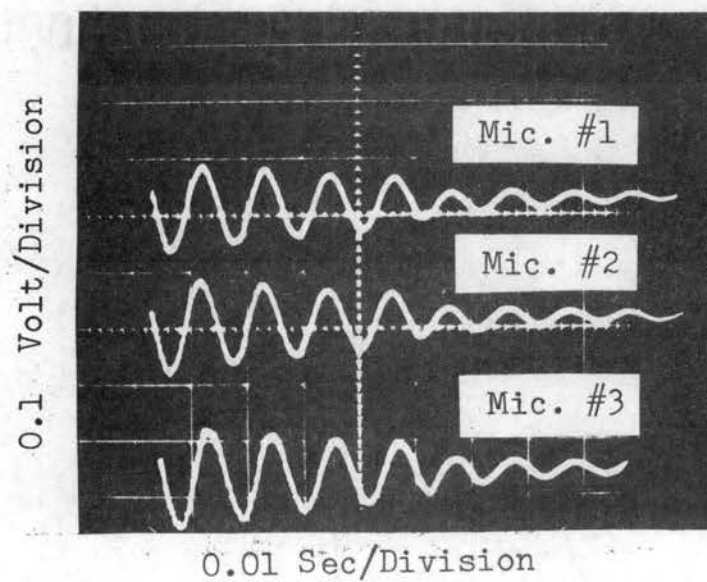
Figure 13.   Pressure Recordings at Three
Different Locations Inside
the Resonator

Measured pressures had less than 5 per cent variation. The readings were compared with the referenced sensitivities given in Table IV, Appendix B.

Electronic Pulse Generating Apparatus

The pulse generating mechanism was essentially that of Simpson (24) with minor modifications. Input frequencies were in the region in which the driving system responded well to the transient pulse. Typical traces of the generated pulse are displayed in Figures 14 and 15.

The difficulty encountered in attempting to generate the N-wave pressure pulse was mainly due to the response of the speaker system. A N-wave can be developed by many methods, and poses no large problem (6). Actual sonic boom pressure signatures can be recorded by means of a good magnetic tape, and can be accurate providing the frequency response of the recording apparatus is sufficiently good to preserve the low frequency signals. Difficulty arises when the recorded trace is affected directly by the output of the generating device. The loudspeaker, being a second order system, will not respond identically to the form of the transient N-wave. Second order systems must have finite rise time, thus creating an error in the reproduction of the N-wave pulse.

The pulse generating equipment and monitoring devices used in the experimental work are illustrated in Figure 16. A sawtooth wave generator was used as the primary driving

0.1 Volt/Division

0.01 Sec/Division
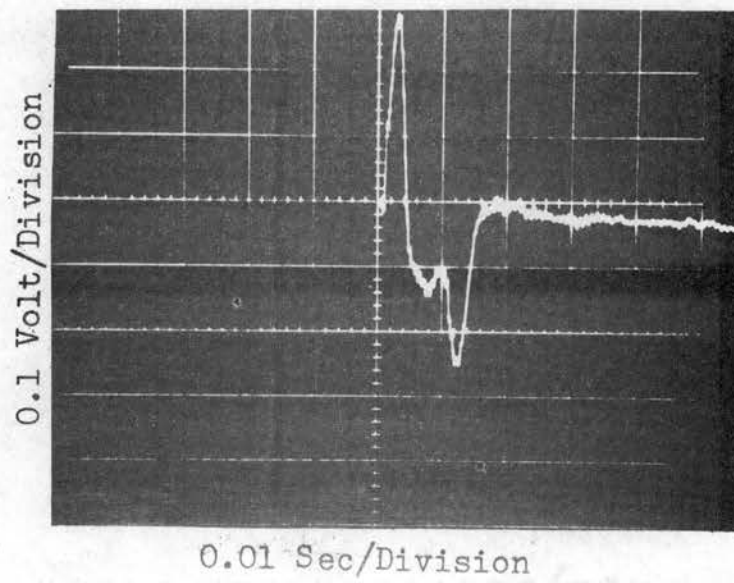
Figure 14. N-wave Pulse Generated
at 100 cps

0.1 Volt/Division

0.005 Sec/Division
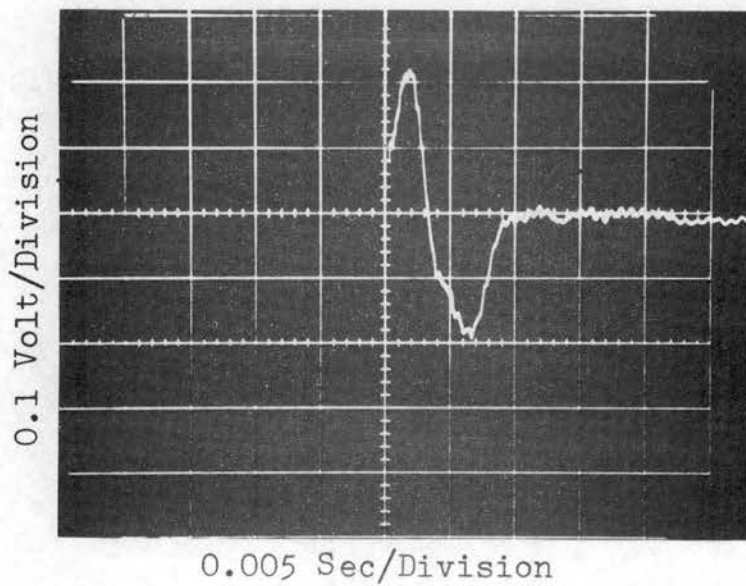
Figure 15. N-wave Pulse Generated
at 167 cps
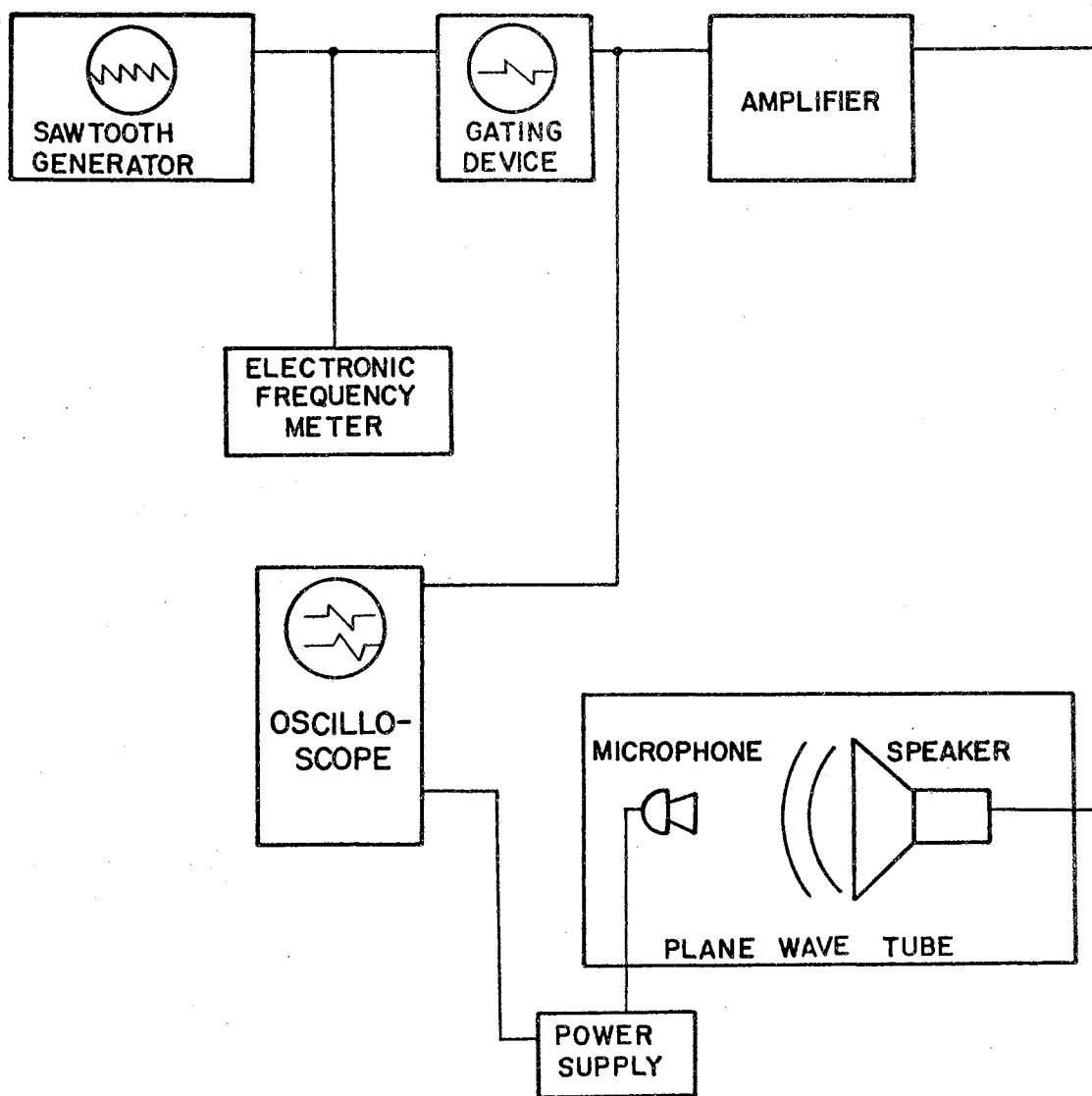
Figure 16. Block Diagram of Pulse Generating Equipment and Monitoring Devices

device and its output was fed into a gating device which
enabled the aperiodic N-wave pulse to be developed. The
shape of the N-wave was altered by means of a d-c bias.
Signal shape was varied to compensate for discrepancies in
the response of the loudspeaker. The correct wave form
was achieved by monitoring the output of the loudspeaker
with a condenser microphone and altering the bias on the
gating device.

Transient pulse generation by the preceding method
proved excellent, being both economical and repeatable.
The time base can be altered and monitored on the counter.
The height of the signal can be varied, both at the sawtooth
generator, and at the output of the amplifier. Shaping of
the pulse can be accomplished by the bias at the gating
network. Elaborate generating devices could be designed
to control the output of the loudspeaker, but any system
that is to accurately reproduce a transient signal will be
limited by the transient response of the driving transducer.

The Strain Gauge Instrumentation

The strain sensing device and its' associated circuitry
were the most sensitive portions of the entire instrumentation
setup.

A semiconductor micro-miniature strain gauge was used
as the primary sensing device. This gauge is one of the most
sensitive devices of this type that is manufactured. Semi-
conductor gauges are distinguished from the conventional foil

gauge principally by their high gauge factors. The higher
the gauge factor, the greater is the possible output with
conventional strain gauge circuitry. The gauge is fabri-
cated from single-crystal silicon. It exhibited very good
dynamic properties, thermal stability and linear per-
formance. The range over which the strains were measured
were well below the recommended range for the gauge.
Recorded strains at the one micro-inch/inch level are
reliable and accurate providing proper calibration pro-
cedure is followed. The instrumentation setup and cali-
bration procedure are described in Appendix B.

A tedious and time consuming procedure is necessary
in mounting the strain gauge. Figure 17 illustrates the size
of the gauge. Difficulty arises while attempting to solder
the leads to the terminals, as there is only 0.02 inch
separating the points in which the wires must be soldered.

A bridge amplifier meter was used in a two gauge
configuration, with the second gauge serving as a dummy
gauge. The amplifier provided the initial amplification
in the circuitry. The output of the bridge was fed into a
fixed gain amplifier, and subsequently into the recording
device. A block diagram of this arrangement is illustrated
in Figure 18. A digital voltmeter was used to insure that
the bridge remained balanced.

The recording device was an ultra-violet galvonometer
recorder, with fluid damped galvonometers. Damping was
such that overshoot to a step input was about 5 per cent.
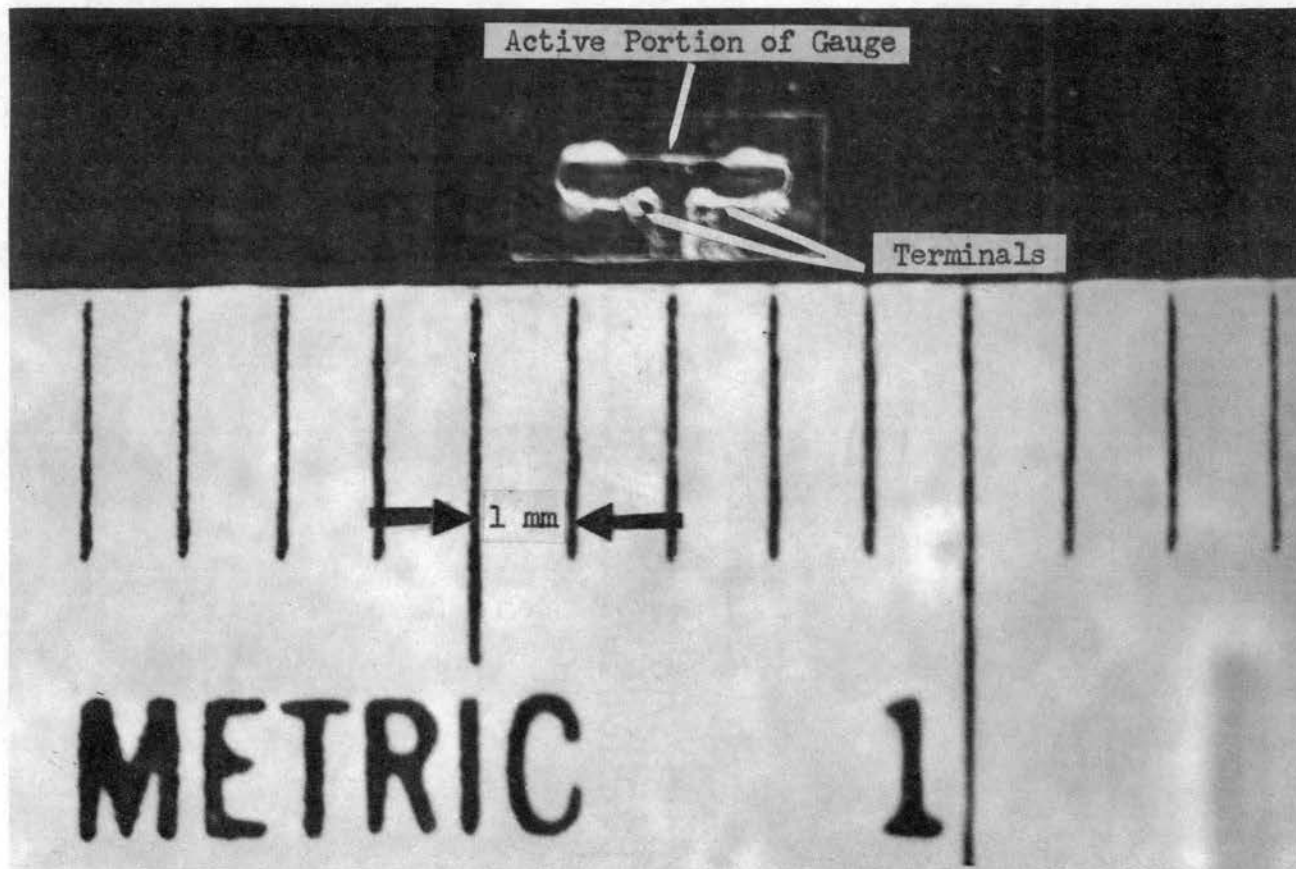
Figure 17. Semiconductor Strain Gauge and Its Relative Size
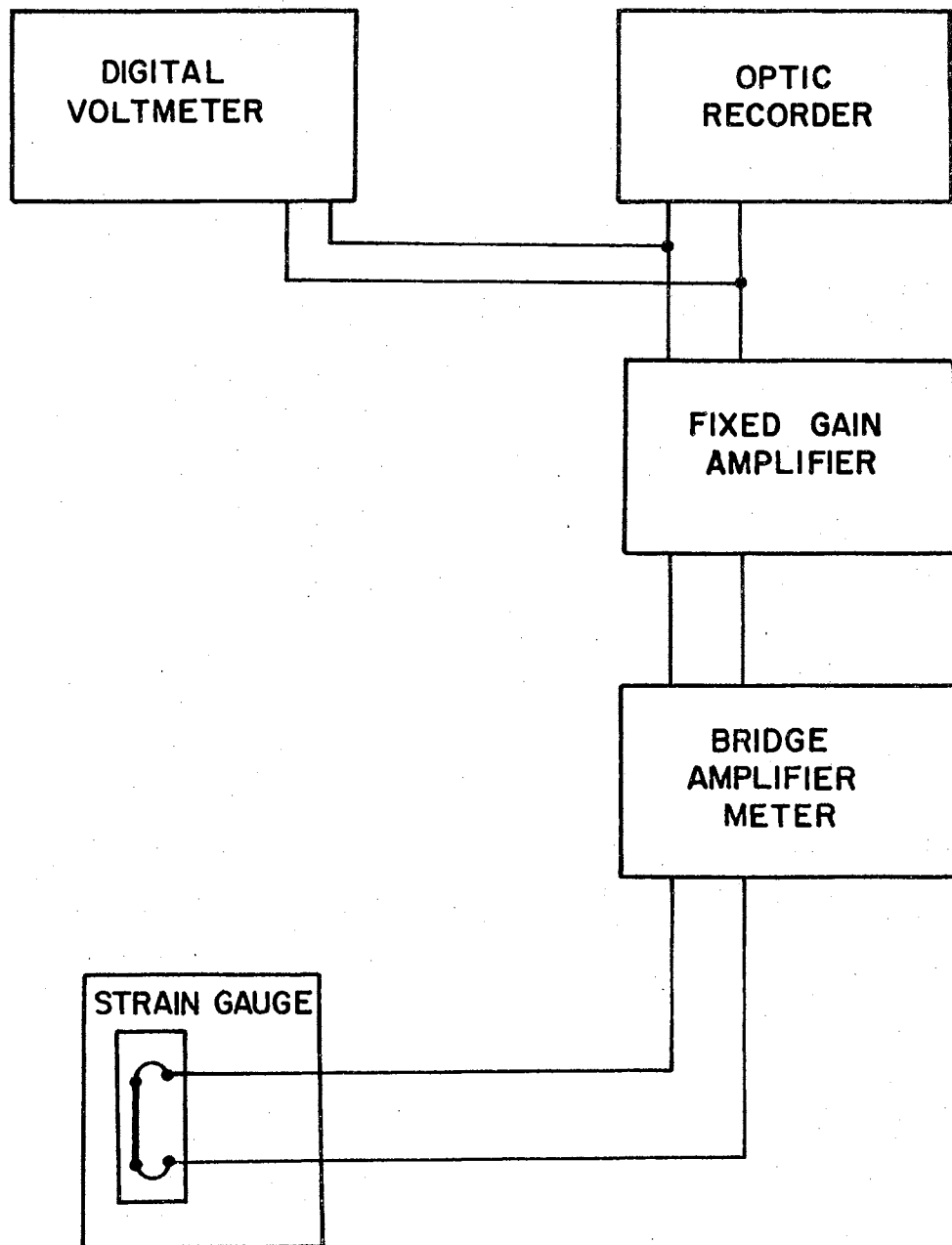
Figure 18. Block Diagram for Strain Gauge
Instrumentation

Time responses recorded had much less overshoot. The natural frequency of the galvonometers were 1000 cps.

The entire strain recording instrumentation performed well. The signal to noise ratio was good, considering the high amplifications used. The entire system was extremely sensitive and would reflect very slight pressure variations.

CHAPTER V

EXPERIMENTAL RESULTS

The overall objectives of the experimental work may be summarized as follows:

1. to furnish experimental results for verification of the strain-time response of the simply supported panel in a baffle subjected to a normal incidence N-wave;

2. to obtain data that would give a closer evaluation of the contribution of the higher modes on the response of the panel;

3. to verify that the results obtained on the analog computer for the lumped-parameter, damped, two degree-of-freedom model will suffice in predicting the response of a simply supported panel in the wall of a Helmholtz resonator;

4. to compare the response of the simply supported panel in the baffle to that of the panel coupled to the resonator.

On the basis of previous work in this area (24), in which experimental verification of a lumped parameter model for the transient response of a resonator was done, a low frequency lumped parameter description was assumed, and the

48

experimental tests were run to validate the assumption or to
disprove the idealization.

<div align="center">Determining the Modulus of Elasticity
for the Aluminum Panel</div>

The edge support conditions in the experimental model
could not be determined exactly. Therefore, properties of
the material were determined prior to making tests for the
natural frequency and damping measurements.

The value for Poisson's ratio was assumed to be 0.33.
This value is predominate among all the different types of
aluminum. The extensive experimentation required to obtain
a more accurate value than the published value was not
warranted. Poisson's ratio does not appreciably affect
the natural frequency of the panel since it appears in the
denominator of the frequency expression as the quantity
$\sqrt{1 - \mu^2}$.

The modulus of elasticity varies quite radically from
specimen to specimen, and can range from 50 per cent less
than the published value, to 50 per cent more than the
published value. An ultrasonic technique was used to
determine the modulus of elasticity of the aluminum panel
by the measurement of the speed of propagation through the
material. The measurement was accomplished by utilizing a
commercial pulsing unit and two piezoelectric transducers
constructed of lead zicronate, with frequencies 2.25 mega-

cycles. One transducer was used as a sending unit, while the other transducer received the pulsed signal. Initially, the transducers were placed together, and with the aid of an oscilloscope, the position of the start of the pulse was observed. The aluminum specimen was placed between the sending and the receiving transducers, and the position of the delayed pulse was observed. The time delay, caused by the longitudinal wave propagation through the material, was recorded, and the velocity of propagation computed. Thickness of the material was measured with a micrometer.

The relationship $V = \sqrt{E/\rho}$, where V is the speed of propagation, and ρ is the density of the material, was used to calculate a value for E. The time delay was measured on a scale of 0.1 micro-sec/cm and could be recorded to an accuracy of 0.1 of a cm yielding an overall accuracy of .01 of a micro-sec.

Velocity was calculated at 205,000 in/sec. Density of the aluminum specimen was 98.85×10^{-3} #/in^3. This resulted in a value, $E = 10.76 \times 10^6$ psi.

The experimental value is in close agreement with the published value. The modulus of elasticity for aluminum is generally taken as 10×10^6 psi.

Natural Frequency and Damping Measurements

Shock excitation tests were performed on the aluminum panel in the baffle. The tests consisted of exciting the panel with a transient type input and observing the residual

free relaxation oscillations. The oscillations were
recorded from the output of the semiconductor gauge
mounted at the center of the panel. Figure 19 shows
an oscilloscope trace displaying the decaying oscil-
lations.
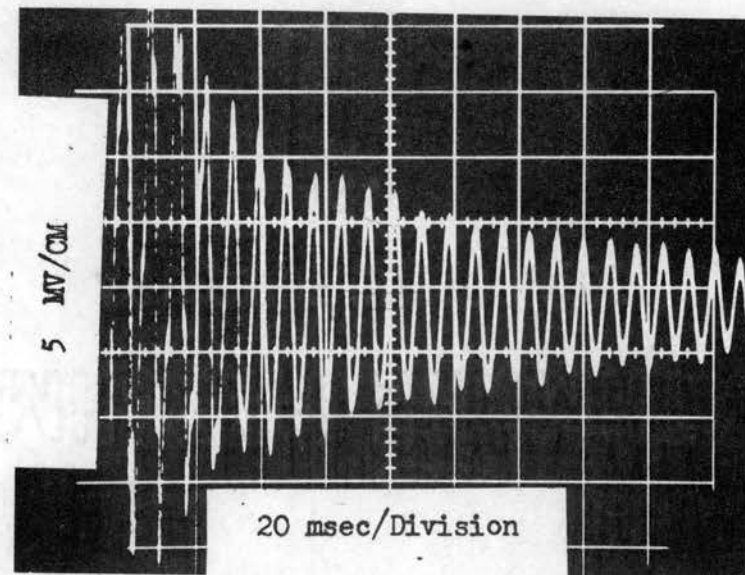
Figure 19. Free Vibration Trace of
Center of Aluminum Panel

The damped natural frequency was computed from the
response trace. Sweep rate of the oscilloscope multiplied
by the length in cm yields the damped natural period. The
damped natural frequency f_d, is related to the undamped
natural frequency f_o through the expression $f_d = \sqrt{1 - \zeta^2}\, f_o$,
where ζ is the damping factor. The case in which ζ is
small, f_d and f_o are practically equal.

A theoretical estimation of the fundamental frequency for the panel was made from the well-known expression (3,4) for natural frequencies of simply supported plates;

$$f_o = \frac{\pi h}{2} \sqrt{\frac{E}{12(1-\mu^2)\rho}} \left(\frac{r^2}{a^2} + \frac{s^2}{b^2} \right) \qquad (5\text{-}1)$$

where

a = horizontal dimension

b = vertical dimension

h = thickness of panel

E = modulus of elasticity

ρ = density of panel

μ = Poisson's ratio.

The fundamental frequency 99 cps was computed from the expression (5-1). Figure 19 indicates the damped natural frequency is about 119 cps. The correction for $\zeta = 0.05$ yields the undamped natural frequency of 118cps. A deviation from the theoretical estimation was expected, but to a lesser degree. A closer agreement between the theoretical and the measured value would have occurred if the knife edges supporting the aluminum panel had been more accurate. Slight variations of the edges were compensated for, by tightening the edge frames more securely. This caused the support conditions to be some combination between a simply supported edge condition, and a clamped edge condition. The deviation in the edge conditions explains the increase in natural frequency.

An estimate of the damping for the system was obtained
from the same residual free oscillation recording. An
assumption was made that the dissipation of the energy in
the system was mainly in the form of viscous damping. A
small amount of structural damping does exist, and can be
observed in the decaying oscillation curve as the straight
line portion; but for the most part, viscous damping was
predominant. The logrithimic decrement method, in which
amplitudes of succeeding peaks indicate to what degree
viscous damping is present, was utilized in obtaining a
value for the damping factor. A value of $\zeta = 0.05$ was
obtained. This value is not far removed from damping
factors found in experimental measurements on large glass
windows. A representative value for of a large plate
glass window is of the order 0.08 to 0.1.

Contribution of the higher modes, as observed in the
decay traces, appears to be negligible. However, the panel
is a distributive system, and capable of being excited in
an infinite number of mode shapes. The proportional affect
of the higher modes on the fundamental natural frequency is
unknown. Some of the deviation between the theoretical
and measured frequency could be attributed to this phenomena.

A similar type of test was performed on the test
resonator. Measurements were accomplished with pressure
microphones and a residual pressure trace was recorded. The
resonator was designed to insure no cavity leakage. Wherever
a joint occurred, gaskets were used, and a rubber "O"-ring

was utilized in the interior sliding baffle.

A typical trace of the residual cavity pressure oscillations is shown in Figure 20. This trace was recorded from a resonator of cavity dimensions, cavity volume 960 cu. in., neck diameter 7.13 inches and neck length 0.375 inches.
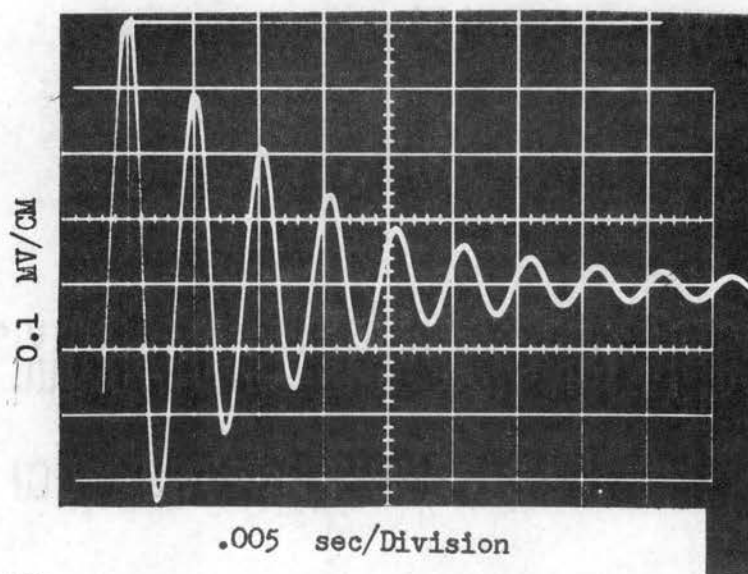
Figure 20. Residual Pressure Oscillations in Test Resonator

The theoretical estimation of the natural frequency by expression (A-4), yields a value of 175 cps, whereas, the measured value is about 181 cps. The agreement between theoretical and measured values was good. A deviation of only 3 to 5 cps was observed for various configurations that were tested, ranging from 80 cps to around 200 cps.

The damping factor was estimated for the resonator in a similar fashion as for the aluminum panel. Calculations for various configurations indicated the damping factor had a consistent value about 0.06. All tests conducted to estimate the damping factor were done using a transient excitation. Figure 20 shows clearly the presence of only a single frequency, and this predominated as long as the input wave length was three to four times the characteristic dimension of the cavity, or longer.

The natural frequency and damping measurements were conducted for the purpose of obtaining representative values for use in the analog study. The study was somewhat oriented toward a particular test configuration and the experimental values for the natural frequencies were a good check on the theoretical estimations. The damping values obtained experimentally were close enough to use in analytical work for predicting the transient response studies to follow.

Time Response Measurements of the Simply Supported Panel in a Baffle

The predicted response of the distributive system was validated by strain measurements on the panel. The panel was subjected to various N-wave pressure pulse durations and strain recordings were made by the use of the semiconductor gauge. The measured strain was compared to the predicted strain.

Predicted response curves were derived using a straight line approximation to the N-wave pulse. The negative pressure was assumed to be the same magnitude as the positive counterpart. The measured value of damping was used to define the damping coefficient for the panel, however, the theoretical frequencies for the panel were used in the analysis. The transient response of the panel was obtained by methods outlined in Chapter II, and subsequent numerical values were obtained by the use of a high speed digital computer.

The recording speed was limited and the response curves were close together and had to be spread out for a good comparison with the predicted values. Consequently, the traces had to be read and replotted on expanded time scales.

Figure 21 is a typical recording of the pressure pulse and the strain at the center of panel. The upper trace represents the pressure input recorded by the condenser microphone and the lower trace shows the output of the strain gauge. Contribution of the higher modes is apparent in the residual era, but have little affect in the forcing era. A second set of blips on the pressure channel is caused by reflections of the wave in the plane wave tube. Since the tube is 32 feet in length, the reflected signal returns in approximately 0.06 seconds. The pressure pulse was adjusted in amplitude as close as possible to 0.2 psf.

Figure 22 shows a comparison between the predicted
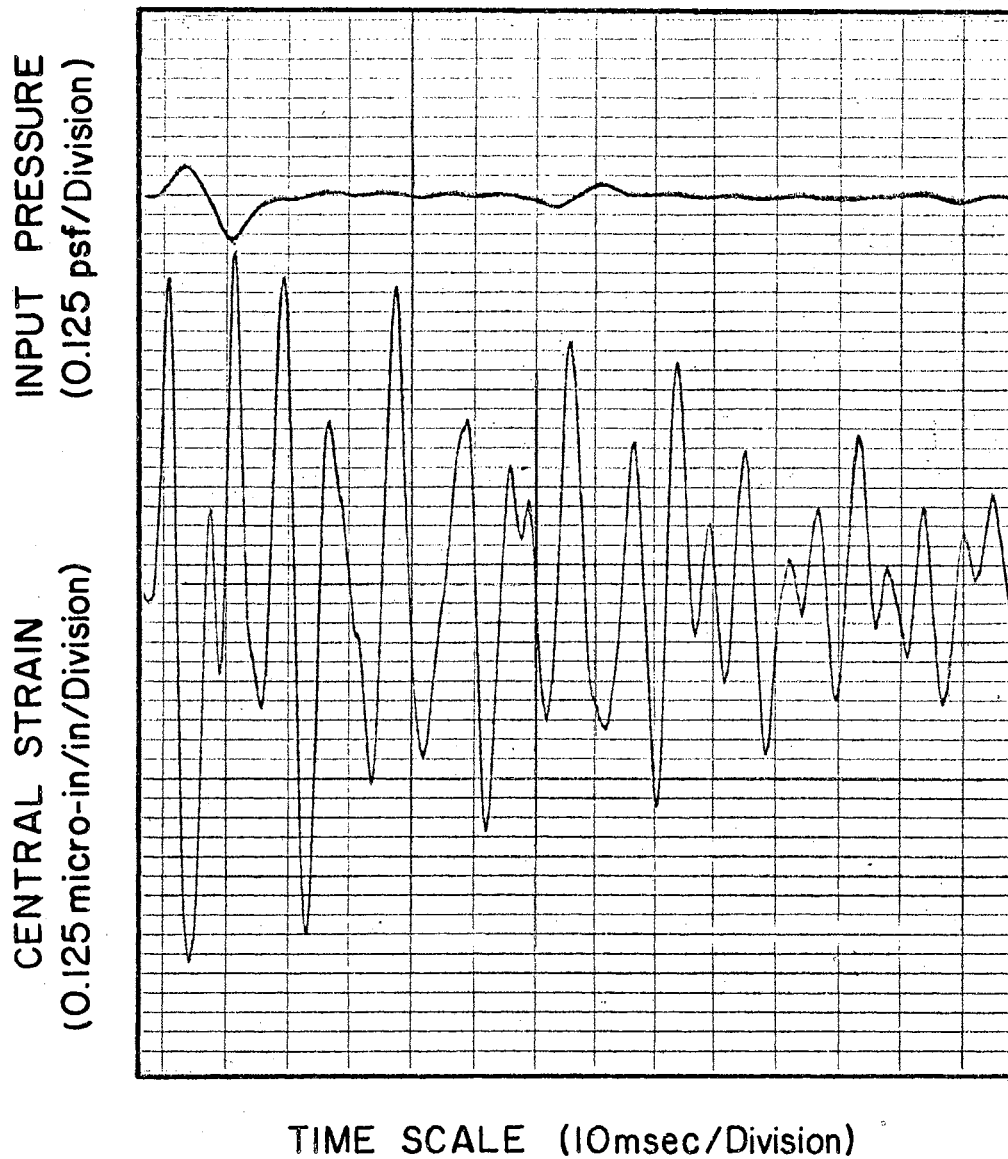
Figure 21. Typical Recorder Trace for Measured
Strain and Input Pressure, $\tau = 0.01$ sec

strain response and the measured strain response for a N-wave
input of .00672 sec. duration. Amplitude agreement between
the measured and the predicted strain response is quite good.
There is a small phase shift in the measured response from
the predicted responses. This shift causes the measured
amplitudes to reach their maximum value before the predicted
results. The phase shift can be attributed to the difference
in the predicted natural frequencies and the measured fre-
quency. The difference in the frequency is great enough
that an appreciable shift on the time axis is observed in
the strain response curve. Close agreement exists between
the amplitude of predicted strain and the amplitude of
measured strain at the first two peaks. The measured response
falls below the predicted values later in the response
curve. This is due to more damping in the system than the
assumed value used in the analytical prediction.

Other inherent errors could be in the delicate balancing
of the bridge circuit used in the system. A correction
factor to adjust the response for the change in natural
frequency is difficult. The response is composed of the
contribution of all the modes. These modes with their
associated frequency determine the response of the system.
A correction for the frequency would involve correcting for
all the higher natural frequencies. A corresponding change
in the geometric model or variation of the physical proper-
ties of the material would have to be made in that case.
Figure 23 is a computed response of the center of the baffle

TIME (2.5 msec/Division)

Figure 22. Comparison of Predicted Strain
Response to Measured Strain
for Center of Panel in Baffle,
P = 0.2 psf N-wave,
τ = 0.00672 sec
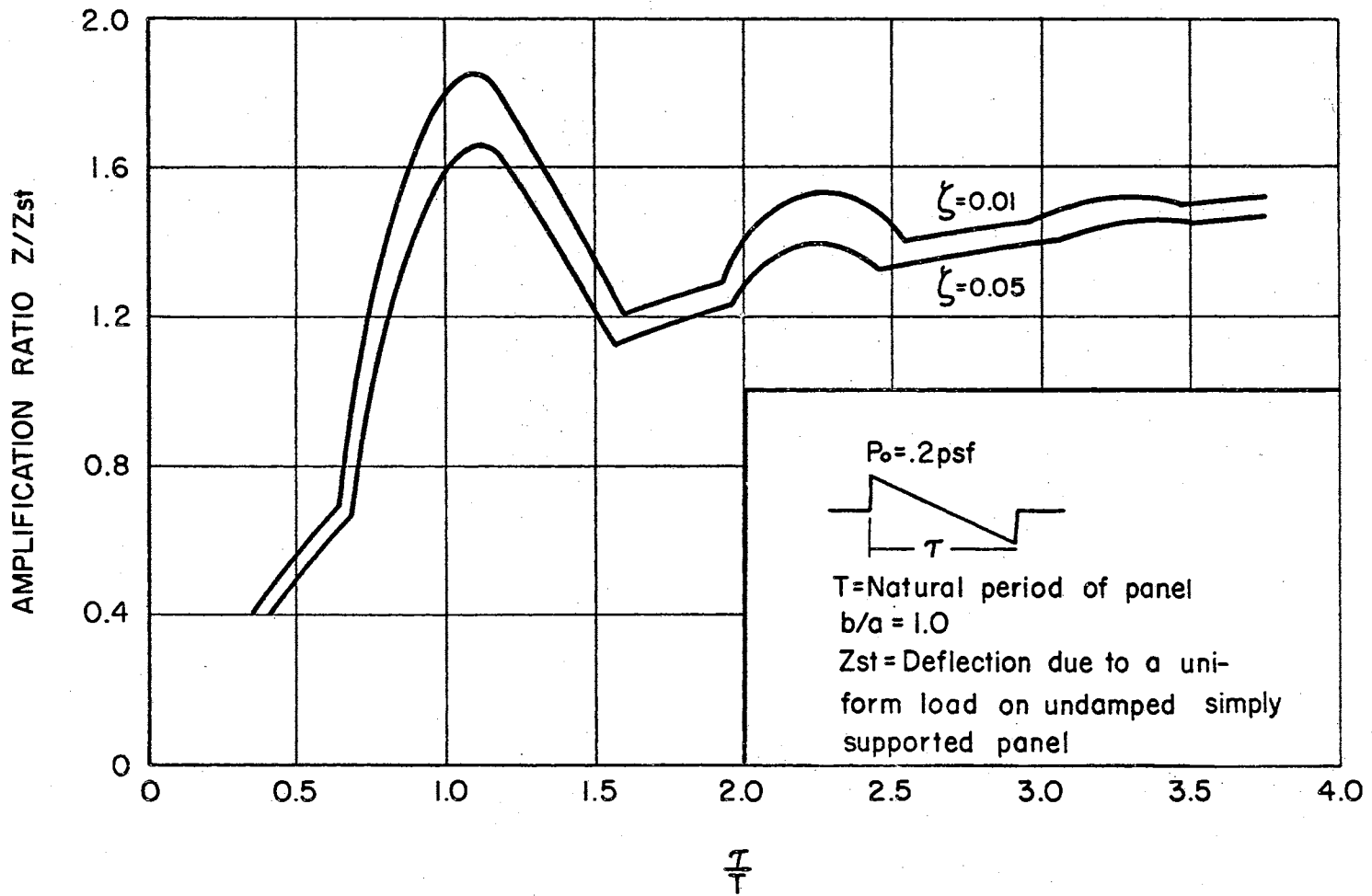
Figure 23. Normalized Center Response of Damped Simply Supported
Panel to Various τ/T N-wave
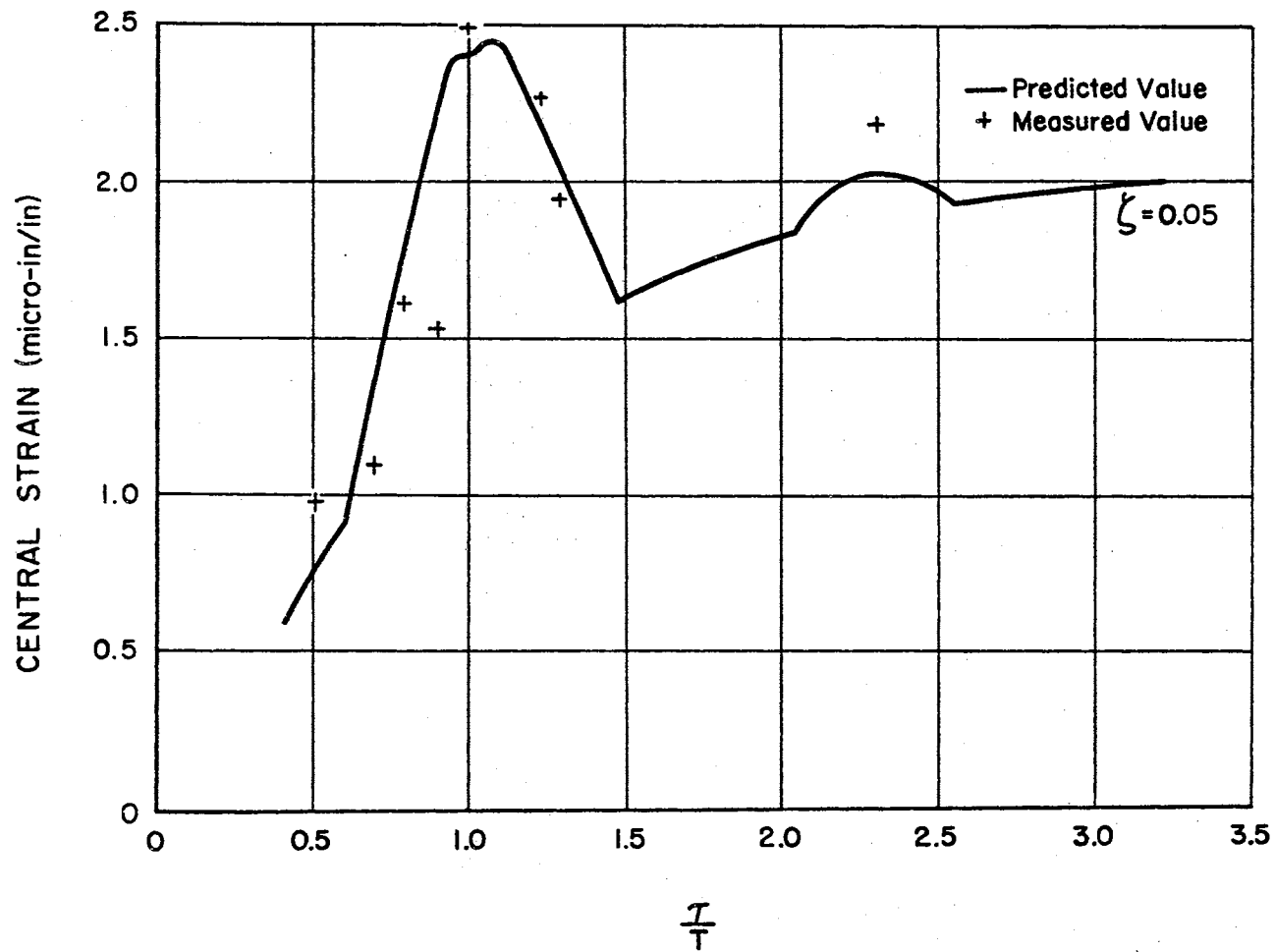
Figure 24. Comparison of Predicted and Measured Strain for
Panel, P = 0.2 psf, ζ = 0.05

for various forcing ratios.

Figure 24 shows a comparison between the predicted strain and the measured strain for the panel in the baffle with a normal incidence N-wave. All work was performed with a normal incidence pressure pulse. At large values of τ/T the sound producing system would not respond to the shape of a N-wave and consequently data was not taken in that region.

<div align="center">

Time Response Measurements of the Panel
Coupled to the Helmholtz Resonator

</div>

Time response measurements for the panel coupled to the resonator were performed to ascertain the validity of the lumped parameter two degree-of-freedom model in the transient situation. Several response traces for the center of the panel are presented. Figures 25, 26, 27, and 28 display the time responses and show the comparison between the predicted and measured response. This phase shift is discussed in the next section, and doesn't appear to affect the amplitude appreciably. However, maximum values occur slightly behind the predicted maximums.

Predicted values were based on a straight line idealization of the N-wave because of the limited capability of the function generator in the analog study. The difference between the actual input and the assumed input caused the phase difference. Input pressure of the N-wave was adjusted before each run to 0.2 psf.
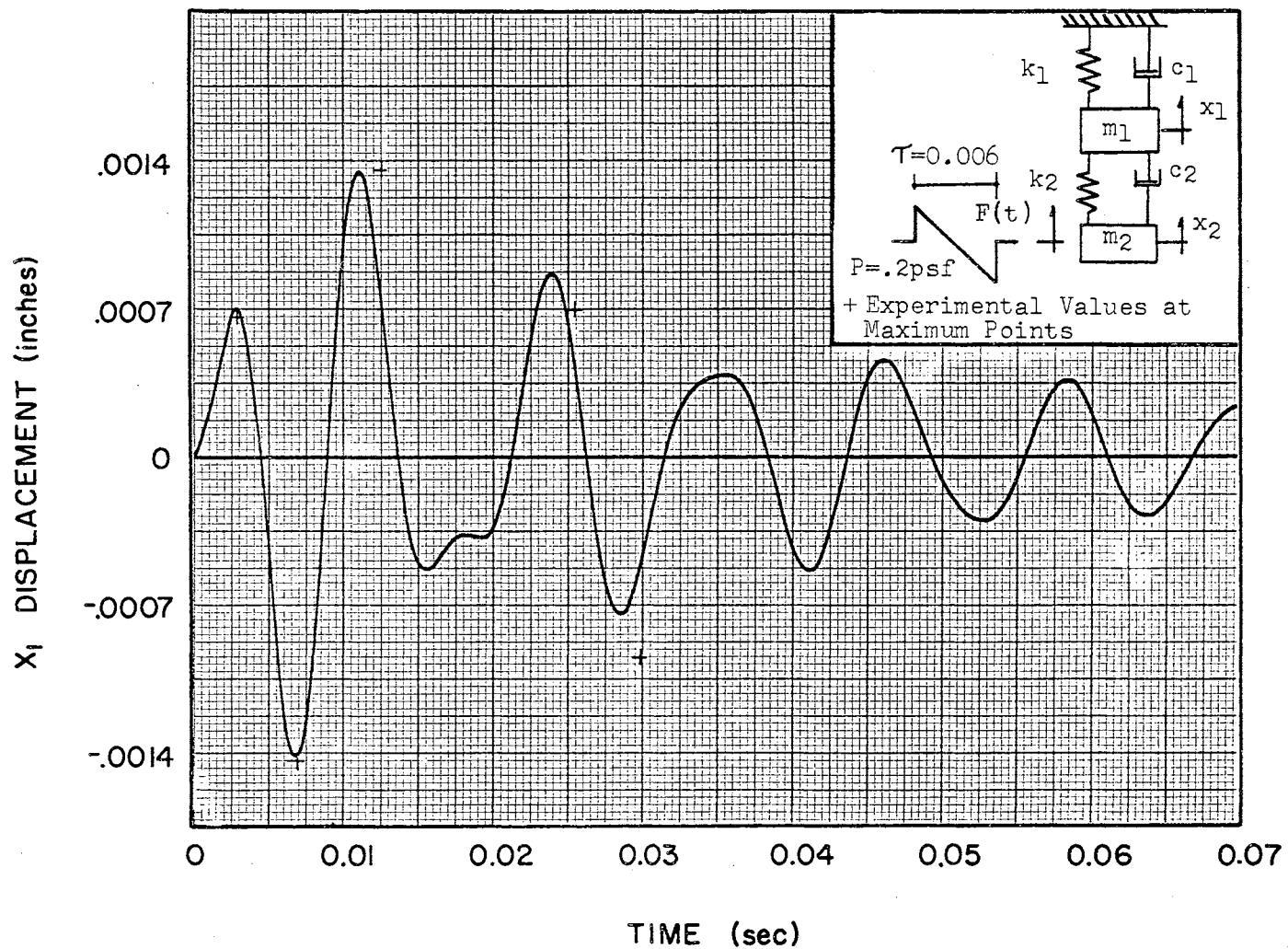
Figure 25. Comparison of Maximum Points in the Measured and Predicted Time-Response to N-wave, $\tau = .006$ sec
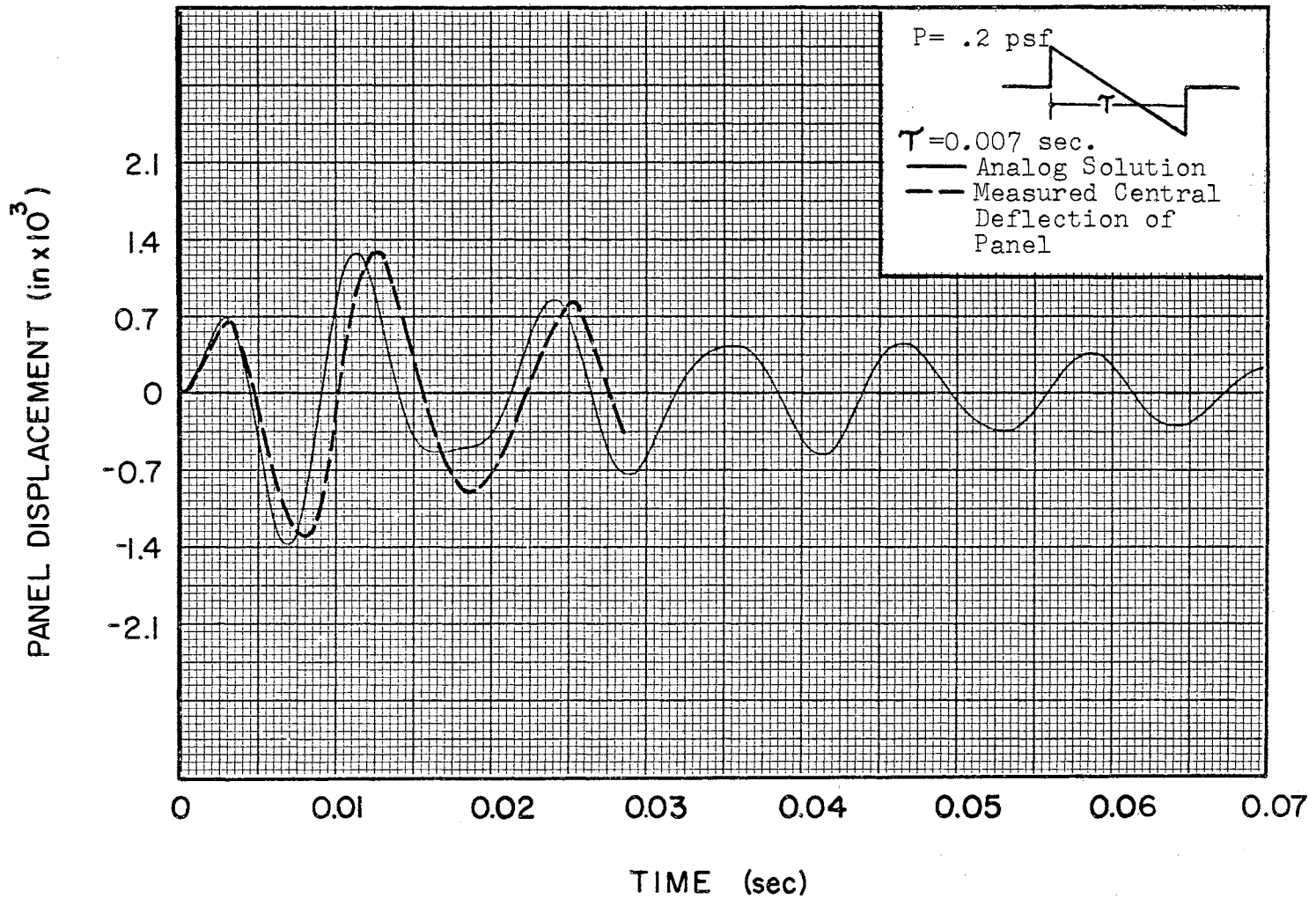
Figure 26. Center Deflection -- Time Response of Panel Coupled to Helmholtz Resonator, P = 0.2 psf, τ = 0.007 sec
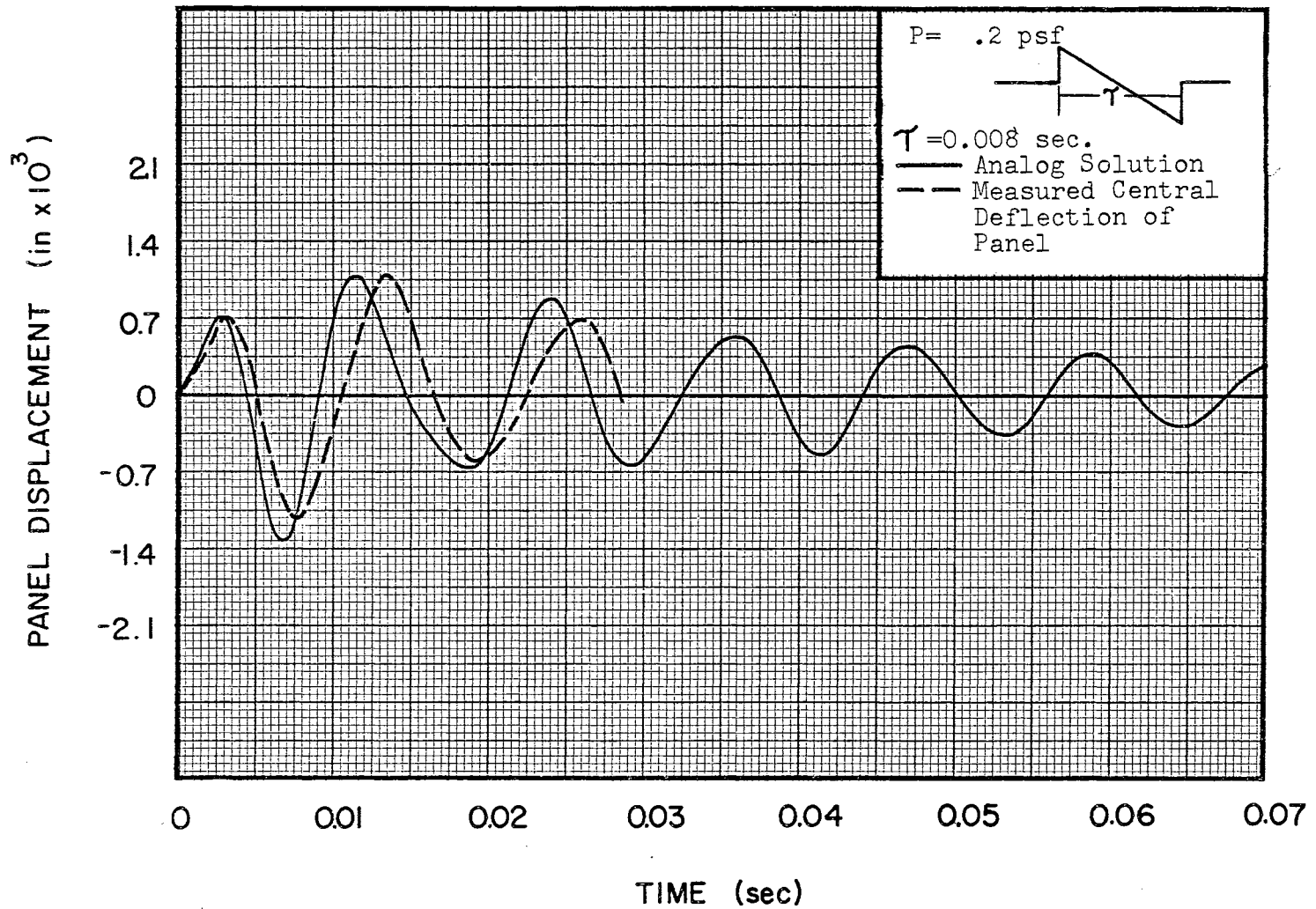
Figure 27. Center Deflection — Time Response of Panel Coupled to Helmholtz Resonator, P = 0.2 psf, τ = 0.008 sec
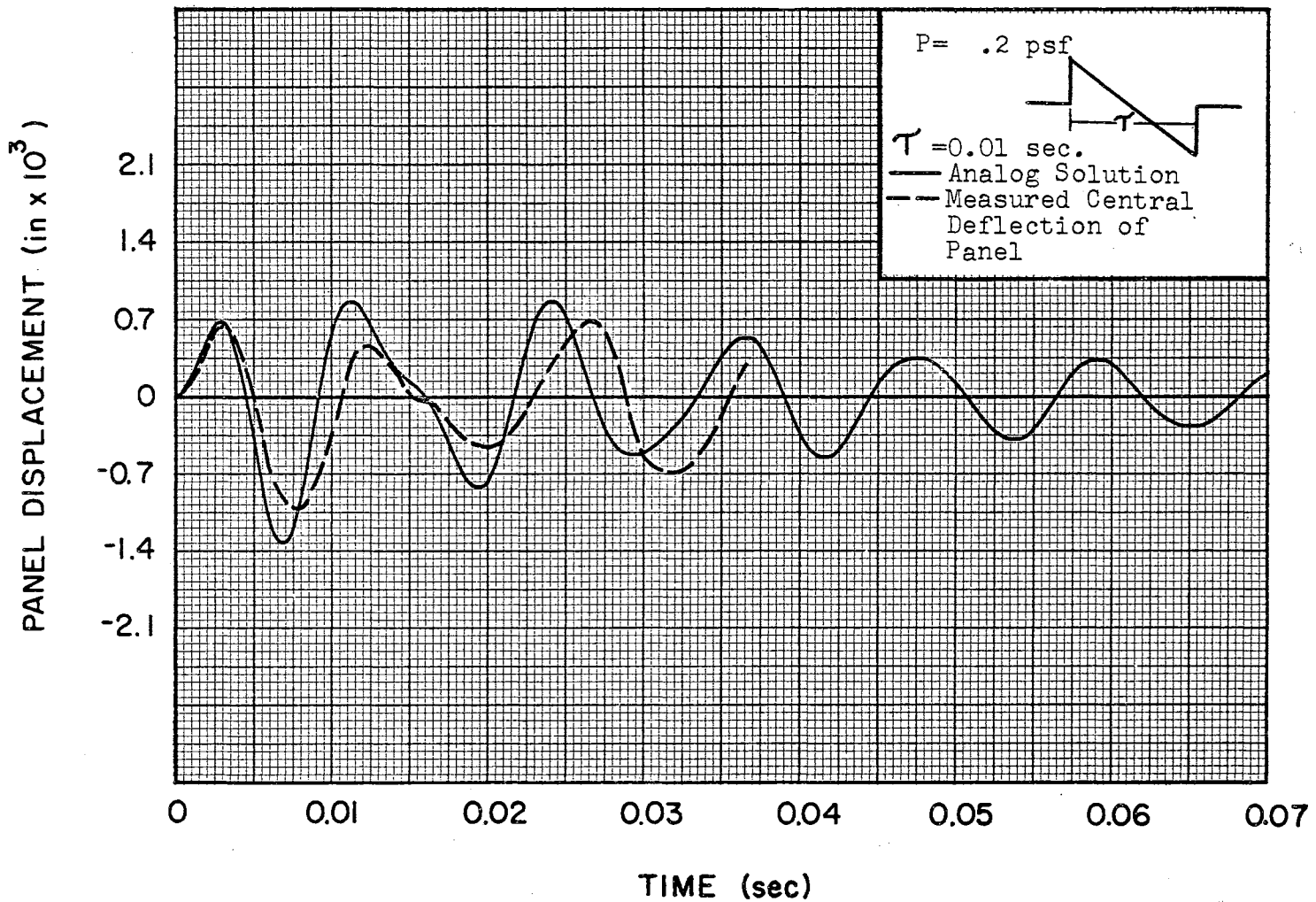
Figure 28. Center Deflection – Time Response of Panel Coupled to
Helmholtz Resonator, P = 0.2 psf, τ = 0.01 sec

Deflection amplitude of the panel coupled to the
resonator was approximately 1.5 times that of the panel
in the baffle. This case was one in which the uncoupled
natural frequency of the resonator was slightly higher than
that of the panel. A N-wave input of 0.006 seconds duration
to the resonator achieved the maximum response of the panel.

The Effect of Pulse Shape on Maximum Response of a Two Degree-of-Freedom System

One of the most important characteristics of the
transient input to a system is the shape of the input pulse.
Investigation (24) has shown that various pulses, like the
square wave, with its' distinct portions of finite jump,
can cause the simple spring mass system to achieve greater
amplitudes than transient pulses with longer rise times.
The most significant parameter of an aperiodic function of
given time duration is the rise time. Rise time is the time
required for the signal to reach its' maximum value. An
examination of the response of a two degree-of-freedom
system will explain why a phase shift occurred between
the measured and the predicted response.

The inherent problem in the experimental pulse generating
apparatus, discussed in detail in Chapter IV, was the dis-
crepancy in the response of the sound reproduction system.
The loudspeaker required approximately two milliseconds to
achieve the maximum peak for the input of the N-wave, although
the rise time in the electrical analog circuit was instan-

taneous. This delay in the experimental pulse generation, although seemingly small, caused a distinct change in the system's overall response. To illustrate this effect, the same idealized model was investigated analytically by the use of the digital computer. The time response of the upper mass, which represents the response of the panel, was observed. Straight line segments were used to approximate the N-wave.

Figure 29 displays the computed time response of the upper mass as a result of varying the rise time for four different variations of N-wave pulses with the same time duration.

The shift in the measured data from the predicted results can be explained by observing the plotted responses. Shorter rise time caused the maximum peaks to occur quicker. As the rise time became longer, the response was somewhat slower, and the maximum points occurred at a later time. The maximum value on the second peak increased as the rise time increased and caused the N-wave to resemble a skewed sine pulse. Thus, the maximum response was somewhat greater and, as predicted in the case of a simple system, the sine pulse caused more response than the corresponding N-wave.

The investigation of the damped two degree-of-freedom model explains the shift in the data. A concluding statement can be made concerning the damping in the system. Measured amplitudes were less than predicted amplitudes which indicate that damping in the physical model, was
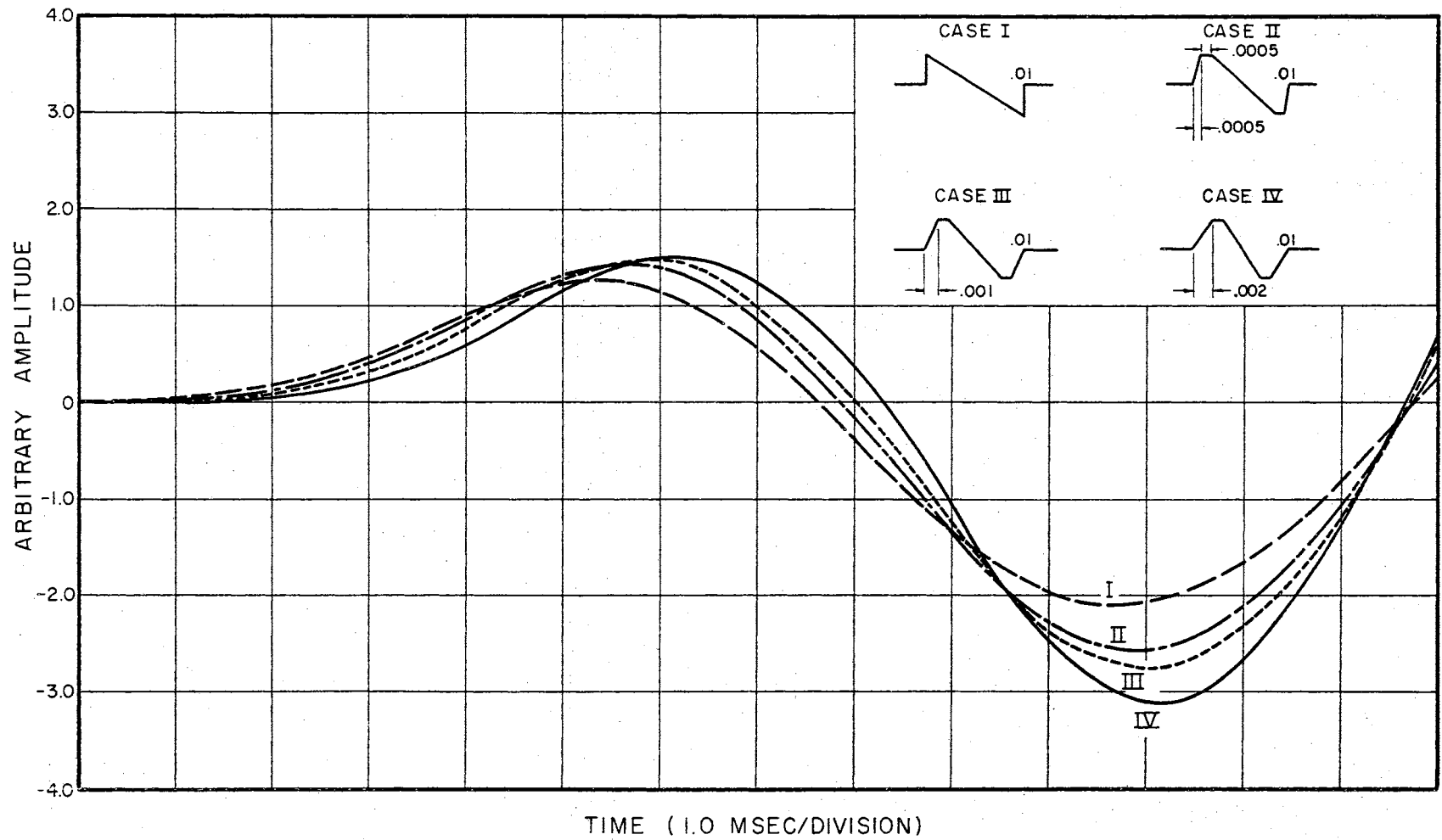
Figure 29. Effect of Pulse Shape on Upper Mass in Two
Degree-of-Freedom System

somewhat greater than the assumed value used in the analog study. This damping would cause a further shift in the measured response from the predicted response.

Prediction of Window-Room Damage Conditions

Typical single rooms and window size configurations that could occur in residential dwellings are tabulated in Tables II and III. The natural frequencies of the glass windows were computed using the assumption of simply supported edge conditions. The frequency of the single room with an open doorway was calculated by the use of the Helmholtz frequency expression (A-4, Appendix A).

Prediction of the worst possible configuration of a window coupled to a room experiencing a sonic boom type input is difficult. Extreme cases, that is conditions in which a maximum response could be expected, might be a more realistic evaluation. An examination of room sizes and window sizes that might be found in typical residential dwellings would lend insight on any changes in the design of structures to prevent sonic boom damage.

The two degree-of-freedom model was shown to represent the system quite well as verified by the measured responses in the laboratory. A coupling frequency for the idealized system can be defined as $f_{21} = \frac{1}{2\pi} \sqrt{\frac{K_2}{M_1}}$. This parameter was investigated for the two degree-of-freedom system and was shown that for small values of f_{21}, the

TABLE II

HELMHOLTZ NATURAL FREQUENCIES OF TYPICAL ROOM SIZES
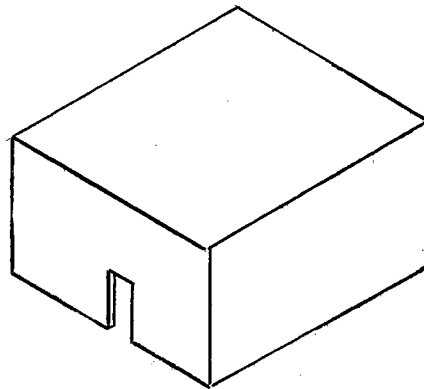
H(ft)	W(ft)	L(ft)	Door Opening (6" Deep)	Natural Frequency(cps)
8	9	12	6 ft–8 in x 30 in.	11.9
8	9	12	6 ft–8 in x 30 in.	10.3
8	12	15	6 ft–8 in x 30 in.	9.2
8	12	18	6 ft–8 in x 30 in.	8.4
8	15	21	6 ft–8 in x 30 in.	6.9
10	12	15	6 ft–8 in x 30 in.	8.2
10	14	18	6 ft–8 in x 30 in.	7.8
10	15	21	6 ft–8 in x 30 in.	6.9
10	9	12	6 ft–8 in x 30 in.	10.6

TABLE III

NATURAL FREQUENCIES OF TYPICAL SIZES OF GLASS WINDOWS

$E = 1 \times 10^7$ psi, Poisson's Ratio $= 0.21$,
Density $= 0.0888$ #/in^3
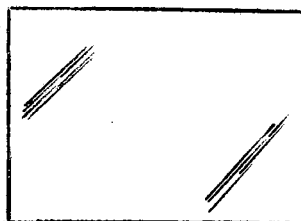
Thickness(in)	a(in)	b(in)	f_{11}(cps)	f_{13}(cps)	f_{31}(cps)
1/16	24	24	2 1.0	104.9	104.9
1/16	12	12	83.9	419.9	419.9
1/16	30	30	13.4	67.2	67.2
1/8	60	72	5.7	24.5	32.7
1/8	48	60	8.6	35.6	50.8
1/8	60	60	6.7	33.7	33.7
3/16	48	60	12.9	53.2	75.9
3/16	60	60	10.1	50.4	50.4
3/16	60	72	8.5	36.5	48.8
3/16	48	48	15.7	78.7	78.7
1/4	48	60	17.2	70.9	101.2
1/4	60	72	11.4	48.7	65.1
1/4	72	84	8.1	35.5	45.4

response of the panel mass will be large (21). This implies
that when the quantity (K_2), the stiffness of the air in the
cavity volume, is small then the coupling frequency will also
be small. As the value for the mass M_1 increases, the
coupling frequency decreases.

A large room would be one in which the stiffness of the
air is small. The large volume of air acts similar to a
soft spring in the simple spring mass system. The fact
that a large panel would cause the mass M_1 to increase is
apparent. Intuitively one can associate a large plate
glass window to a large room volume and the air having a
pushing or an oscillating affect on the window when dis-
turbed. Thus, when a large window's natural frequency is
approximately the same as the cavity natural frequency,
adverse affects can occur during a sonic boom input of time
duration near the natural period of the cavity.

As mentioned in the preceding paragraphs, nearly
every conceivable structural configuration will exist in
practice. An examination of typical room configurations
and their natural frequencies is shown in Table II. A
room size of 12 feet by 18 feet with a window of 48x60x1/8
inches would be a case in which the undamped natural fre-
quencies of the window and room are approximately the same.
Since the room volume is quite large, the coupling frequency
will be low.

The aforementioned plate glass window, when considered
as a panel alone and subjected to a sonic boom pressure wave,

can withstand a considerable amount of overpressure. The
simple panel stresses caused by the N-wave pressure pulse
for a peak pressure of 3 psf will be 2500 psi. The
coupling of a tuned system, a cavity resonance about the
same as the window frequency, will increase the stress to
approximately 4000 psi. The working strength of glass is
around 6000 psi with a reduction to 4000 psi for long term
loading. Approximately fifty per cent of the windows would
be expected to break at a stress level of 6000 psi. Any
supersonic aircraft flying on a day when winds are gusting,
can possibly create a dynamic amplification that could cause
the stress level to equal or exceed 6000 psi. If the window
size were increased to 60x72x1/8 and mounted in a slightly
larger room a stress level of 54000 psi would result for the
same conditions.

A physical structure such as a residential dwelling
will have a complex interaction of halls, adjoining rooms,
and multiply connected windows. Each adjoining system of
rooms will affect the others.

Since the sonic boom pressure wave is considered by
most people to be relatively weak when compared to the
design wind load, intuitively, a plate glass window designed
properly should not fail for the sonic boom overflights.
However, structural members such as plastered ceilings,
windows and flexible ceilings, which in the past have not
been load carrying members would possibly fail. The cumu-
lative damage factor that will be induced by wind, settling,

and temperature changes is a cause for concern. The push-
pull effect of the sonic boom might cause a fatigue failure
after many cycles of overpressure.

The analysis of sonic boom effects will have to be
accomplished by a generalized approach rather than trying
to treat each situation as an isolated problem. The lumped
parameter model seems like a logical method of treatment.

CHAPTER VI

PRACTICAL CONSIDERATIONS AND APPLICATIONS

TO TRANSIENT PANEL OSCILLATIONS

The following excerpt appeared in an article in the

Daily Oklahoman, May 18, 1964:

> "The sonic boom went off and then the glass
> just bulged out", is how a witness described the
> shattering of a large display window Sunday
> afternoon at Kinney's Shoe Store 3718 NW 23.
> The 8 by 11-foot plate glass window popped
> out shortly after 1 p.m. The FAA said a sonic
> boom did occur at approximately the same time
> but they refused further comment until they
> have completed an investigation.

A detailed investigation was undertaken by the author

in conjunction with R. L. Lowery* on the factors causing the

window breakage.

Figures 30 and 31 show a general view of the structure

and the plate glass window that was broken. The dimensions

of the structure were approximately 100 feet by 78 feet by

13 feet. Window dimensions were 96 inches by 120 inches

by $\frac{1}{4}$-inch. The window was mounted so that about $\frac{1}{4}$-inch of

its periphery was clamped in the mullion. Previous history

on the window and mullion was unknown, but it seems that

both were in good condition prior to the breakage.

---

* Associate Professor, Oklahoma State University
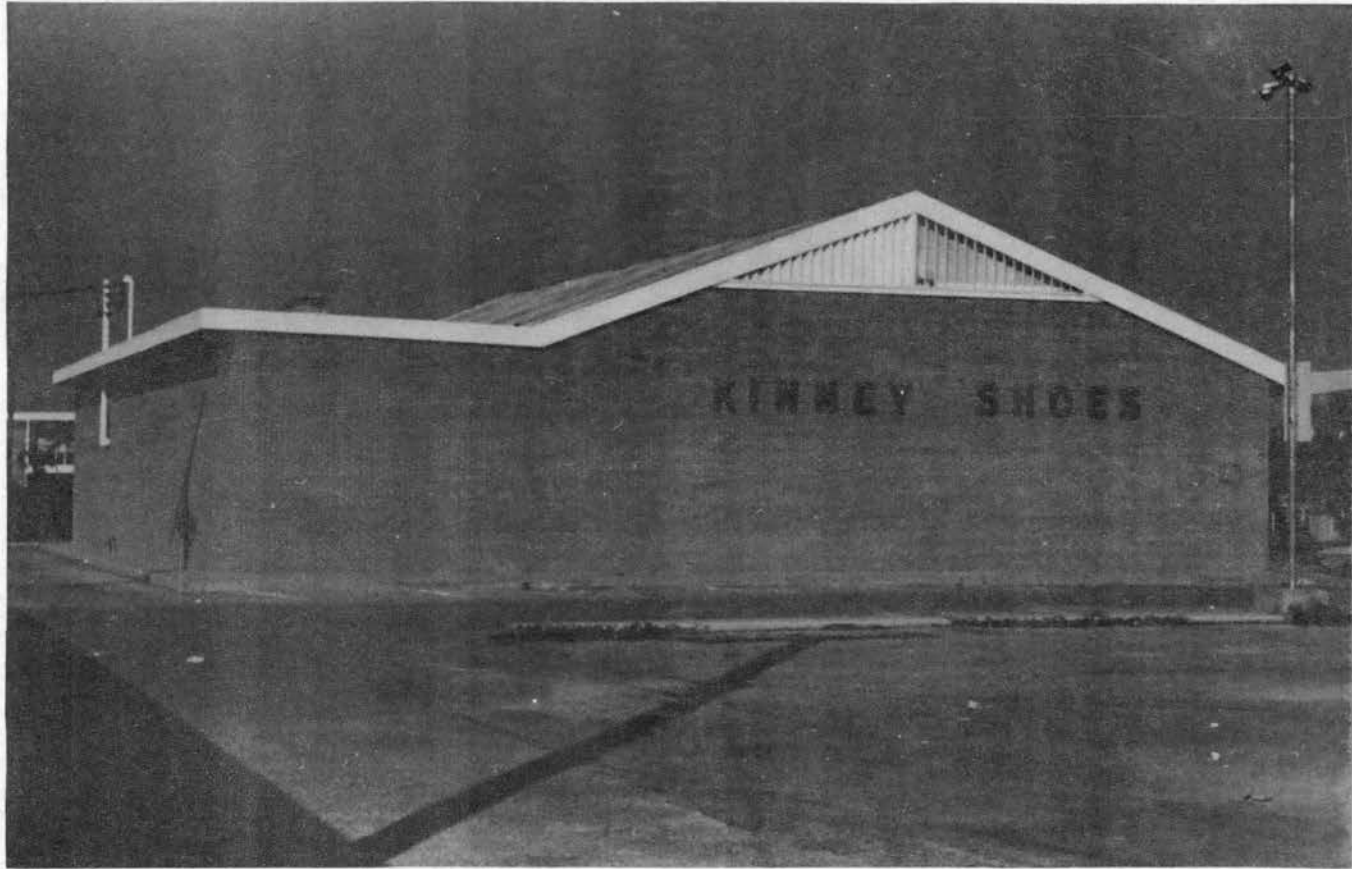
Figure 30. General View of Structure

Figure 31. Location of Window Sustaining Damage

A practical and convenient assumption was made to treat the plate glass window as simply supported on all edges. This assumption leads to analytical simplicity and enables one to arrive at some conclusions rather quickly. Boundary conditions have little effect except for the lowest modes. Results of the previous stated assumptions would apply, approximately, for all the higher modes, regardless of the edge conditions.

Simply supported edge conditions imply that the moment and deflection is zero at the edges of the window. This assumption is partially in error, due to the fact that the mullions are somewhat flexible and a small deflection will occur at the supports. A small amount of moment, caused by the clamping effect of the mullion, will exist at the periphery.

The actual pressure signature of the sonic boom was not recorded at the damage location but at a test location in the vicinity of the structure. The recorded pressure trace was assumed to be the same pressure-time history that was experienced by the window. A normal incidence pressure wave condition was assumed. The normal incidence wave is the most severe case, and therefore, no analysis of a traveling pressure wave was performed. The traveling wave would be one in which the pressure signature would vary in the x-direction, y-direction, and vary with time. The exact pressure-time history was not available, and probably in future analysis of structural damage, the exact pressure

will rarely be known accurately. The assumption of a normal incidence N-wave is a good engineering approximation to the problem.

The natural frequency of the window (the replacement) was determined experimentally. The experimental measurement consisted of shock excitation of the window utilizing a differential transformer as the sensing transducer. The measured frequency was approximately five cycles per second (Figure 32). Measured frequency was about 20 per cent higher than the calculated, simply supported panel frequency of 4.2 cycles per second. A higher frequency than simply supported conditions implies that the system would tend to be somewhat clamped at the edges. This is a mixed boundary condition, rather than the assumed simply supported edge condition. A physical system would seldom be found in which exact mathematical boundary conditions were satisfied. A compromise on edge conditions was required in order to obtain a satisfactory solution.

Figure 33 shows the recorded sonic boom pressure signature, and the corresponding straight line approximation used for computational purposes. The expressions for the displacement, strain and stress, derived in Chapter II, were used to compute the time history of each quantity.

The displacement for the undamped panel in the forcing era is as follows:
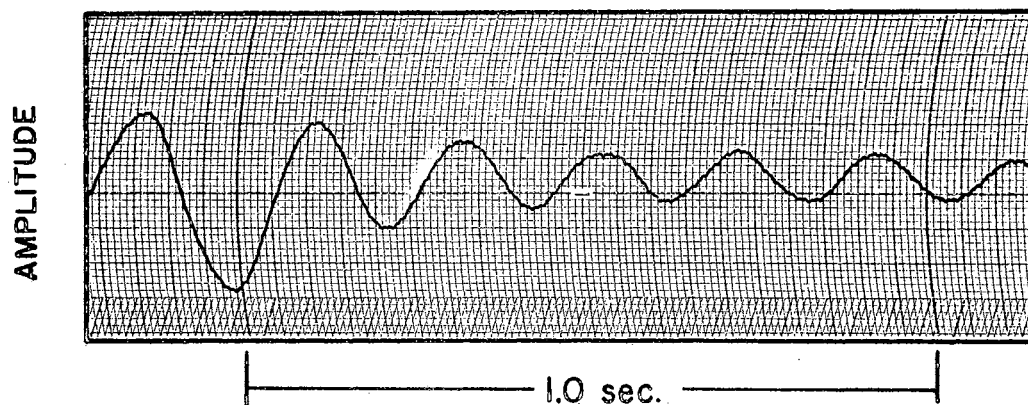
Figure 32. Free Vibration Trace of Window
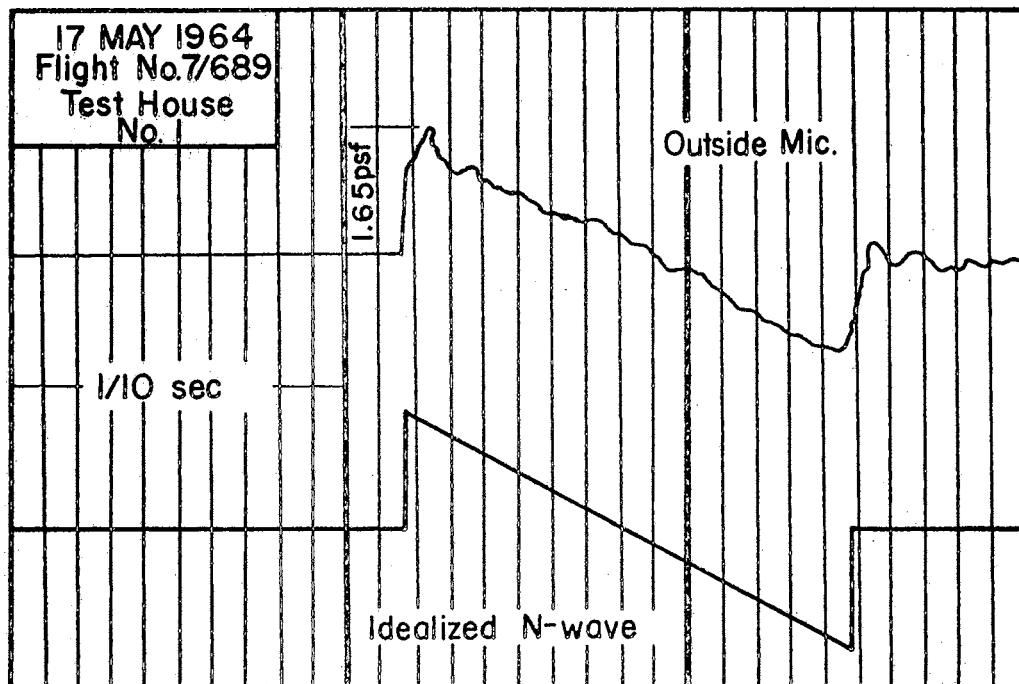
Figure 33. Comparison of Actual Pressure Signature and
Idealized Straight Line Approximation

$$z_{rs}(t) = \frac{4abP_o}{rs\pi^2 M_{rs}\, \omega^2_{rs}} \left[1 - \frac{t}{\tau_1} - \cos \omega_{rs}t + \frac{\sin \omega_{rs}t}{\tau_1 \omega_{rs}} \right] \cdot$$

$$\frac{\sin r\pi x}{a} \cdot \frac{\sin s\pi y}{b} \tag{6-1}$$

and for the residual era,

$$z_{rs}(t) = \frac{4abP_o}{rs\pi^2 M_{rs}\, \omega^2_{rs}} \quad \cos \left[\omega_{rs}(\tau_1 - t) \right]$$

$$+ \frac{\sin}{\omega_{rs}\, \tau_1} \left[\omega_{rs}(\tau_1 - t) \right] - \cos \omega_{rs}\, t$$

$$+ \frac{\sin \omega_{rs}\, t}{\omega_{rs}\, \tau_1} \quad \frac{\sin r\pi x}{a} \quad \frac{\sin s\pi y}{b} \cdot \tag{6-2}$$

The strains and stresses then become (see Timoshenko, Love, or any reference on theory of elasticity),

$$e_x(x,\ y,\ t) = \frac{-h}{2} \quad \frac{\partial^2}{\partial x^2} \left[z_{rs}(x,\ y,\ t) \right] \tag{6-3}$$

$$e_y(x,\ y,\ t) = \frac{-h}{2} \quad \frac{\partial^2}{\partial y^2} \left[z_{rs}(x,\ y,\ t) \right] \tag{6-4}$$

$$\sigma_x(x,\ y,\ t) = \frac{\epsilon}{1 - \mu^2} \quad \left[\epsilon_x + \mu\, \epsilon_y \right] \tag{6-5}$$

$$\sigma_y(x,\ y,\ t) = \frac{\epsilon}{1 - \mu^2} \quad \left[\epsilon_y + \mu\, \epsilon_x \right] \cdot \tag{6-6}$$

Figures 34, 35, and 36 show the plots of the computed time response of the center of the window for the displacement, strain and stress, respectively, based on the contributions of the first 25 modes. The curves represent an undamped system. Damping was present and can be observed in
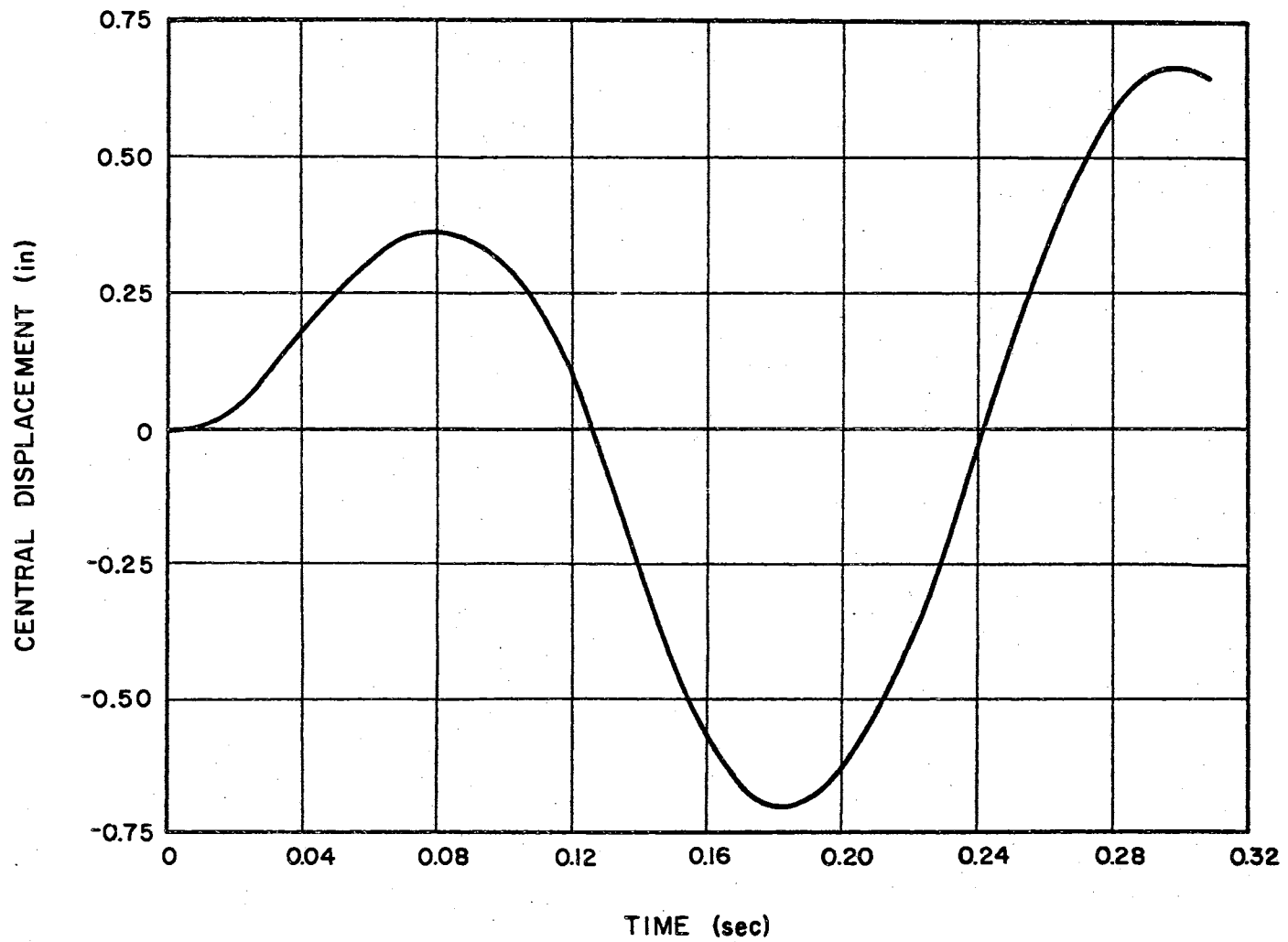
Figure 34. Displacement Time Response for Center of Window to Normal Incidence N-wave
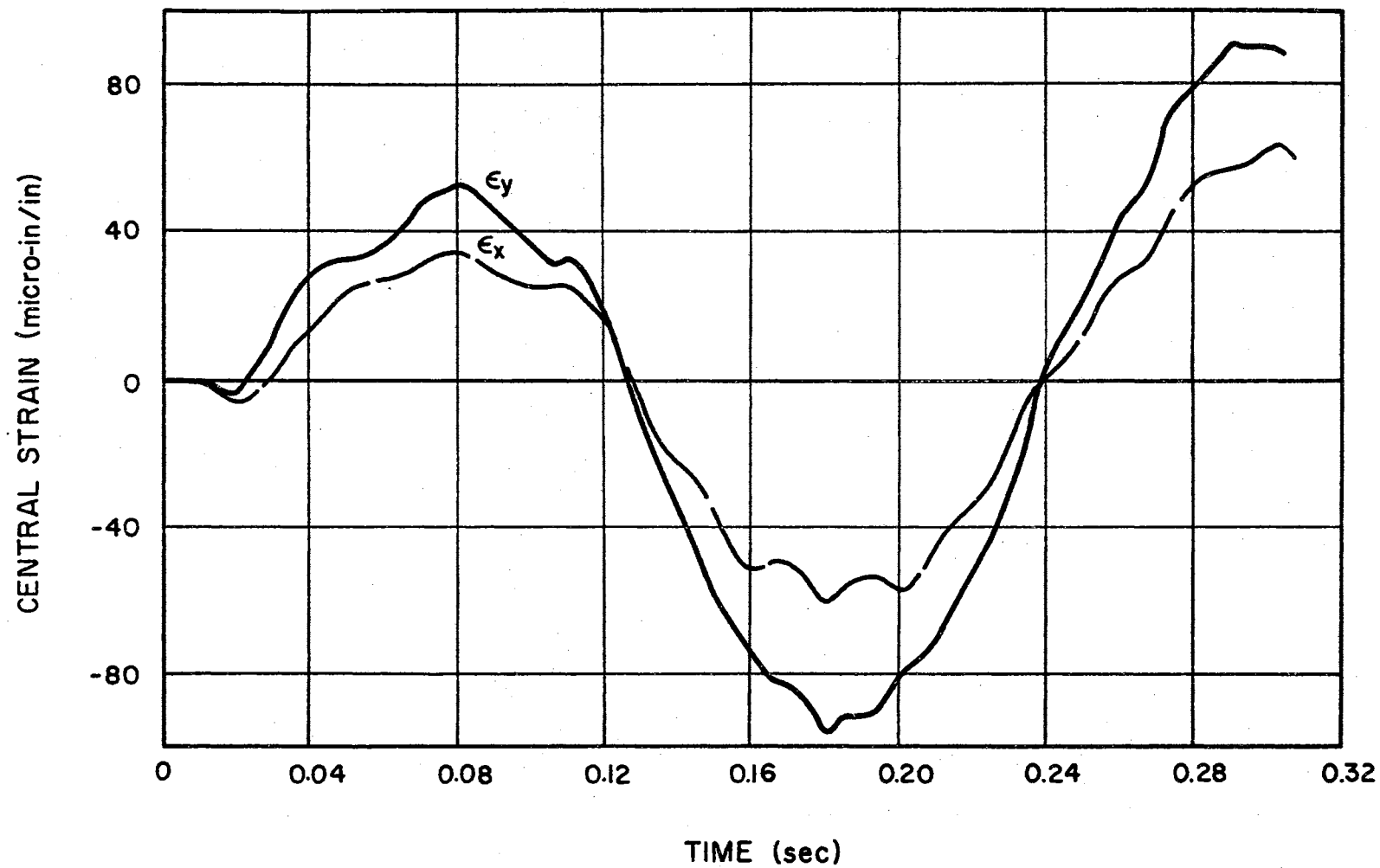
Figure 35. Stress-Time History of Center of Window to Normal Incidence N-wave
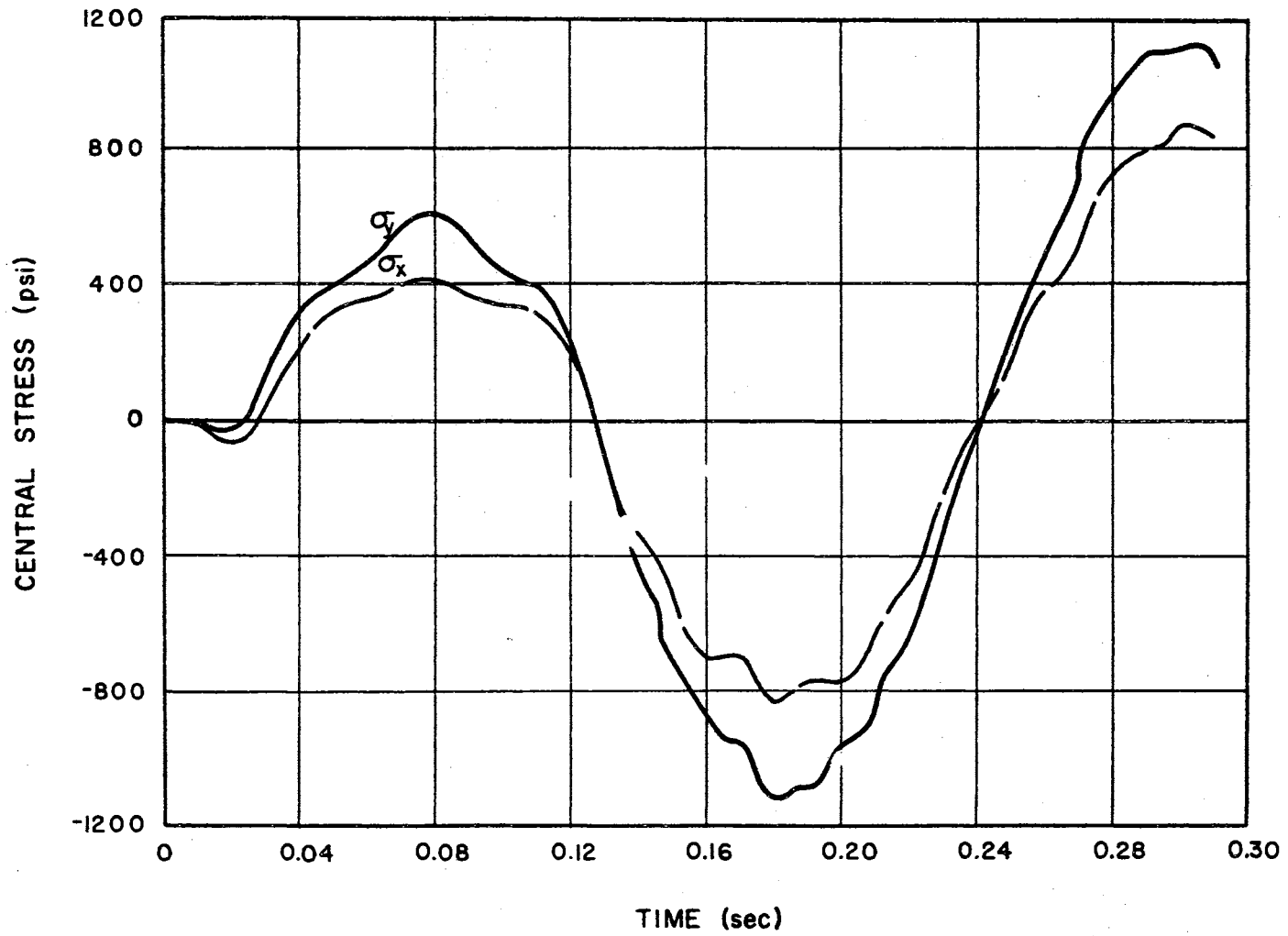
Figure 36. Stress-Time Response of Center of Window to Normal Incidence N-wave

the free vibration decay curve of Figure 32. The damping factor for the window, computed from the free vibration curve was about 0.08. The plotted curves represent a limiting value for the displacement, strain and stress, as the inclusion of damping will reduce the amplitude.

The effect of the higher modes is displayed in Figure 37. A plot is shown of the stress-time response, considering the contribution of the first 25 modes, and one in which only the fundamental mode contribution is considered. The difference in the maximum stress between the first mode contribution and the inclusion of the first 25 modes is less than three per cent. Inherent error in the unknown edge conditions could be expected to cause more than the deviated three per cent error.

Figure 38 is a plot of the stress amplitude at the center of the window for various ratios of N-wave forcing durations to the natural period of the window. A dashed line to the curve shows the maximum central stress for the input pressure signature recorded for the specific flight in which the window was broken. The stress curve is plotted for the peak pressure of 1.65 pounds per square foot. The value for the maximum stress was somewhat less than the maximum that could have occurred at the corresponding peak pressure input if the forcing duration had been tuned to the period of the panel. A N-wave input duration of 0.190 seconds would have resulted in a 40 per cent higher stress amplitude for the same input pressure.
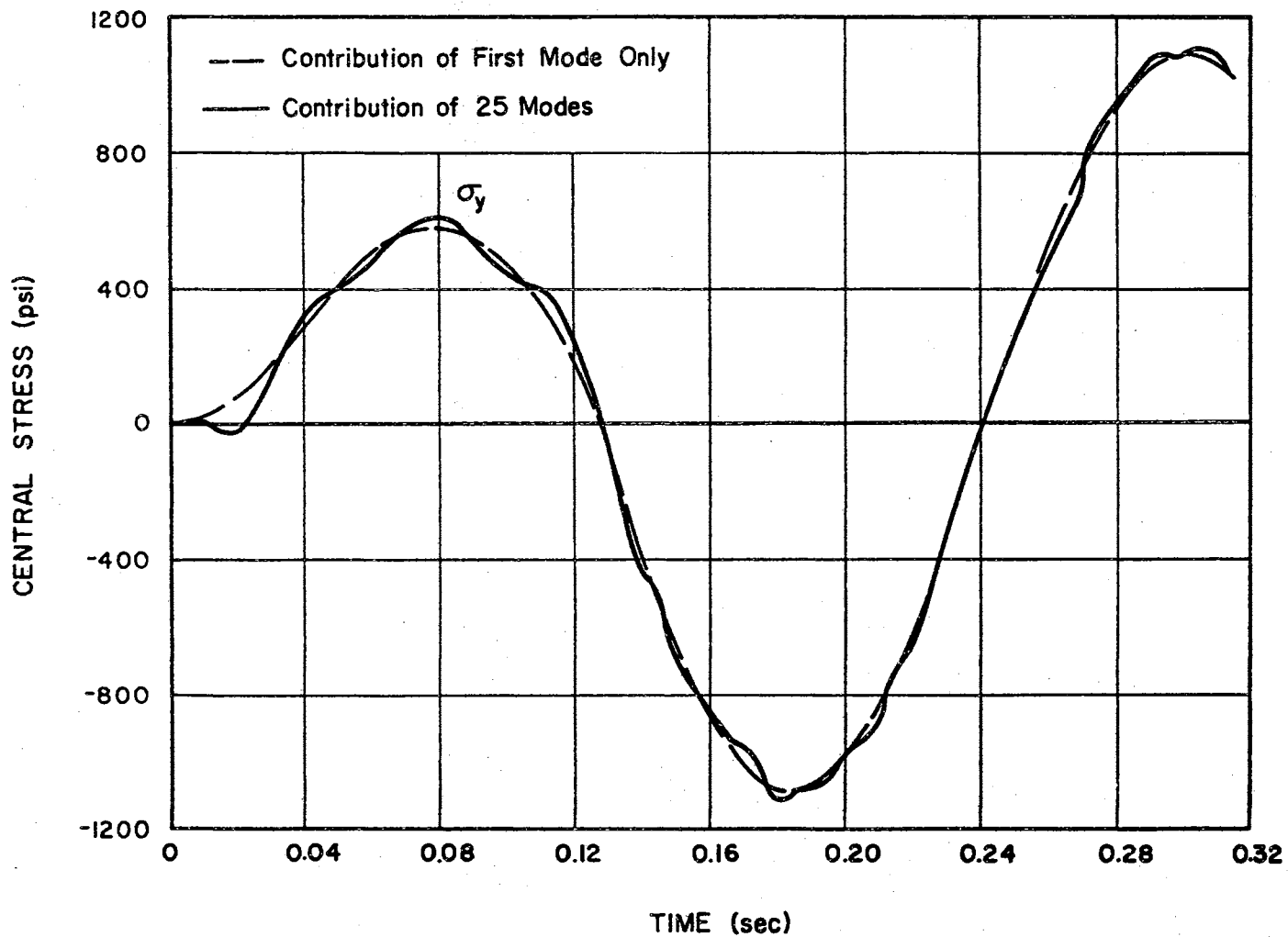
Figure 37. Comparison of the Stress-Time History of the Fundamental Mode Response to the Response of the First 25 Modes With N-wave Input, P =1.65 psf
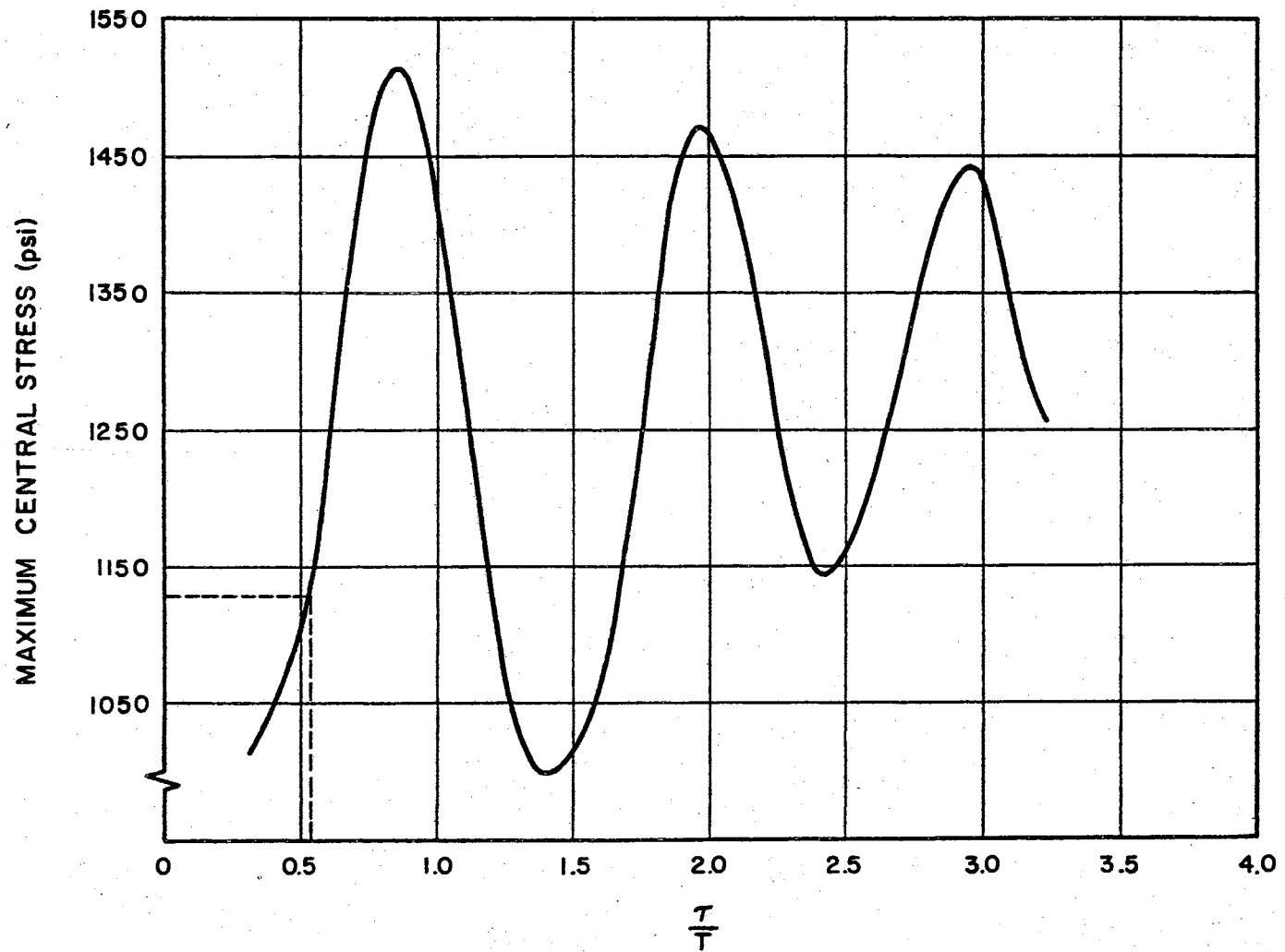
Figure 38. Maximum Central Stress for Various N-wave $\frac{\tau}{T}$ Ratios for 25 Mode Contributions, P = 1.65 psf

Lumped Mass Representation

A lumped mass representation of the physical structure was utilized to enable a comparison between the response of the panel in the baffle and the lumped parameter system. The floor plan of the physical structure and a lump parameter idealization of the system is illustrated in Figure 39.

The static deflection of the mass M_1 of the lumped system is calculated from the expression:

$$X_{st} = \frac{F}{K_1 + K_2} = \frac{132}{478} = 0.276 \text{ inches.}$$

This deflection is due to a static load of 1.65 psf on the equivalent lumped mass system. The parameters, K_1 and K_2 were arrived at by the method given in Appendix A. Figure 40 is a normalized maximum response curve extracted from reference 28. This plot, showing the response of a simple undamped oscillator, enables a comparison to be made between lumped mass analysis and distributive analysis. The ratio $\frac{\tau}{T} = 0.675$ is shown on the graph as a dashed line.

This input would result in a maximum response ratio of 1.8. The maximum dynamic deflection for the input is

$$X_m = 1.8(X_{st}) = 1.8(0.276) = 0.5 \text{ inches.}$$

The absolute maximum form the same figure, for the assumed idealized model, would be 2.1(0.276) = 0.58 inches. This maximum displacement is somewhat less than the computed displacement (0.74; Figure 26) by distributive analysis of the panel.
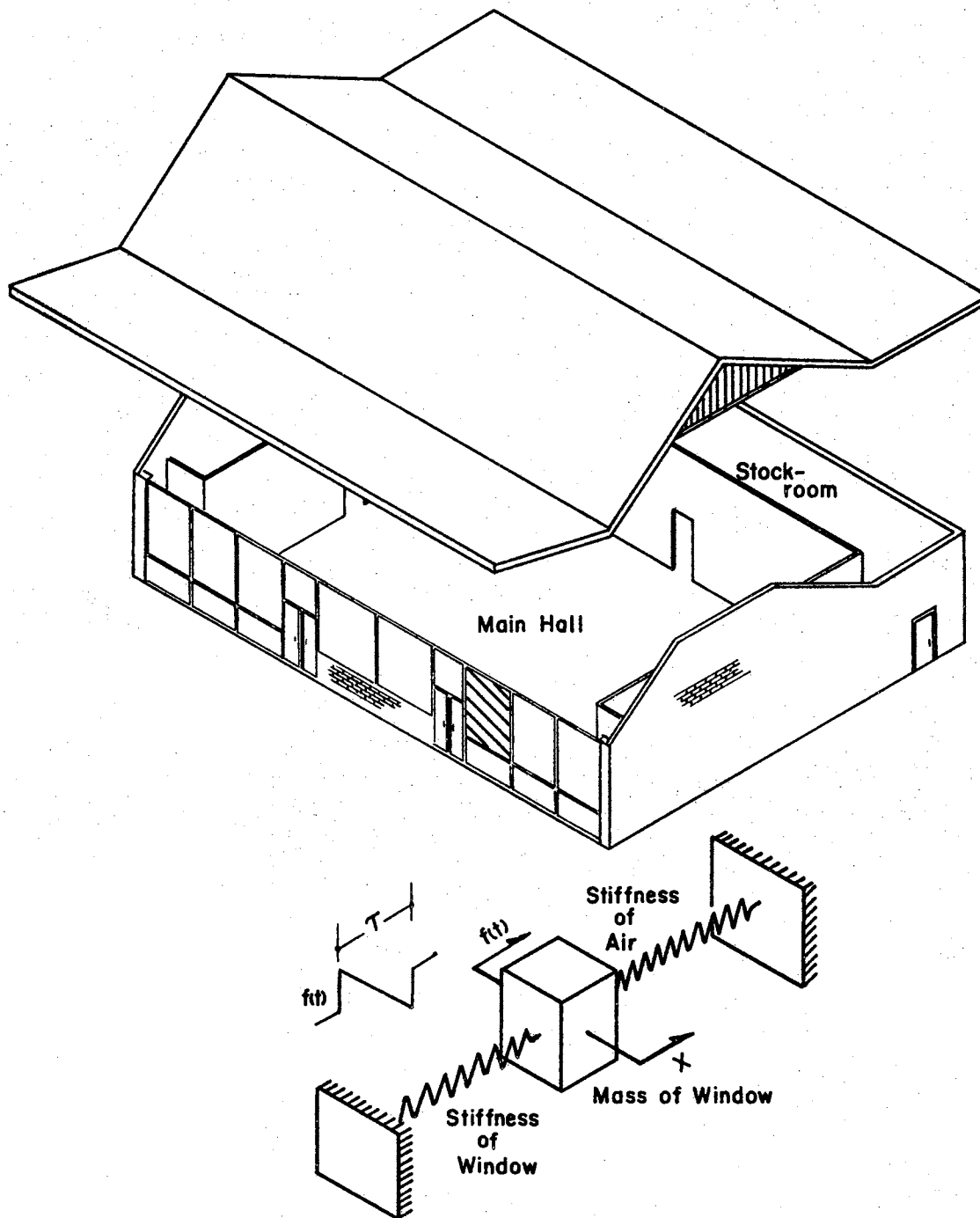
Figure 39. Floor Plan of Structure and Idealized Lumped
Parameter Representation
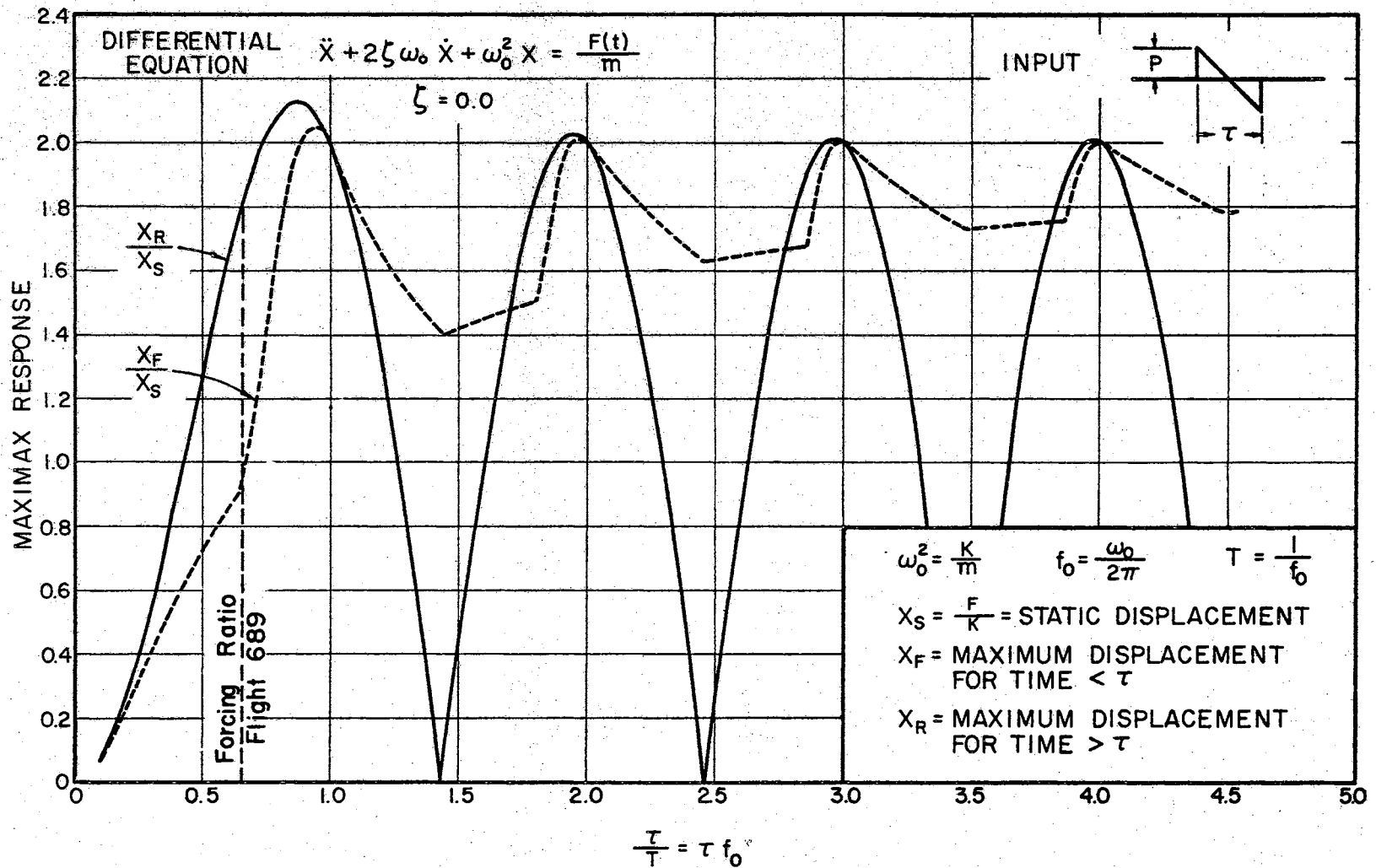
Figure 40. Normalized Response of a Simple Oscillator With
Natural Period T to a N-Wave of Duration τ

Conclusions on the Failure of the Window

In the entire analysis of the Kinney Shoe Store window, there were no stress levels computed which exceeded or approached the working stress of common glass (6,000 psi).

The failure stress of $\frac{1}{4}$-inch plate glass is given by a statistical distribution. A normal distribution curve was assumed for a group of specimens that have been tested under the same conditions, the average breaking strength will occur around 6,000 psi (18). The value of working stress will vary with the different constituent ratios in the glass.

A reduction to about one half the value will occur for long term loading because the material is highly sensitive to strain rate.

A stress amplitude of 1127 psi would cause failure in a very small percentage of cases. The stress amplitude is well below the average on the distribution curve. However, since this isolated incident was the only reported failure of this particular size of window, it may well have been that failure occurred because the glass was faulty. Other intangible factors, as stress risers in the form of scratches, or nicks in the surface of the glass, could have been contributing factors.

Glass windows can experience stress levels near the fracture point if the thickness is small and pressures are large. For certain sizes of windows, the natural period of

the window will be in the right proportion ($\frac{\tau}{T} = 1$) with the forcing period for maximum response. Stress levels in this case will be much higher than for other sizes. The tuning effect, coupled with focusing effects such reflections of the wave from structures in the area or unknown stress risers in the material, can cause large stress amplitudes which may result in the failure of many windows.

A conjecture can be formed in the case of a hypothetical supersonic transport aircraft. A far-field pressure signature of about 0.3 seconds duration would not be un-reasonable. The time duration of the forcing transient implies that peak structural response will occur at about 3.3 cps. A dynamic amplification factor of 2.5 would be realistic. It was shown in Chapter V, that a slower rise time caused the peak ratio to increase slightly over the normal N-wave. Sonic booms in the order of 2 to 2.5 psf might well occur for an aircraft traveling at a speed of 3.0 mach. This pressure, coupled with the dynamic ampli-fication factor, would yield a maximum pressure of 6.25 psf.

A recent publication by Pittsburg Plate Glass Company (18) shows a plate window 96x120x$\frac{1}{4}$ inches would be approved for a 14 psf with a safety factor of 4.2. This safety factor would state, using a statistical probability table from the same article (18), that about 1.3 windows would "probably" fail, out of 1,000 specimens.

The need for the understanding of the effects of sonic booms on structural elements cannot be overemphasized.

With the development of a supersonic transport, sonic booms will be a frequent occurrence over the entire country side. Marginal structural elements, such as plaster ceilings, windows, and framing members will be subjected to severe overpressures. Attention will have to be diverted to the structural design of these elements to avoid failures in this new loading environment.

Any useful response analysis of a complex structure will necessitate an idealization of an equivalent mathematical model for the system. Analysis of distributed complex structures with hallways, windows, flexible ceilings, multi-story dwellings, and odd geometric configurations are extremely difficult and somewhat specific. The time required to obtain an exact solution for a specific configuration is probably not worth the effort. The time could be well spent in developing general design methods applicable to an entire group or type of problems.

In the analysis of the window failure, various contributing factors were ignored in the one degree-of-freedom idealization of the system. The ceiling and the pressure oscillations which were created by the ceiling pumping the air in the room could have been a contributing factor. Although there were eight windows of approximately the same size in the store front, only one window failed. There was no apparent explanation why others didn't break. Each window was vibrating after the boom passed and was oscillating at a different phase. Phase difference could

be a contributing factor. Thus it is easy to conclude that there is no exact method of analyzing the response of complex structures and stating precisely what occurred in the failure of a window to a sonic boom.

CHAPTER VII

CONCLUSIONS AND RECOMMENDATIONS

The lumped parameter representation of the panel coupled
to the Helmholtz resonator served as a good predictor for
the panel response. Experimental results obtained from a
simply supported panel indicated that panel response can be
greater when coupled to the resonator than in the baffled
case alone.

The increase in panel response when the resonator
natural frequency is approximately the same as the panel
natural frequency is cause for concern. Physical structures
can exist in which this situation might be very pronounced.

The analog computer was utilized to obtain response
plots for the lumped parameter analysis and the digital
computer was used in the distributive analysis.

Distributive analysis of panel response is limited in
its' usefulness toward complex physical systems. The
coupling and interaction of walls, flexible ceilings and
windows will necessitate a general analysis and a prediction
of the response by a lumped parameter model.

The difficulties encountered in the investigation were
mainly of an instrumentation nature. The pulse generating
apparatus was adequate but lacked the quality required for

excellent results. Knife edges supporting the panel should be ground rather than milled in future work in this area. The following specific conclusions are given as a result of this investigation:

1. The lumped parameter model for the two degree-of-freedom system of a panel coupled to the resonator allows reasonably good prediction of the dynamic response of the panel. The model can be extended to encompass more complicated systems such as multiple-connected windows, two interconnected cavities, etc.

2. The duration of the N-wave to the natural period of the panel has a marked affect on panel response. When this ratio is approximately one, amplification ratios for a lightly damped system are of the order 2.0.

3. Consideration of the contribution of the fundamental mode only is deemed adequate for prediction of panel response to sonic booms.

4. A magnification factor of 2.6 can occur when a panel is coupled to an acoustic resonator having a natural frequency close to that of the panel.

5. In the case of the panel coupled to the resonator, the time duration of the N-wave is of less importance than in the case of the baffled panel alone.

6. Intangible factors, such as internal panel defects, support imperfections, state of disrepair, etc., are important and must be considered in the overall analysis and prediction of damage due to sonic booms.

7. External damping material reduces the amplitude of the panel in all cases. A damper type of window mounting could help resist sonic boom damage.

8. The rise time of a transient pulse for a given time duration is the parameter which is most influential on the magnitude and location of the peak response.

Recommendations

The following areas appear to offer scope for further work:

1. Identification of the lumped parameters and application of the lumped parameter theory to a residential dwelling. Parameters, such as hallway dimensions, door openings, and room size need to be described in terms of masses and springs in lumped systems, and the results verified by measurements with a sonic boom input.

2. An investigation of the neck correction factors for multiple degree-of-freedom system

of resonators. These correction factors
will enable better predictions of the
parameters in a complicated structure.

3. The area of fatigue of metal fasteners and
the development of improved methods of
fastening wall board, plaster, and other
materials. Repeated sonic boom pressure
waves for an extended period of time can
cause conventional fasteners to vibrate
loose. Fatigue is associated with
repetitive type loading and will eventu-
ally have to be considered in predicting
the finite life of items subjected to the
sonic boom overpressures.

4. The interaction of structural elements such
as ceilings and windows or multiple-
connected windows to transient type inputs.

5. Construction of a full size test facility in
which a resonator effect coupled to various
sizes of panels can be investigated. Sizes
of openings, windows and interconnection of
cavities could be altered to achieve maximum
pressure and maximum response conditions.

6. Investigation of cavity response, in which the
input pressure wave length is of the same
order of magnitude as the cavity dimensions.
Sonic booms can have wave lengths in the

vicinity of 175 to 200 feet. Large auditoriums, train terminals and air terminals will have dimensions near this fundamental wave length. Lumped parameter representation for a resonator response has been applied with the limitation that the wave length of the incoming sound be large compared to the cavity dimensions. Experimental results show that this is not extremely important as long as the wave length is three to four times as large. What effect will the long wave have on pressure oscillations in large rooms? Will standing waves be excited that will adversely affect the response of large windows coupled to the structure?

7. Investigation of the maximum amplitude of a damped single degree-of-freedom system for a decaying sinusoidal forcing input. Enclosures which are lightly damped can have oscillations for many cycles (40).

Preliminary investigation showed in the case of the lightly damped system ($\zeta = 0.05$) with a damped sinusoidal input ($\zeta_F = 0.05$), an amplification factor of 3.6. The forcing period was the same as the natural period of the system.

The assumption of a decaying type input to the simple system uncoupled the system and changes the amplification ratio. However, the response to the damped sine input

should define a limiting value for the amplification ratio.

BIBLIOGRAPHY

1. Andrews Associates, Inc., and Hudgins, Thompson, Ball
        and Associates, Inc., "Final Report on Studies of
        Structural Response to Sonic Booms," for the
        Federal Aviation Agency, Vol. 1, February 5, 1965.

2. ARDE Associates, "Response of Structures to Aircraft
        Generated Shock Waves," WADC Technical Report,
        Pages 58-169, April, 1959.

3. Beranek, L., Acoustics, McGraw-Hill Book Co., 1954.

4. Biggs, J., Structural Dynamics, McGraw-Hill Book Co.,
        1964.

5. Bowles, R., B. Sugarman, "The Strength and Deflection
        Characteristics of Large Rectangular Glass Panels
        Under Uniform Pressure," Glass Technology, Vol. 3,
        No. 5, October, 1962.

6. Broom, P. W., "The Laboratory Generation of Sonic Booms,"
        University of Washington, Masters Thesis, 1963.

7. Cheng, D. H., "Some Dynamic Effects of Sonic Booms on
        Building Structural Elements," Langley Working
        Paper, No. 25, NASA.

8. Clarke, M. J., and J. F. Wilby, "Subjective Response of
        Sonic Bangs," Aero. Res. Council London Cir.,
        October, 1961.

9. Crandall, I. B., Theory of Vibrating Systems and Sound,
        2nd Edition, D. VanNostrand Company, 1927.

10. Crocker, M. J., "Theoretical and Experimental Response
        of Panels to Travelling Sonic Boom and Blast
        Waves," Wyle Laboratories Report, WR 66-2, January,
        1966.

11. Handbook of Analog Computation, Pub. No. L800 0001 OA
        Electronic Associates, Inc., Long Branch, New
        Jersey.

12. Hoover J., A. Ross, "Sonic Booms and Large Glass
        Windows."

13. Lamb, H., _Dynamical Theory of Sound_, Dover.

14. Little, R. W., Rayleigh-Ritz Energy Method (unpub.).

15. Lyon, I., "The Impedance of a Resistance Loaded Helmholtz Resonator," _Journal of the Acoustical Society of America_, Vol. 25, No. 5.

16. Mase, G. E., "Transient Response of Linear Visco-elastic Plates," _Journal of Applied Mechanics_, September, 1960, page 589.

17. Ostergren, S. M., "Shock Response of a Two Degree-of-Freedom System," Air Research and Development Command, United States Air Force, ASTIA Document No. AD 202096.

18. Pittsburg Plate Glass Company, "Glass Performance Under Wind Load," Product Development Technical Memorandum, February, 1962.

19. Pretlove, A. J., "Free Vibrations of a Rectangular Panel Backed by a Closed Rectangular Cavity," _Journal of Sound and Vibrations_, Vol. 2, No. 3, pages 197-209.

20. Rayleigh, J. W. S., _The Theory of Sound_, Volumes 1 and 2, Dover Publications.

21. Reddy, N. N., "Transient Response Spectra of Double Acoustical Resonators," (unpub. Ph.D. thesis, Oklahoma State University, 1967).

22. Richards, E. J., "Noise Problems Associated with Supersonic Flight with Emphasis on Structural Aspects of the Problem," _Israel Journal of Technology_, February, 1964, Vol. 1.

23. Samulon, H., "Investigations on Acoustic Resonators," _Journal of the Acoustical Society of America_, Vol. 19, No. 1, 1947.

24. Simpson, J. D., "The Transient Response of a Helmholtz Resonator with Application to Sonic Boom Studies," Thesis, Oklahoma State University, May, 1966.

25. Stewart, G. W., "Acoustic Wave Filters," _Physical Review_, 1922, Vol. 20, pages 528-551.

26. Stewart, G. W., "Acoustic Wave Filters," _Physical Review_, 1922, Vol. 23, pages 520-524.

27. Stewart, G. W., "Acoustic Wave Filters," _Physical Review_, 1925, Vol. 25, pages 90-98.

28. Timoshenko, S., _Theory of Plates and Shells_.

29. Timoshenko, S., _Vibration Problems in Engineering_.

30. Thompson, W. T., _Laplace Transformation_, Prentice-Hall Inc., Englewood Cliffs, New Jersey, 1960.

31. Ungar, E., "Response of Plates to Moving Shocks," _Aerospace Engineering_, March, 1961.

APPENDIX A

LUMPED MASS CONSIDERATIONS FOR THE SYSTEM

Helmholtz Resonator

A suitable mathematical model to represent the Helmholtz
resonator, whether it be electrical or mechanical analog,
will be dependent on the frequency of the input sound. If
the wavelength of the pressure input is of sufficient length,
then the assumption that the pressure inside the cavity
volume is uniform is adequate. This implies that there is
no change in kinetic energy in the cavity volume itself.
The cavity volume then acts as a spring and absorbs and
relinquishes potential energy. Previous investigators have
stated the following assumptions for the lumped parameter
system representing the Helmholtz Resonator (20):

1. Input wavelength is long in comparison with
    the largest dimensions of the cavity. This
    restriction on the forcing input insures that
    standing waves in the cavity volume and in the
    neck of the cavity are not excited.

2. Adiabatic compression occurs within the cavity
    volume. This condition merely implies that the
    wave propagation is so rapid that temperature

changes are unimportant.

3.   The cavity volume of air has compression with-
out acceleration.

4.   The air contained in the neck of the resonator
has acceleration without compression.

Thus, the air in the neck behaves as a mass, while the
air in the cavity volume acts like a spring.
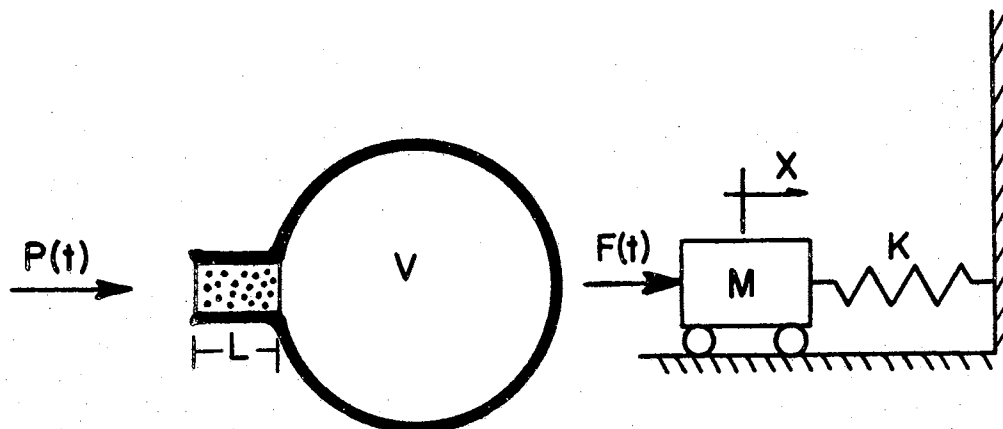
Figure 41.   Simple Helmholtz Resonator and Equivalent
Lumped Parameter System

If   represents the displacement of the air in the neck,
as shown in Figure 41   , and utilizing the mathematical
expression for adiabatic compression:

$$PV^{\gamma^1} = C, \qquad\qquad (A-1)$$

the differential equation of motion can be obtained in a
straight forward manner (3),

$$\rho_o L_e A \; \frac{d^2 X}{dt^2} \; + \; \frac{\gamma p_o}{V} \; A^2 X = P(t) \; A \tag{A-2}$$

where

ρ_o is density of air,

L_e is an effective length of the neck.

Using a volumetric displacement, $\bar{X} = AX$ and replacing
$p_o \gamma$ by its' equivalent, $\rho_o c^2$, the differential equation
takes the form of,

$$\frac{\rho_o L_e}{A} \; \frac{d^2 \bar{X}}{dt^2} + \frac{\rho_o c^2}{V} \; \bar{X} = P^1(t) \tag{A-3}$$

and the natural frequency of the system then becomes

$$f_o = \frac{c}{2\pi} \sqrt{\frac{A}{V L_e}} \; . \tag{A-4}$$

This equation was used to compute the frequency using a
correction factor for the length of the neck as
$L_e = L + 1.57 \; (r)$ where r is the radius of the neck (3).
The expression is a good prediction for the natural frequency
and as stated previously, measured values agreed quite well
with the predicted values.

Consideration of an Equivalent Lumped System
for the Simply Supported Panel
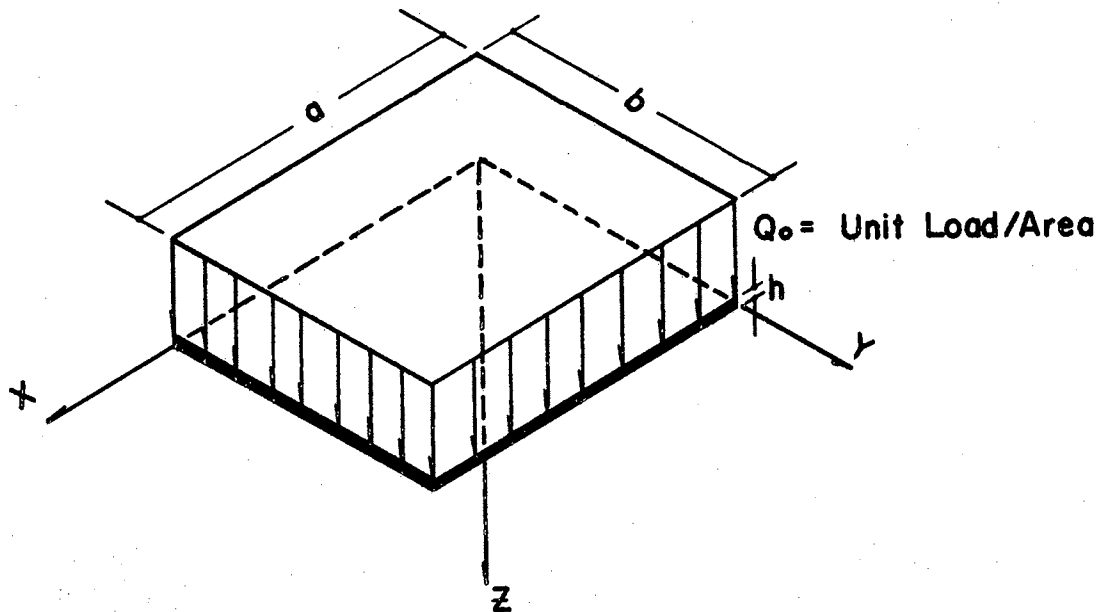
Figure 42. Simply Supported Uniform Load Configuration

For a uniform loaded, simply supported plate, the well-known expression for the deflection is given by (28),

$$z(x, y) = \frac{16\ Q_0}{\pi^6\ D} \sum_{r=1,3,5}^{\infty} \sum_{s=1,3,5}^{\infty} \frac{\text{Sin}\ \frac{r\pi x}{a}\ \text{Sin}\ \frac{s\pi y}{b}}{rs\ \frac{r^2}{a^2} + \frac{s^2}{b^2}} \cdot$$

$$\text{Cos}\ (\omega t - \gamma) \ . \tag{A-6}$$

If one considers only the fundamental mode, i.e., when r=1, s=1, this states that all points on the panel are moving in phase with each other and the expression for the displace-

ment reduces to

$$z = z_0 \, \text{Sin} \, \frac{\pi x}{a} \, \text{Sin} \, \frac{\pi y}{b} \, , \qquad (A\text{-}7)$$

where z_0 is the central displacement. The velocity is obtained by differentiating z;

$$\dot{z} = \dot{z}_0 \, \text{Sin} \, \frac{\pi x}{a} \, \text{Sin} \, \frac{\pi y}{b}, \qquad (A\text{-}8)$$

where $\dot{z}_0$ is the central velocity of the panel.

The kinetic energy of the plate T in terms of the deflection z is given by

$$T = \tfrac{1}{2} \, m\dot{z}^2 = \frac{h}{2} \int_0^b \int_0^a \rho \dot{z}_0^2 \, \text{Sin}^2 \, \frac{\pi x}{a} \, \text{Sin}^2 \, \frac{\pi y}{b} \, dxdy \qquad (A\text{-}9)$$

$$T = \tfrac{1}{2} \left[\rho \, \frac{abh}{4} \right] \dot{z}_0^2 \, . \qquad (A\text{-}9a)$$

Therefore, the equivalent mass or the mass constant considering only the fundamental mode, is one-fourth of the total mass of the plate. This mass, sometimes is expressed as the so called generalized mass, and is usually obtained by using the relation,

$$M = m \int_A \, \Phi^2 \, (x,y) \, dA \qquad (A\text{-}10)$$

where Φ (x,y) is the mode shape and m is the actual mass of the plate.

The potential energy of the simply supported plate with a uniform load is obtained in a straight forward manner:

Considering the fundamental mode or r=1, s=1

$$Z = Z_0 \, \text{Sin} \, \frac{\pi x}{a} \, \text{Sin} \, \frac{\pi y}{b}$$

then the potential energy U is obtained by integrating the expression,

$$U = \int_0^{Z_0} \int_0^b \int_0^a Q_0 \, \text{Sin} \, \frac{\pi x}{a} \, \text{Sin} \, \frac{\pi y}{b} \, dx \, dy \, dZ. \tag{A-11}$$

Defining constants,

$$Z_0 = Q_0 \, K_1 \tag{A-12}$$

and

$$K_1 = \frac{16}{\pi^6 \, D \left(\frac{1}{a^2} + \frac{1}{b^2} \right)^2} \quad , \tag{A-13}$$

the potential energy is obtained by integration:

$$U = \int_0^{Z_0} \int_0^b \int_0^a \frac{\Psi}{K_1} \, \text{Sin} \, \frac{\pi x}{a} \, \text{Sin} \, \frac{\pi y}{b} \, dx \, dy \, d\Psi \tag{A-14}$$

$$U = \frac{4ab}{\pi^2 K_1} \frac{Z_0^2}{2} \tag{A-14a}$$

$$U = \frac{1}{2} \left[\frac{(a^2 + b^2)^2}{a^3 b^3} \right] Z_0^2 \, . \tag{A-14b}$$

The equivalent spring constant as derived in terms of the central deflection is

$$k_{eq} = \frac{(a^2 + b^2)^2 \pi^4 \, D}{4a^3 b^3} \, . \tag{A-15}$$

A check on the natural frequency of the plate is made by the expression,

$$f_o = \frac{1}{2\pi} \sqrt{\frac{K_{eq}}{m_{eq}}} \qquad\qquad (A\text{-}15a)$$

resulting in,

$$f_o = \frac{\pi h}{2} \sqrt{\frac{E}{12\ \rho\ (1 - \mu^2)}} \left(\frac{1}{a^2} + \frac{1}{b^2}\right) \ . \qquad (A\text{-}16)$$

This expression above is the same expression for the fundamental frequency by Timoshenko (28) using the theory of elasticity.

Then the equivalent lumped parameter model to describe the distributed system will take the equivalent spring constant, and the equivalent mass as obtained in expressions (A-9a) and (A-15) above. This equivalent method will reduce the distributed system to the lumped system with the following implications:

1. A preservation of the natural frequency; the lumped parameter system will have the same natural frequency as the fundamental natural frequency of the distributed system.

2. The equivalent was obtained in terms of central velocity and central deflection, therefore, a center point of the panel should correspond to the same displacement of the lumped mass system.

APPENDIX B

LIST OF MAJOR INSTRUMENTATION AND CALIBRATIONS

Calibrations

Three factory-calibrated Altec microphones, a Tektronic
oscilloscope, and a semiconductor strain gauge with an
optic galvonometer type recorder, were the main devices used
in obtaining the measurements. The calibration curves for
the microphones showed a flat response from 20 to 4000
cycles per second. The sensitivity of the microphones are
-54.5 db (reference being 1 volt per dyne per centimeter),
this corresponding to 1.095 pounds per square foot per
volt. A very slight difference in the microphones was
observed and is tabulated in Table IV. The reference
sensitivity of the microphone was taken as 1.1 psf/volt
because of the inherent difficulty in reading the oscillo-
scope to a high accuracy.

The balancing and calibration of the semiconductor
strain gauge was extremely tedious. The semiconductor
strain gauge is a highly sensitive gauge with a gauge
factor of 115. The gauge factor is given as

$$GF = \frac{\Delta R}{\epsilon R} \qquad \qquad (B-1)$$

where

    ΔR is the change in resistance of the gauge,

    R is the resistance of the gauge,

    ϵ is the strain (in/in).

A high gauge factor will cause the gauge to output a large change in resistance for a small amount of strain.

Ideally, calibration of the strain gauge would consist of introducing an accurately known pressure on the plate and observe the response. This type of calibration could not be realized in this experimental work because of the nature of the transducer and the unknown boundary conditions. The gauge was bonded to the test item for the simple reason that the strains were unknown. Once the strain gauge was bonded, it could not be transferred to a known strain situation for calibration purposes. If the gauge factor and the gauge resistance is known, the system can be calibrated without a direct strain reading. This method was used since the gauge manufacturer provided the gauge factor and gauge resistance within a tolerance of $\pm$ 1 per cent.

The calibration method consists of determining the system's response to the introduction of a small resistance change and calculating an equivalent strain from it. The change in resistance is done by shunting a high-value precision resistance across the gauge. This change was accomplished by the use of a manual calibration knob provided on the bridge amplifier meter. The bridge was

TABLE IV

MICROPHONE SENSITIVITY COMPARISONS

Frequency (cps)	$\dfrac{\#2 \text{ Microphone}}{\#1 \text{ Microphone}}$	$\dfrac{\#3 \text{ Microphone}}{\#1 \text{ Microphone}}$
20	1.02	1.00
30	1.06	1.02
40	1.07	1.05
50	1.00	.98
60	1.07	1.04
70	1.06	1.01
80	1.05	1.02
90	1.07	1.04
100	1.09	1.06
110	1.07	1.03
120	1.08	1.08
130	1.09	1.03
140	1.05	1.06
150	1.03	1.00
160	1.07	1.02
170	1.11	1.07
180	1.03	1.03
190	1.03	1.03
200	1.04	1.00

#1 Microphone (Serial No. 3892)   #2 Microphone (Serial No.
#3 Microphone (Serial No. None)   3854)

balanced prior to the shunting process, and was accomplished with the aid of a digital voltmeter. Accuracy of balancing the bridge was critical, and could not be balanced by the meter on the commercial amplifier unit itself. The balancing of the bridge was accomplished with the entire detection, amplification and recording devices connected on line. This was done to insure no loading affect would alter the balancing. The manual calibration switch was depressed and released about six to eight times a second and the output of the bridge was noted on the digital voltmeter to be 51 MV. This output was placed in the detection and recording system, by substituting an oscillator at the specified voltage and frequency through the fixed gain amplifier, and subsequently placed into the optic recorder, in which the signal was recorded. A calibration factor was then determined in terms of micro-in/in per inch deflection on the recorder.

The calibration of the differential transformer used in measuring deflections at the center of the plate, was accomplished by a direct method. The differential transformer was placed on a vibrator at a known amplitude and the displacement and the phase shift was observed on an oscilloscope for the frequency range in consideration.

Table V shows the output of the transformer and phase difference over the frequency range.

Figure 43 shows the filtered and unfiltered trace of the differential transformer displaying the carrier frequency on the unfiltered trace.

TABLE V

DIFFERENTIAL TRANSFORMER CALIBRATION

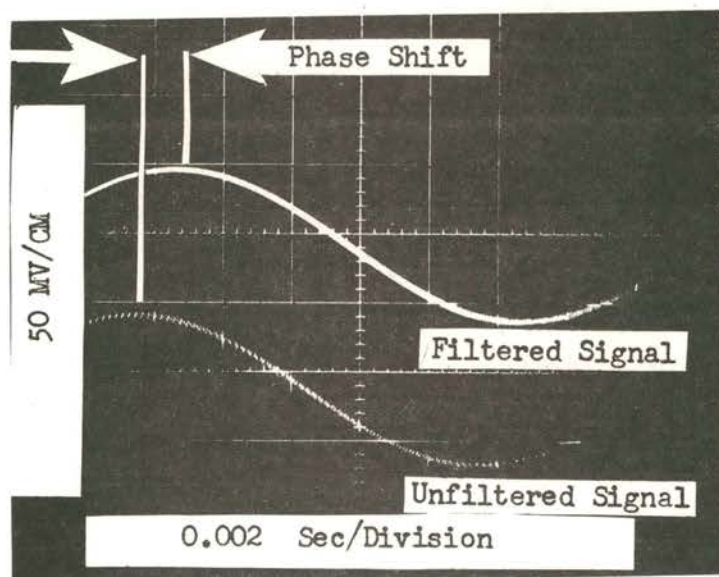| Frequency(cps)	Output(mv)	Phase Angle($^\circ$)	Displacement(in)
80	115 mv	28.8°	.004
90	115 mv	32.4°	.004
100	115 mv	36°	.004
110	115 mv	39.5°	.004
120	113 mv	43.2°	.004
125	110 mv	45°	.004
130	110 mv	47.5°	.004
140	105 mv	49.8°	.004

Figure 43. Differential Transformer
Output Through Band Pass
Filter, Lower Cutoff 2cps
- Upper Cutoff 900 cps

The scope calibration and linearity of the traces were so close that no discernible error could be visually detected. The sensitivities of the two beams were identical. There was no discernible difference in the linearity or sensitivities of the two beams.

Instrumentation

Microphone System---Model 21BR150 Condenser Microphone, Serial No. 3854; 165 Base; Model 526B Power Supply, Serial No. 608; Manufacturer; Altec Lansing Corporation.

Microphone System---Model 21BR150 Condenser Microphone, Serial No. 3892; 165 A Base; Model 526B Power Supply, Serial No. 606; Manufacturer; Altec Lansing Corporation.

Microphone System---Model 21BR150 Condenser Microphone, Serial No. None; 165 A Base; Model 526B Power Supply, Serial No. None; Manufacturer; Altec Lansing Corporation.

Dual Beam Oscilloscope---Model 502; Manufacturer; Tektronix; Serial No. 022893.

Tone Burst Generator---Type 1396-A; Manufacturer; General Radio Company; Serial No. 354.

Power Amplifier---Model MC 75; Manufacturer; McIntosh.

Dual Beam Oscilloscope---Model 322; Manufacturer; DuMont Laboratories, Inc.; Serial No. 9X78.

Strain Gauge Amplifier---Model BAM-1; Manufacturer; Ellis Associates; Serial No. 2076.

Fixed Gain Amplifier---Model 450 A; Manufacturer; Hewlett Packard; Serial No. 010-05479.

Oscilloscope Camera---Model 3620; Manufacturer; Analab; Serial No. 246; Periscope; Model 3600; Manufacturer; Analab; Serial No. 109.

Recording Oscillograph---Model 5-124; Manufacturer; Consolidated Electrodynamics Corporation; Serial No. 6307.

Linear Differential Transformer---Model 70 CDT-050; Manufacturer; Sanborn; Serial No. EG.

Band Pass Filter---Model 330 M; Manufacturer; Krohn-Hite; Serial No. 2959, .2cps - 20 KC.

Strain Gauge----Type PAI-05-120; Semiconductor; Manufacturer; Micro-Systems, Inc.

VITA

GERALD D. WHITEHOUSE

Candidate for the Degree of

Doctor of Philosophy

Thesis: COUPLED AND UNCOUPLED PANEL RESPONSE TO SONIC
BOOM TYPE INPUTS

Major Field: Mechanical Engineering

Biographical:

Personal Data: Born in Sapulpa, Oklahoma, May 17,
1936, the son of Stephen Ted and Mary Frances
Whitehouse. Married to Lilliun Ross, June 7,
1958. Father of two daughters, Carol and Linda.

Education: Graduated from Sapulpa High School, Sapulpa,
Oklahoma, 1954; received the Bachelor of Science
Degree in Mechanical Engineering from the Uni-
versity of Missouri-Rolla in June 1958. Graduated
with Master of Science in Mechanical Engineering
from Oklahoma State University in May, 1964;
completed requirements for the Doctor of Philoso-
phy Degree in September, 1966.

Professional Experience: Engineering assistant, Ethyl
Corporation, summer of 1957. Engineer, Douglas
Aircraft Company, June, 1958, to May, 1959. Comp-
any grade officer in the Corps of Engineers,
May, 1959, to January, 1963. Graduate research
and graduate teaching assistant, Oklahoma State
University, January, 1963, to June, 1966. Sonic
Boom consulting work, summer of 1964, spring of
1966.

Organizations: Member of Pi Tau Sigma (national
honorary mechanical engineering fraternity),
Theta Tau (professional engineering fraternity),
Alpha Phi Omega (service fraternity), ASME,
Engineer-in-training; State of Oklahoma.